Bregnard *et al. Parasites Vectors* (2021) 14:168
https://doi.org/10.1186/s13071-021-04646-0

Parasites & Vectors

RESEARCH Open Access

Masting by beech trees predicts the risk of Lyme disease

Cindy Bregnard[1*], Olivier Rais[2] and Maarten Jeroen Voordouw[1,3]

Abstract

Background: The incidence of Lyme borreliosis and other tick-borne diseases is increasing in Europe and North America. There is currently much interest in identifying the ecological factors that determine the density of infected ticks as this variable determines the risk of Lyme borreliosis to vertebrate hosts, including humans. Lyme borreliosis is caused by the bacterium *Borrelia burgdorferi* sensu lato (s.l.) and in western Europe, the hard tick *Ixodes ricinus* is the most important vector.

Methods: Over a 15-year period (2004–2018), we monitored the monthly abundance of *I. ricinus* ticks (nymphs and adults) and their *B. burgdorferi* s.l. infection status at four different elevations on a mountain in western Switzerland. We collected climate variables in the field and from nearby weather stations. We obtained data on beech tree seed production (masting) from the literature, as the abundance of *Ixodes* nymphs can increase dramatically 2 years after a masting event. We used generalized linear mixed effects models and AIC-based model selection to identify the ecological factors that influence inter-annual variation in the nymphal infection prevalence (NIP) and the density of infected nymphs (DIN).

Results: We found that the NIP decreased by 78% over the study period. Inter-annual variation in the NIP was explained by the mean precipitation in the present year, and the duration that the DNA extraction was stored in the freezer prior to pathogen detection. The DIN decreased over the study period at all four elevation sites, and the decrease was significant at the top elevation. Inter-annual variation in the DIN was best explained by elevation site, year, beech tree masting index 2 years prior and the mean relative humidity in the present year. This is the first study in Europe to demonstrate that seed production by deciduous trees influences the density of nymphs infected with *B. burgdorferi* s.l. and hence the risk of Lyme borreliosis.

Conclusions: Public health officials in Europe should be aware that masting by deciduous trees is an important predictor of the risk of Lyme borreliosis.

Keywords: Beech tree, *Borrelia burgdorferi*, Climate, *Fagus sylvaticus*, *Ixodes ricinus*, Lyme borreliosis, Masting, Tick-borne disease, Tick population ecology

*Correspondence: cindy.bregnard@unine.ch
[1] Laboratory of Ecology and Evolution of Parasites, Institute of Biology, University of Neuchâtel, Neuchâtel, Switzerland
Full list of author information is available at the end of the article

Background

Ticks and tick-borne diseases represent a significant health problem for humans and their companion animals [1]. Tick-borne pathogens cause both morbidity and mortality in their vertebrate hosts. A recent report by the US Centers for Disease Control and Prevention (CDC) found that tick-borne diseases in the USA had more than doubled over a period of 13 years (> 22,000 cases in 2004 to > 48,000 cases in 2016) with Lyme borreliosis accounting for 82% of all tick-borne disease reports [2]. The incidence of Lyme borreliosis and other tick-borne diseases is also increasing in Europe and Canada [3–8]. The explanation for this increased incidence of tick-borne disease is multi-factorial [9] and includes climate change [7, 8], changes in human land use [10, 11] and even socio-economic changes [12–14]. To understand the epidemiology of tick-borne diseases, it is critical to identify the ecological factors that influence the density of infected ticks because this variable determines the risk of infection to vertebrate hosts, including humans [15].

Lyme borreliosis is the most common vector-borne disease in the northern hemisphere [16, 17]. The causative agents are spirochete bacteria belonging to the *B. burgdorferi* sensu lato (s.l.). complex, which are transmitted among vertebrate hosts by *Ixodes* ticks. In Europe, the sheep tick (*Ixodes ricinus*) is the main vector that maintains *B. burgdorferi* s.l. in nature [18]. The life cycle of *I. ricinus* involves three active stages: larva, nymph and adult. Blood meals are required for larvae and nymphs to develop to the next stage and for egg production in adult female ticks. Immature *I. ricinus* ticks feed on a large variety of vertebrate hosts [18–20]. Larvae acquire *B. burgdorferi* s.l. after feeding on an infected host, as transovarial transmission of *B. burgdorferi* s.l. is believed to be rare or non-existent [21–23]. These engorged infected larvae moult into and overwinter as infected nymphs, which search for new vertebrate hosts the following spring and can transmit the infection during the nymphal blood meal [24]. In contrast, adult female ticks usually feed on incompetent reservoir hosts, such as deer, and therefore do not contribute directly to the maintenance of Lyme borreliosis in nature [25–27].

The infection risk of Lyme borreliosis to vertebrate hosts is determined by the density of infected nymphs and infected adult female ticks. The density of infected nymphs (DIN) is the most important risk factor because nymphs are more numerous and less noticeable than adult female ticks [10, 15, 28–30]. The DIN describes the probability for a host to acquire the pathogen from an infected nymph in its habitat [31]. In practice, the DIN is often estimated as the product of two other variables, the density of nymphs (DON) and the nymphal infection prevalence (NIP), the latter being the percentage of nymphs infected with *B. burgdorferi* s.l. [15]. The phenomenon of the seasonal risk of Lyme borreliosis is well known because the DON and the DIN vary dramatically over the seasons. The seasonal phenology of *I. ricinus* nymphs differs among geographic locations, but in continental Europe it is bimodal and consists of a large spring peak followed by a smaller autumn peak [32–34]. In contrast, the ecological factors driving inter-annual variation in the risk of Lyme borreliosis are less well studied because it requires long-term studies with good information on the DIN [35, 36]. From a public health perspective, understanding the ecological factors that cause inter-annual variation in the DIN, and hence in the risk of infection, is important for developing control strategies to reduce the incidence of Lyme borreliosis.

The ecological drivers underlying spatiotemporal variation in the DIN are a combination of abiotic (e.g., climate) and biotic factors (e.g., abundance of vertebrate hosts and vegetation). *Ixodes* ticks spend more than 98% of their time off the host [37, 38], and they have to cope with seasonal changes in temperature and precipitation. Their life history traits (development, survival, and reproduction) are highly sensitive to different climate variables. For example, tick development rates and survival rates increase with temperature and relative humidity, respectively [37, 39–41], suggesting that warmer and wetter environments should increase nymphal density and the risk of Lyme borreliosis.

Tick population ecology is also highly sensitive to the abundance of vertebrate hosts because all motile tick stages must blood feed to graduate to the next stage in the life cycle [42, 43]. Immature ticks (larvae and nymphs) feed on small mammals, such as rodents, which often exhibit dramatic inter-annual fluctuations in population size [44, 45]. An important source of food for many rodent species is the fruit (also called mast) of forest trees, and the annual production of this fruit can also vary dramatically among years [46–49]. Studies on *Ixodes scapularis* ticks in North America have shown that masting events increase the abundance of rodents in the following year, which increases larval feeding success, which in turn increases the DON and the DIN 2 years after the masting event [35, 50–52]. In Europe, two recent long-term studies have shown that seed production by trees increased the DON 2 years later [53, 54]. However, direct evidence that natural fluctuations in tree seed production influence the DIN and hence the risk of Lyme borreliosis is still lacking in Europe.

The aim of this study was to better understand the ecological factors that influence the inter-annual variation in the DIN and hence the risk of Lyme borreliosis. We used a long-term study to test whether the NIP and the DIN

have changed along an altitudinal gradient in Switzerland. Specifically, we used data from a 15-year study that monitored the monthly abundance of *I. ricinus* nymphs and adult ticks and their *B. burgdorferi* s.l. infection status at four different elevations on Chaumont Mountain, in the canton of Neuchâtel, Switzerland. We had previously analyzed this long-term data set and shown that the DON doubled over time at this study location and that seed production by European beech trees had a strong and positive effect on the DON 2 years later [54]. If the NIP remains constant over time, we expect that the DIN would double over the duration of the study and that beech masting would be important for explaining interannual variation in the DIN with the expected 2-year time lag.

Methods

Study location

The study was conducted on the south-facing slope of Chaumont Mountain, which is part of the Jura Mountains, and is in the canton of Neuchâtel, in western Switzerland. Four tick sampling sites, referred to as low, medium, high and top, were established at elevations of 620, 740, 900, and 1073 m above sea level (a.s.l.), respectively, and have been previously described [55–57]. There is logging in the area, and there are hiking trails and recreation areas for the public. The forest on Chaumont Mountain is mainly composed of European beech (*Fagus sylvatica*; 28.6%), Norway spruce (*Picea abies*; 28.5%), European silver fir (*Abies alba*; 20.4%), sycamore maple (*Acer pseudoplatanus*; 5.9%), European ash (*Fraxinus excelsior*; 3.7%), Scots pine (*Pinus sylvestris*; 2.3%), sessile oak (*Quercus petraea*; 2.3%), willow (*Salix* ssp.; 2.1%), common whitebeam (*Sorbus aria*; 1.6%), and European hornbeam (*Carpinus betulus*; 1.0%).

Sampling *I. ricinus* ticks in the field

Questing *I. ricinus* nymphs and adult ticks were collected monthly over a period of 15 years (January 2004 to December 2018) at each of the four elevation sites. The sampling protocol has been described previously [57]. Briefly, a 1-m^2 cotton flag was dragged across low vegetation over a transect distance of 120 m at the medium, high and top elevation sites; each transect of 120 m consisted of six drags of 20 m. At the low elevation site, the transect distance was 100 m and consisted of five drags of 20 m. The flag was inspected every 20 m, and nymphs and adult ticks were counted separately and placed in collection vials. This method of tick collection targets questing ticks and removes them from the environment, which means that they cannot be encountered on future sampling occasions and they cannot contribute to future tick population growth. The same person (Olivier Rais) conducted all of the 3427 drags (4 elevations × 15 years × 12 months × 5 or 6 drags = 4140 drags). No dragging was performed on days when there was snow on the ground (hereafter referred to as snow days). Over the study period (15 years × 12 months = 180 sampling dates), a total of 34 snow days occurred, which resulted in missing data for 713 drags.

Selection of ticks for testing of *B. burgdorferi* s.l. infection

Questing *I. ricinus* nymphs and adult ticks were placed in separate plastic vials (length: 9.5 cm; diameter: 1.6 cm) containing grass collected at the field sites to maintain a high relative humidity. Vials were brought to the laboratory and ticks were kept alive and at room temperature until DNA extraction. Over the 15 years of the study, we collected a total of 41,972 *I. ricinus* ticks at the four elevation sites: 32,823 nymphs and 9149 adult ticks (4658 males and 4491 females). For each combination of elevation site and sampling date (4 elevation sites × 15 years × 12 months = 720 combinations), a maximum of 40 questing *I. ricinus* ticks (20 nymphs, 10 adult females, 10 adult males) was selected for subsequent testing of *B. burgdorferi* s.l. infection.

DNA extraction of whole ticks

Total DNA was extracted from live *I. ricinus* ticks within 10 days after field collection using ammonium hydroxide (NH_4OH), as previously described [56]. Briefly, entire ticks were lysed in 100 µl of 0.7 M NH_4OH solution and boiled at 100 °C for 15 min. After allowing the solution to cool, tubes were opened and boiled again for 15 min to allow the ammonia to evaporate [58]. DNA extractions were stored at −20 °C until further analysis by reverse line blot (RLB).

Detection and identification of *B. burgdorferi* s.l. species by PCR and RLB

The DNA extractions of the ticks were analyzed for infection with *B. burgdorferi* s.l. and the identity of the *B. burgdorferi* s.l. genospecies was determined using PCR and RLB, as previously described [56]. Briefly, the variable spacer region between two repeated copies of the *23S rRNA* and *5S rRNA* genes was amplified using a conventional PCR [59]. The RLB allows us to detect and identify the six *B. burgdorferi* s.l. genospecies present at our study site: *B. burgdorferi* sensu stricto (s.s.), *B. afzelii*, *B. garinii*, *B. valaisiana*, *B. bavariensis,* and *B. lusitaniae*, as well as the relapsing fever spirochete *Borrelia miyamotoi*. The *B. burgdorferi* s.l.-positive PCR products were allowed to hybridize to a Biodyne C membrane (Pall Corp.,

New York, NY, USA) that contained seven genospecies-specific oligonucleotide probes using a Miniblotter 45 (Immunetics Inc., Boston, MA, USA) [59]. Hybridization was visualized by incubating the membrane with enhanced chemiluminescence detection liquid and by exposing the membrane to X-ray film.

Each RLB can process 45 samples and we performed a total of 325 RLBs to process all the ticks. The RLB blots were validated with DNA from cultures of the six *B. burgdorferi* s.l. genospecies to confirm that the genospecies-specific probes were working properly. These cultures of the six *B. burgdorferi* s.l. genospecies were grown fresh whenever they were needed over the duration of the study. We defined the RLB time lag as the time interval between the date of tick sampling and the RLB (this time lag is similar to the time lag between the DNA extraction and the RLB). There was considerable variation in the RLB time lag among the RLBs (nymphs: mean = 859 days, range = 4–5025 days; adult ticks: mean = 914 days, range = 4–3487 days).

The ability of the RLB to detect *B. burgdorferi* s.l. is comparable to that of other molecular detection methods. In a previous study, we used a sample of field-captured *I. ricinus* nymphs ($n = 788$) to show that there was a strong correlation ($r = 0.883$, $P < 0.001$) between the RLB method and a quantitative PCR that targets the *flagellin* gene of *B. burgdorferi* s.l. [60]. In another study, we used Sanger sequencing of nymph-derived *B. burgdorferi* s.l. isolates ($n = 110$) to show that the RLB identifies the correct genospecies for > 95.0% of the samples [61].

Field-collected climate variables

Temperature (T; in °C) and relative humidity (RH; in %) were recorded at 60 cm above the ground at 1 moment in time on the day of tick collection (usually between 10:00 a.m. and 2:00 p.m.) at each tick sampling site using a thermohygrometer (model 615; Testo SA, Lonay, Switzerland). Thus, for each combination of elevation and year, we had a total of 12 field-collected measurements of temperature and relative humidity. The saturation deficit (SD) is a measure of the drying power of the atmosphere (in mmHg) and is calculated using temperature and relative humidity as follows: $SD = (1 - RH/100) \times 4.9463 \times e^{0.0621T}$ [62, 63]. The accuracy of our field-collected climate data was confirmed by comparing them to the weather station data [54].

Weather station climate variables

We also obtained climate data from the Climap-net database of the Federal Office of Meteorology and Climatology MeteoSwiss. Two weather stations close to our study site are in Neuchâtel at 485 m a.s.l. and in Chaumont at 1136 m a.s.l. These weather stations sample, at 200 cm above the ground, the temperature and relative humidity every hour, and the total precipitation each day. We used the data on the daily mean temperature (average of the 24 hourly measurements), the daily mean relative humidity (average of the 24 hourly measurements) and the daily total precipitation. Thus, for each year, we had a total of 365 weather station measurements of these three climate variables. The SD was calculated as previously described. For each of the four elevation sites, we calculated site-specific climate variables by interpolating the data between the two weather stations (Additional file 1: Section 1).

Data on inter-annual variation in tree masting

We previously demonstrated that the abundance of *I. ricinus* ticks depends on the seed production of deciduous trees [54]. The seeds or fruit of forest trees, such as the acorns of oak trees and the beech nuts of beech trees, are often referred to as mast. The annual production of mast by a population of trees in an area is highly variable among years [64]. The MASTREE database contains data on masting (or seed production) for many locations in Europe from 1982 to 2016 for two tree species, European beech (*Fagus sylvatica*) and Norway spruce (*Picea abies*) [65]. In this database, the mast intensity is classified into five classes, namely 1, 2, 3, 4, and 5, which refer to very poor mast, poor mast, moderate mast, good mast, and full mast, respectively [65]. We used the MASTREE database [65] to obtain masting data for the European beech and Norway spruce for the canton of Neuchâtel for the years of our study. These two species account for 57.1% of the trees at our study location.

Statistical methods

The years 2004 and 2005 were excluded from the statistical analysis because they had missing data for the RLB time lag and for the field-collected climate variables with a time lag of 1 and 2 years prior to tick collection. For this reason, the statistical analyses in the main manuscript are restricted to a 13-year period (2006–2018).

Annual cumulative nymph density (CND) is the annual density of nymphs (DON)

The cumulative nymph density (CND) is an estimate of the total annual abundance of questing nymphs per 100 m^2 and was estimated by integrating the area under the curve (AUC) of the monthly questing nymph densities for each year [55, 66]. We used this AUC approach because it is less likely to be biased by missing data (i.e., for the snow days) compared to calculating a simple average for each year. The interpretation of the CND is the theoretical number of questing nymphs per 100 m^2 that

would have been collected if we had sampled ticks daily over the course of a year (as estimated from 12 monthly sampling occasions). If the CND is divided by 365, we obtain the mean daily number of nymphs collected per 100 m^2 (for details, see Additional file 1: Section 2). We assume that the CND represents a small unknown fraction of the density of nymphs that was present in the area. In summary, tick abundance data from 740 monthly transects (and 3,427 individual drags) were collapsed into 60 estimates of CND (15 years × 4 elevations = 60 annual estimates of abundance). The same approach was used to calculate the cumulative adult density (CAD). We previously analyzed the climate variables and ecological variables that influence inter-annual variation in the CND and the CAD at our study location [54]. For consistency with other studies, we will hereafter refer to the CND and the CAD as the DON and the density of adult ticks (DOA), respectively.

Annual nymphal infection prevalence (NIP)

Nymphs that tested negative or positive on the RLB were defined as being uninfected or infected with *B. burgdorferi* s.l., respectively. The nymph infection status is a binomial variable (uninfected and infected nymphs were coded as 0 and 1, respectively) that was used to calculate the annual NIP, which is the percentage of nymphs infected with *B. burgdorferi* s.l. for a given combination of elevation site and year. The same approach was used to calculate the adult infection prevalence (AIP).

Annual density of infected nymphs (DIN)

The annual DIN is a measure of the total annual abundance of questing infected nymphs per 100 m^2 and was estimated by multiplying our annual estimates of the DON by our annual estimates of the NIP (separately for each of the four elevation sites). The interpretation of the DIN is the theoretical number of questing infected nymphs per 100 m^2 that would have been collected if we had sampled ticks daily over the course of a year. The same approach was used to calculate the annual density of infected adults (DIA); we multiplied the DOA by the AIP (separately for each of the four elevation sites).

Annual mean climate variables

To investigate the relationship between climate and the NIP and DIN, we collapsed our monthly or daily weather data into a set of annual means. For the field-collected data, the annual means were calculated over the 12 measurements (i.e., a single measurement for each month). For the weather station data, the annual means were calculated over 365 daily means (i.e., a total of 365 days × 24 measurements/day = 8760 hourly measurements). Thus, the weather station annual means were based on 730 times more data than the field-collected annual means. However, an important advantage of the field-collected data was that they were specific for each of the four elevation sites. In contrast, the Climap-net data came from two weather stations that were located at some distance from the four elevation sites. To facilitate comparison between the slopes of the climate variables, we standardized the climate variables to Z scores (mean of zero and a standard deviation of 1).

Annual tree masting variables

Previous studies [35, 53, 54] have shown that there is a 2-year time lag between masting events and the DON and a 3-year time lag between masting events and the DOA. Our recent analysis of tick abundance at our study location showed that inter-annual variation in the DON and the DOA was strongly associated with the mast scores of European beech trees but not Norway spruce [54]. Taken together, these studies validate our decision to model the DIN and DIA as a function of the European beech mast scores 2 years previously (year $y-2$) and 3 years previously (year $y-3$), respectively. For example, we expect that beech mast scores from the year 2001 predict the DIN in year 2003 (2 years later) and the DIA in year 2004 (3 years later). The same approach was used to model the NIP and the AIP.

RLB time lag

As mentioned in the molecular methods, there was considerable variation in the RLB time lag (range: 4–5025 days), which is the time interval between the date of tick collection (and tick DNA extraction) *versus* the date of the RLB. The ammonium hydroxide solution used to extract the whole tick DNA is not optimal for long-term DNA storage, and we were concerned that the DNA would degrade over time and that our ability to detect *B. burgdorferi* s.l. would decrease with the duration of the RLB time lag. We therefore included the RLB time lag as an explanatory variable (standardized to a Z score) in our statistical analyses. As information on the RLB time lag was missing for the first 2 years of our study (2004 and 2005), we excluded these years from our statistical analyses.

Analysis of NIP

The NIP was modeled using generalized linear mixed effects models (GLMMs) with binomial errors. The fixed effects structure included elevation site (4 levels: low, medium, high, top), the covariate year (rescaled as 1, 2, 3, … 15), the covariate beech mast score 2 years prior (range: 1–5), the covariate DIN in the previous year, the

covariate RLB time lag, and the mean annual climate variables of temperature, relative humidity, SD and precipitation (standardized to Z scores). As time lags are important in tick ecology, we modeled the NIP as a function of the mean climate variables in the present year, the previous year or 2 years prior. As we did not measure the field-collected climate variables in the 2 years prior to the start of our study (e.g., 2002 and 2003), we had to exclude the years 2004 and 2005 from our statistical analysis. The unique identification number for the 720 transects was included as a random factor. We analyzed the NIP at the transect level ($n=4$ sites*180 transects = 720 transects) rather than at the year level ($n=4$ sites*15 years = 60 years) because this approach avoids overdispersion (i.e., by including the transect as a random effect). Overdispersion can be handled by introducing a quasibinomial error function, but this solution cannot be combined with Akaike information criterion (AIC)-based model selection, which is our preferred method for identifying the best model. The same approach was used to model the AIP. All the acronyms of the variables can be found in Table 1.

Analysis of the DIN

Count data follow a Poisson distribution and aggregated count data follow a negative binomial distribution. In our previous analysis of the DON, we found that generalized linear models with negative binomial errors gave the same results as linear models with normal errors [54]. The reason for this is because our estimates of the DON and the DIN (or DOA and DIA) are summary statistics of counts (integrals based on the counts of 12 monthly transects), which follow a normal distribution according to the central limit theorem of statistics. For simplicity, we therefore assumed that the residuals of our DIN values follow a normal distribution; these values were log10-transformed to further improve their fit to the normal distribution. In summary, the log10-transformed DIN values were analyzed using linear models (LMs) using the same explanatory variables as the NIP. The same approach was used to model the DIA. All the acronyms of the variables can be found in Table 1.

AIC-based model selection approach

To identify the best model, we used a model selection approach based on the AIC. Models were ranked according to their AIC values and the Akaike weights, which indicate the percentage support, were calculated for each model. We used the Akaike weights to calculate the model-averaged parameter estimates and their 95% confidence intervals (CIs). For the GLMMs that analyzed the NIP and AIP, we assessed the goodness of fit of the binomial distribution for the best model from the model selection table. For the LMs that analyzed the DIN and DIA, the assumptions of normally distributed residuals and equal variances were assessed for the best model from the model selection table (Additional file 1: Section 3).

We used R version 4.0.3 for all statistical analyses [67]. We used the *lm()* function in the base package to run the LMs with normal errors. We used the *glmer()* function in the lme4 package to run the GLMMs with binomial errors. We used the *mod.sel()* function and the *model.av()* function in the MuMIn package to create the model selection tables and the model-averaged parameter estimates. The raw data used for these statistical analyses can be found in Additional file 2: Table S1.

Results

Overview of the statistical analyses

For brevity, we present the analyses of the NIP and DIN. The analyses of the AIP and the DIA are presented in Additional file 1: Section 4.

Prevalence of *B. burgdorferi* s.l. infection in *I. ricinus*

Over the 15 years of the study and at the four elevation sites, we tested a total of 13,076 *I. ricinus* ticks for infection with *B. burgdorferi* s.l.: 7940 nymphs and 5136 adult ticks (2572 males and 2564 females). The infection prevalence of *B. burgdorferi* s.l. was 15.1% for all ticks (1975/13,076), 12.8% for nymphs (1014/7940) and 18.8% for adult ticks (964/5136), with a similar infection prevalence between males (18.3%; 471/2572) and females (19.1%; 490/2564). The *B. burgdorferi* s.l. genospecies detected in this study (ranked from most common to least common) were: *B. afzelii* (35.6%; 703/1975), *B. garinii* (26.0%; 513/1975), *B. valaisiana* (13.5%; 267/1975), *B. burgdorferi* s.s. (11.0%; 218/1975), *B. bavariensis* (1.2%; 23/1975) and *B. lusitaniae* (0.2%; 3/1975). Another 108 ticks were infected with *B. miyamotoi* (5.5%; 108/1975) while 109 *Borrelia* infections (5.5%; 109/1975) could not be identified to genospecies.

Mixed infections with two or three *Borrelia* genospecies were detected in 6.8% and 0.2% of the infected ticks tested in this study, respectively. Ranked from most common to least common, the *Borrelia* genospecies mixed infections were: *B. garinii* and *B. valaisiana* (3.3%; 65/1975), *B. afzelii* and *B. burgdorferi* s.s. (2.3%; 46/1975), *B. afzelii* and *B. garinii* (0.7%; 13/1975), *B. garinii* and *B. burgdorferi* s.s. (0.2%; 4/1975), *B. afzelii* and *B. valaisiana* (0.1%; 2/1975), *B. afzelii*, *B. burgdorferi* s.s., and *B. miyamotoi* (0.1%; 2/1975), *B. afzelii* and undefined genospecies (<0.1%; 1/1975), *B. afzelii*, *B. burgdorferi* s.s. and *B. garinii* (<0.1%; 1/1975), *B. afzelii*, *B. burgdorferi* s.s. and *B. valaisiana* (<0.1%; 1/1975), *B. bavariensis* and *B.*

Table 1 Acronyms and definitions of the variables used in the present study

Acronym	Description
DIN	Annual density of infected *I. ricinus* nymphs per 100 m^2
NIP	Annual nymphal infection prevalence (% of *I. ricinus* nymphs infected with *B. burgdorferi* s.l.)
S	Site name (categorical factor with 4 levels: low, medium, high, top)
Y	Year of the study (covariate: 1, 2, …, 15)
B	Beech mast score in year $y-2$ (covariate: 1, 2, 3, 4, 5)
RLB	Time lag between tick sampling and the RLB procedure (days)
DIN_{y-1}	Annual density of infected nymphs in year $y-1$ per 100 m^2
T1	Mean temperature in year *y* from the weather station data (°C)
$T1_{y-1}$	Mean temperature in year $y-1$ from the weather station data (°C)
$T1_{y-2}$	Mean temperature in year $y-2$ from the weather station data (°C)
RH1	Mean relative humidity in year *y* from the weather station data (%)
$RH1_{y-1}$	Mean relative humidity in year $y-1$ from the weather station data (%)
$RH1_{y-2}$	Mean relative humidity in year $y-2$ from the weather station data (%)
SD1	Mean saturation deficit in year *y* from the weather station data (mmHg)
$SD1_{y-1}$	Mean saturation deficit in year $y-1$ from the weather station data (mmHg)
$SD1_{y-2}$	Mean saturation deficit in year $y-2$ from the weather station data (mmHg)
PR1	Mean precipitation in year *y* from the weather station data (mm)
$PR1_{y-1}$	Mean precipitation in year $y-1$ from the weather station data (mm)
$PR1_{y-2}$	Mean precipitation in year $y-2$ from the weather station data (mm)
T2	Mean temperature in year *y* from the field-collected data (°C)
$T2_{y-1}$	Mean temperature in year $y-1$ from the field-collected data (°C)
$T2_{y-2}$	Mean temperature in year $y-2$ from the field-collected data (°C)
RH2	Mean relative humidity in year *y* from the field-collected data (%)
$RH2_{y-1}$	Mean relative humidity in year $y-1$ from the field-collected data (%)
$RH2_{y-2}$	Mean relative humidity in year $y-2$ from the field-collected data (%)
SD2	Mean saturation deficit in year *y* from the field-collected data (mmHg)
$SD2_{y-1}$	Mean saturation deficit in year $y-1$ from the field-collected data (mmHg)
$SD2_{y-2}$	Mean saturation deficit in year $y-2$ from the field-collected data (mmHg)

valaisiana (< 0.1%; 1/1975), *B. bavariensis* and *B. lusitaniae* (< 0.1%; 1/1975) and *B. burgdorferi* s.s. and *B. valaisiana* (< 0.1%; 1/1975).

Mean NIP at each of the four elevation sites

The mean NIP for the four elevation sites ranged from 10.8% to 15.3% and are shown in Fig. 1 and Table 2. Importantly, these mean estimates of the NIP do not consider the effects of any other explanatory variables.

Model selection analysis of the NIP

The full model selection table for all 232 models is presented in Additional file 1: Section 5. For the NIP, the best two models had a combined support of 94.0% (Table 3). These two models each had 47.0% of the support (Weight1 in Table 3) and contained the explanatory variables of year (Y), RLB time lag (RLB), and weather station mean annual precipitation in the present year (PR). The only difference between these two models was that the second model contained elevation site (S), whereas the first model did not (Table 3).

For the individual explanatory variables, there was strong support for RLB time lag (100.0%), year (100.0%) and weather station mean annual precipitation in the present year (PR; 93.8%), moderate support for site (48.2%), and low support for weather station mean annual relative humidity in the present year (RH1; 5.7%; Table 4). None of the other explanatory variables had a support > 1.0% (Additional file 1: Section 5).

Model-averaged parameter estimates for the NIP

To determine the direction and statistical significance of the explanatory variables on the NIP, we present the model-averaged parameter estimates (and their 95% CIs) on the logit scale (Additional file 1: Section 5). We also back-calculated the effect sizes of the explanatory variables on the NIP on the original scale with respect to the following reference conditions: the site was low elevation,

the year was 2006, and the covariates of RLB time lag and weather station precipitation in the present year were set to 0 (i.e., the mean values on the *Z* score scale).

The NIP was significantly different between the four elevation sites (Fig. 1; Additional file 1: Section 5). Compared to the low elevation site, the NIP was 13.4% lower at the medium (Medium–Low contrast = −0.195, 95% CI = −0.467 to 0.077), 23.6% lower at the high (High–Low contrast = −0.358, 95% CI = −0.653 to −0.063) and 9.4% lower at the top (Top–Low contrast = −0.135, 95% CI = −0.481 to 0.211) elevation site. Year had a negative and significant effect (slope = −0.145 per year, 95% CI = −0.181 to −0.108), indicating that the NIP was decreasing over time at Chaumont Mountain (Figs. 2, 3). Over the 13-year period of the study (2006–2018), the NIP on the original scale decreased by 77.1% to 78.6% at the four elevation sites (Figs. 2, 3). The RLB time lag had a negative and significant effect on the NIP (Fig. 4; slope = −0.184 per standard deviation, 95% CI = −0.285 to −0.083). Increasing the RLB time lag by one standard deviation (e.g., 881 days) decreased the NIP on the original scale by 12.6%–13.6% at the four elevation sites (Fig. 4). The weather station mean annual precipitation in the present year had a negative and significant effect on the NIP (Fig. 5; slope = −0.311 per standard deviation, 95% CI = −0.447 to −0.174). Increasing the weather station mean annual precipitation in the present year by one standard deviation (e.g., 0.5 mm of precipitation) decreased the NIP on the original scale by 22.4%–24.0% at the four elevation sites (Fig. 5). In summary, the explanatory variables of year, RLB time lag, and precipitation in the same year all had significant negative effects on the NIP.

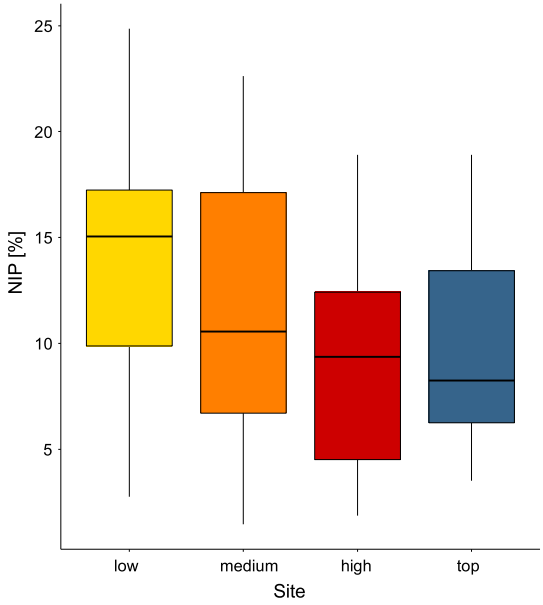

Fig. 1 Boxplot of the effect of elevation site on the nymphal infection prevalence (*NIP*), which is the percentage of *I. ricinus* nymphs infected with *B. burgdorferi* s.l.. For each of the four elevation sites, the NIP values are shown for the 15 years of the study (2004–2018). Compared to the low elevation site, the NIP was 13.4%, 23.6%, and 9.4% lower at the medium, high, and top elevation sites, respectively. The boxplots show the median (black line), 25th and 75th percentiles (edges of the box), and minimum and maximum values (whiskers)

Mean DIN at each of the four elevation sites

The mean DIN was inversely related to the altitudinal gradient; it was highest at the low elevation site and lowest at the top elevation site (Table 2; Fig. 6). If the low elevation site is set as the reference, the mean DIN at the medium, high, and top elevation sites were 40.2%, 66.9%, and 91.7% lower, respectively (Fig. 6). Importantly, these mean estimates of the DIN do not consider the effects of any other explanatory variables.

Model selection analysis of the DIN

The full model selection analysis with 314 models is presented in Additional file 1: Section 6. For the DIN, the top three models had a combined support of 80.0% (Weight 2 in Table 5). The best model had 47.0% of the support (Table 5), explained 82.5% of the variation in the DIN and contained the explanatory variables of elevation site (S; partial $r^2 = 28.3\%$), year (Y; partial $r^2 = 14.8\%$), site:year interaction (S:Y; partial $r^2 = 4.2\%$), beech mast score 2 years prior (B; partial $r^2 = 5.8\%$), and weather station mean annual relative humidity in the present year (RH1; partial $r^2 = 6.1\%$).

The support for the individual explanatory variables was as follows (Table 6): site (100.0%), year (100.0%), site:year interaction (92.0%), beech mast score 2 years prior (69.1%), weather station mean annual relative humidity in the present year (RH1; 50.8%), RLB time lag (31.2%), weather station mean annual precipitation in the previous year (PR_{y-1}; 20.0%), and weather station mean annual saturation deficit in the present year (SD1; 16.1%). None of the other explanatory variables had a support > 2.5% (Additional file 1: Section 6).

Model-averaged parameter estimates for the DIN

To determine the effects of the explanatory variables on the DIN, we present the model-averaged parameter estimates on the log10-transformed scale (Additional file 1: Section 6). We also back-calculated the effect sizes of the explanatory variables on the DIN on the original scale with respect to the following reference conditions: the

Table 2 Mean NIP and mean DIN for the four elevation sites on Chaumont Mountain

Site	NIP[a] (%)	NIP 95% CI	DIN1[b]	DIN1 95% CI	DIN2[b]	DIN2 95% CI
Low	15.3	15.0–15.6	2969	1882–4684	8.1	5.2–12.8
Medium	11.9	11.6–12.2	1775	1125–2800	4.9	3.1–7.7
High	10.8	10.4–11.1	983	623–1552	2.7	1.7–4.3
Top	12.7	12.3–13.1	246	156–388	0.7	0.4–1.1

Values in Table 2 are presented as the means and their 95% confidence intervals (CIs). These means and 95% CIs were calculated from linear models that only contained the explanatory factor of elevation site.

[a] The NIP is the percentage of *I. ricinus* nymphs infected with *B. burgdorferi* s.l..

[b] The DIN is the number of questing *B. burgdorferi* s.l.-infected *I. ricinus* nymphs per 100 m^2. The DIN is given as the total for the whole year (DIN1) or the daily average (DIN2). DIN1 is calculated by multiplying the DON by the NIP. DIN2 is calculated by dividing the DIN1 by 365 days.

Table 3 Model selection results for the generalized linear mixed effects models of the NIP

Rank	Model structure	*df*	logLik	AIC	ΔAIC	Weight1	Weight2
1	NIP ~ *Y* + RLB + PR	5	−2363.1	4736.2	0.0	47.0	47.0
2	NIP ~ *Y* + RLB + PR + S	8	−2360.1	4736.2	0.0	47.0	94.0
3	NIP ~ *Y* + RLB + RH1	5	−2365.4	4740.8	4.6	5.0	99.0

Model selection results are shown for the generalized linear mixed effects models (GLMMs) with binomial errors of the NIP response variable. The explanatory variables were site, year, beech masting index 2 years prior, DIN from the previous year, RLB time lag, and the climate variables obtained from the weather stations and the field. The models are ranked according to their Akaike information criterion (AIC). Of the 232 models in the set, only the 3 top models are shown for which the cumulative support (Weight2) > 99.0%. Shown for each model are the model rank (Rank), model structure (see Table 1 for the acronyms of the explanatory variables), model degrees of freedom (*df*), log-likelihood (logLik), AIC, difference in the AIC value from the top model (ΔAIC), model weight (Weight1), and cumulative model weight (Weight2). The results from the full model selection are shown in Additional file 1: Section 5

Table 4 Support for the five most important explanatory variables of the NIP

Rank	Explanatory variable of interest	Support (%)
1	RLB	100.0
2	Year	100.0
3	PR	93.8
4	Site	48.2
5	RH1	5.7

The support for the 5 most important explanatory variables is shown from the AIC-based model selection table of the NIP. This support is calculated as the sum of the Akaike weights for all the models in the set that include that particular explanatory variable (see Table 1 for the acronyms of the explanatory variables). Additional file 1: Section 5 shows the results for all the explanatory variables.

site was low elevation, the year was 2006, the beech mast score 2 years prior was set to 1 and the other covariates were set to 0 (i.e., the mean values on the *Z* score scale).

The interaction between site and year indicated that the change in the DIN over time differed between the four elevation sites (Fig. 7; Additional file 1: Section 6). Over the 13-year period (2006–2018), the DIN decreased at the low (slope = −0.018 per year, 95% CI = −0.059 to 0.023), medium (Medium–Low contrast of the slope = −0.023, 95% CI = −0.072 to 0.027), high (High–Low contrast of the slope = −0.027, 95% CI = −0.076 to 0.023) and top (Top–Low contrast of the slope = −0.088, 95% CI = −0.138 to −0.037) elevation site. Over the 13-year period (2006–2018), the DIN decreased by 38.7%, 67.2%, 70.7%, and 94.6% at the low, medium, high, and top elevation sites, respectively (Fig. 7). Due to the significant interaction between site and year, it does not make sense to interpret the differences in intercept between the four elevation sites (Fig. 7; Additional file 1: Section 6).

The beech mast score 2 years prior had a positive and significant effect on the DIN (slope = 0.067 per class; 95%CI = 0.029 to 0.105; Figs. 8, 9). Increasing the beech mast score 2 years prior from 1 (poor mast) to 5 (full mast) increased the DIN by 85.5% at each of the four elevation sites on Chaumont Mountain (Fig. 9). The weather station mean annual relative humidity in the present year had a negative and significant effect on the DIN (Fig. 10; slope = −0.166 per standard deviation, 95% CI = −0.253 to −0.079). Increasing the weather station mean annual relative humidity in the present year by one standard deviation (1.8% of relative humidity) decreased the DIN by 31.8% at each of the four elevation sites on Chaumont Mountain (Fig. 10).

Other models contained other explanatory variables that had the following effects on the DIN. The RLB time lag had a negative and significant effect on the DIN (slope = −0.131 per standard deviation, 95% CI = −0.215 to −0.047; Additional file 1: Section 6). The weather station mean annual precipitation in the

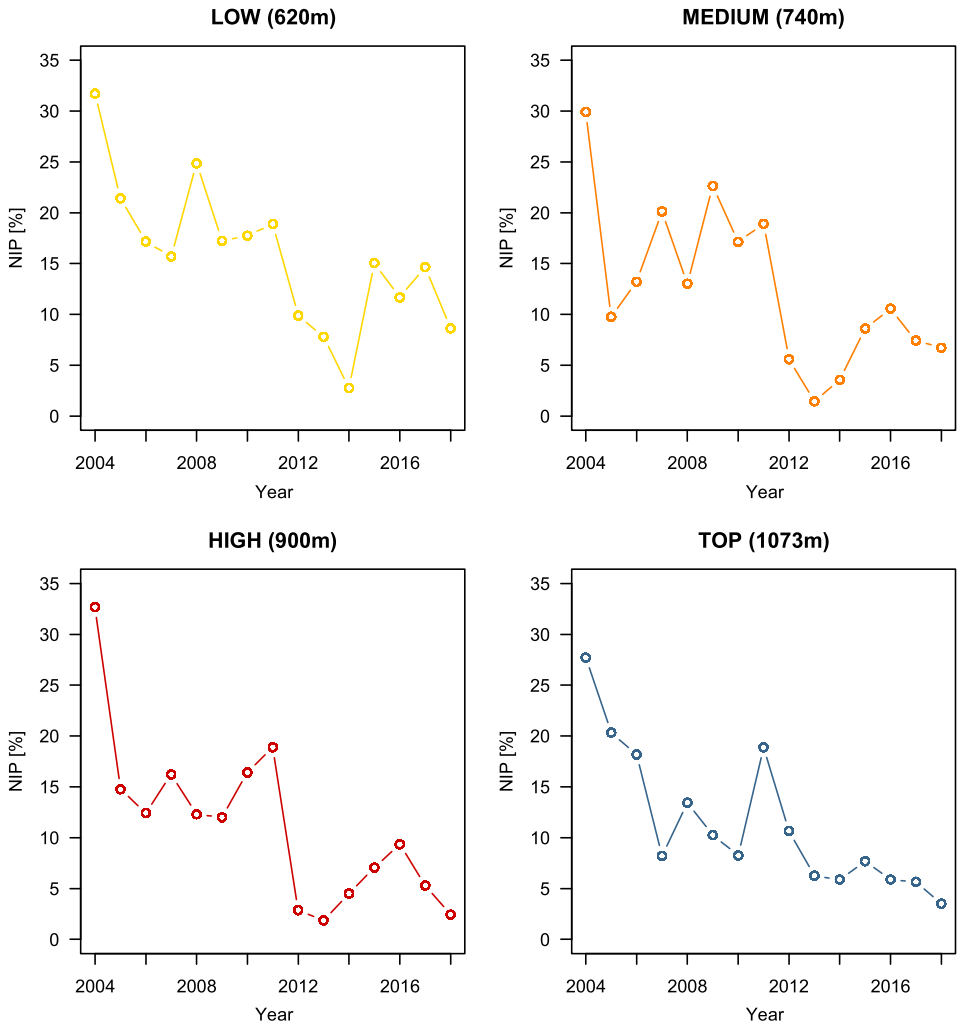

Fig. 2 Decrease in the NIP over the 15 years of the study (2004–2018) for each of the four elevation sites on Chaumont Mountain. Each estimate of the NIP is based on a maximum of 240 nymphs (12 months × 20 nymphs per month)

previous year had a negative and significant effect on the DIN (slope = −0.108 per standard deviation, 95% CI = −0.183 to −0.033; Additional file 1: Section 6). The weather station mean annual saturation deficit in the present year had a positive and significant effect on the DIN (slope = 0.205 per standard deviation, 95% CI = 0.079 to 0.330; Additional file 1: Section 6).

In summary, the DIN decreased over time at the four elevation sites and significantly so at the top elevation site. The DIN increased significantly with tree seed production 2 years prior and decreased significantly with the relative humidity in the present year.

Discussion

Forecasting exposure risk is an important strategy for preventing the spread of tick-borne diseases. In Europe and North America, there is much interest to determine which ecological factors are influencing the abundance of *Ixodes* ticks and their associated pathogens. To address this question, we measured the abundance of *I. ricinus* ticks infected with *B. burgdorferi* s.l. over a period of 15 years in an area of Switzerland where Lyme borreliosis is endemic. The NIP decreased on average by 77.8% over the 13-year study period at the four elevation sites. The inter-annual variation in the NIP was best explained by year, time

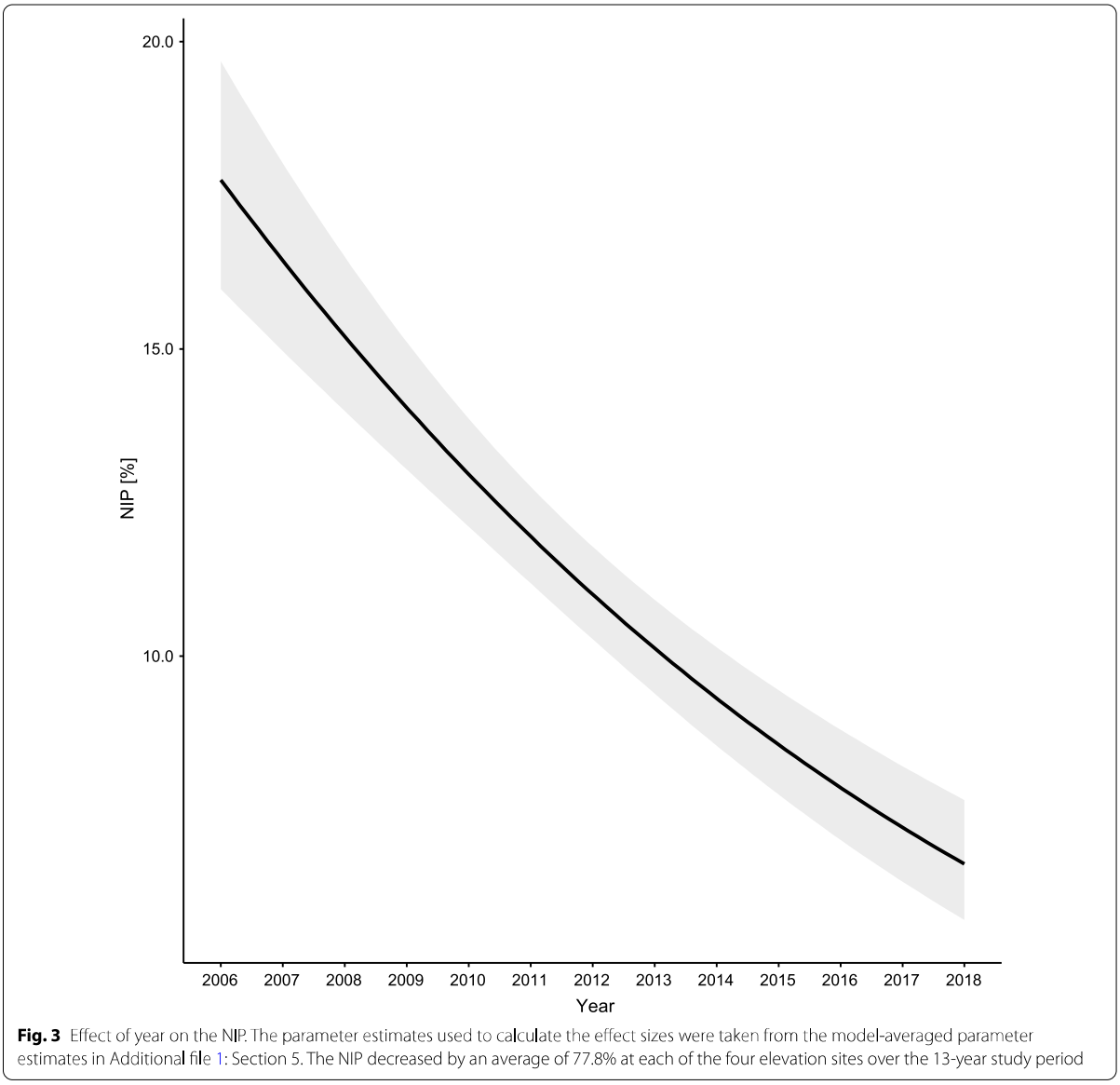

Fig. 3 Effect of year on the NIP. The parameter estimates used to calculate the effect sizes were taken from the model-averaged parameter estimates in Additional file 1: Section 5. The NIP decreased by an average of 77.8% at each of the four elevation sites over the 13-year study period

lag between tick sampling and pathogen detection (the RLB time lag), and the mean annual precipitation in the present year. The DIN decreased over the 13-year study period at all four elevation sites, but the decrease was only significant at the top elevation. The inter-annual variation in the DIN was best explained by site, year, site:year interaction, abundance of beech tree seeds 2 years prior, and the mean annual relative humidity in the present year.

As the DIN is the product of the DON and the NIP, we expect that the factors driving the DON and the NIP should also drive the DIN [31, 35]. Using the data from the present study, we had previously shown that elevation site, year, beech masting 2 years prior, and mean annual relative humidity in the present year were the ecological factors that influenced inter-annual variation in the DON [54], and these same four factors also influenced inter-annual variation in the DIN in the present study. Similarly, year, RLB time lag, and mean annual precipitation in the present year influenced both the NIP and the DIN (although these explanatory variables were not in the top model for the DIN). The explanatory variable of year had a positive effect on the DON, but a negative effect on the NIP,

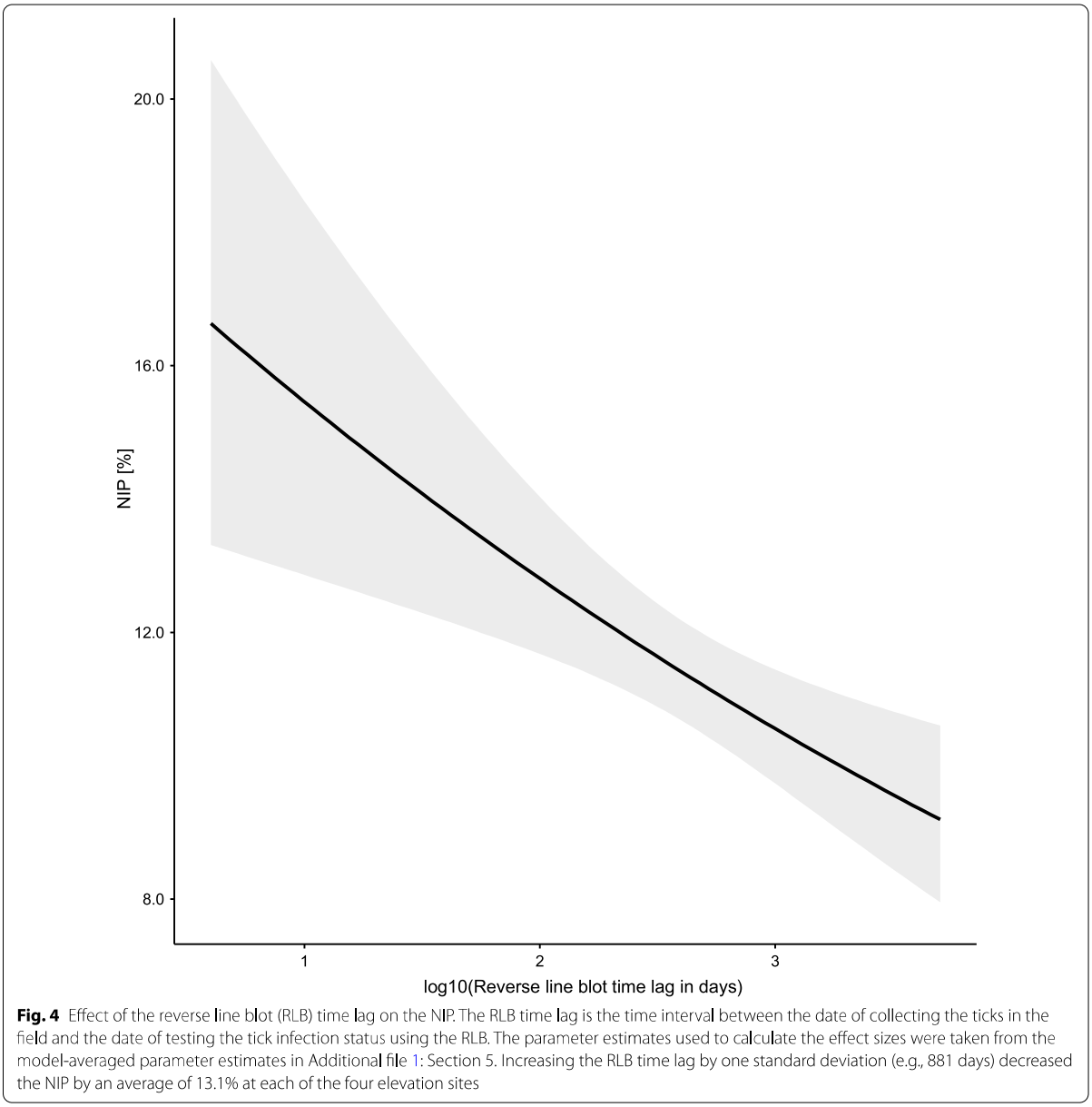

Fig. 4 Effect of the reverse line blot (RLB) time lag on the NIP. The RLB time lag is the time interval between the date of collecting the ticks in the field and the date of testing the tick infection status using the RLB. The parameter estimates used to calculate the effect sizes were taken from the model-averaged parameter estimates in Additional file 1: Section 5. Increasing the RLB time lag by one standard deviation (e.g., 881 days) decreased the NIP by an average of 13.1% at each of the four elevation sites

and these two opposing effects resulted in a net negative effect of year on the DIN at the low, medium, and high elevation sites that was not significant. At the top elevation site, the DON, NIP, and DIN all decreased dramatically over the study period. Other explanatory variables, such as beech masting 2 years prior and relative humidity, are important for the DON but not for the NIP, and *vice versa* for the RLB time lag and precipitation. The effects of these explanatory variables on the DIN were therefore reduced.

One of the most important results of this study is our demonstration of a strong and positive association between seed production by beech trees 2 years prior and the DIN. We had previously shown using the same data from the present study that the beech masting index 2 years prior was highly significantly associated with inter-annual variation in the DON [54]. The discovery that masting events can drive inter-annual variation in the DON and DIN of *Ixodes* nymphs with a 2-year time lag was first made in North America [35,

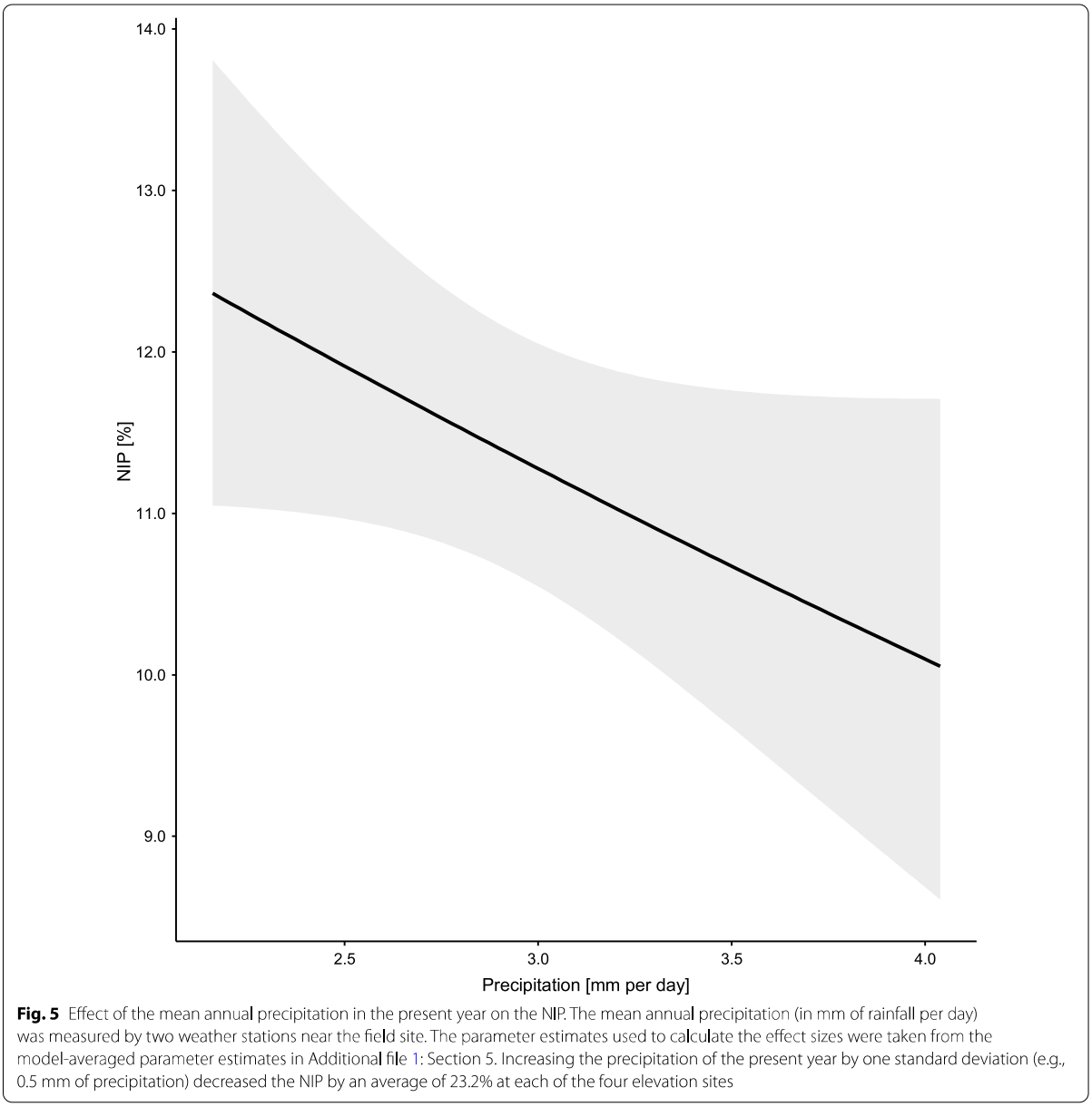

Fig. 5 Effect of the mean annual precipitation in the present year on the NIP. The mean annual precipitation (in mm of rainfall per day) was measured by two weather stations near the field site. The parameter estimates used to calculate the effect sizes were taken from the model-averaged parameter estimates in Additional file 1: Section 5. Increasing the precipitation of the present year by one standard deviation (e.g., 0.5 mm of precipitation) decreased the NIP by an average of 23.2% at each of the four elevation sites

50, 51]. The chain of causality is as follows: mast seeding in year y increases the abundance of small mammals, deer, and larval ticks in year $y+1$ [35, 44, 51, 68–74]. Higher densities of larval ticks feed on higher densities of small mammals in year $y+1$, which in turn increases the abundance of nymphs in year $y+2$ [35, 36, 50–52, 75, 76].

In Europe, there is a growing body of evidence that masting events of deciduous trees influence the DIN of *I. ricinus* ticks. A 9-year study in Germany found a 2-year time lag between the masting of European beech trees (*Fagus sylvatica*) and the DON, but did not measure the DIN [53]. A 7-year study in Poland found a 2-year time lag between the masting of oak trees and the incidence of Lyme borreliosis in human patients, but this study did not measure tick abundance [77]. An 18-year study in central Europe found the expected 1-year time lag between rodent

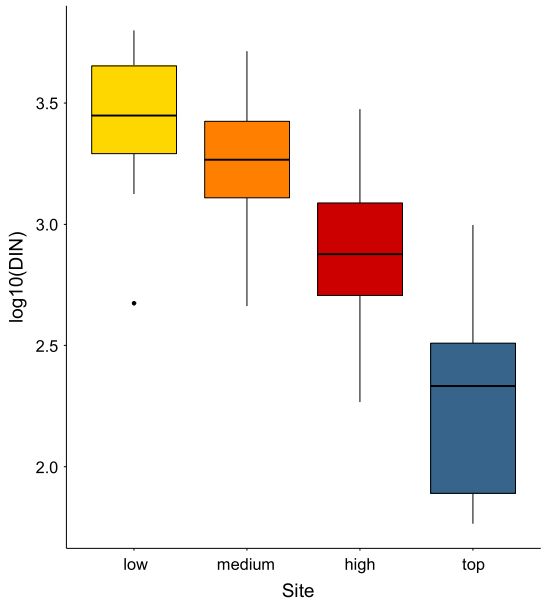

Fig. 6 Boxplot of the effect of elevation on the density of infected nymphs (*DIN*). The DIN is the annual estimate of the number of infected questing *I. ricinus* nymphs per 100 m^2 sampled by the dragging method. For each of the four elevation sites, the DIN values are shown for the 15 years of the study (2004–2018). Compared to the low elevation site, the mean DIN at the medium, high, and top elevation sites were 40.2%, 66.9%, and 91.7% lower, respectively. The boxplots show the median (black line), 25th and 75th percentiles (edges of the box), minimum and maximum values (whiskers), and outliers (solid circles)

densities and the incidence of tick-borne diseases in human patients, but this study did not measure tick abundance or tree seed production [78]. A 3-year study in the Netherlands found a strong correlation between masting in year y and rodent densities in year $y+1$, and between rodent densities in year $y+1$ and the DIN in year $y+2$, but this study did not find any correlation between mast seeding in year y and the DIN in year $y+2$ [36]. Thus, our long-term study is the first demonstration in Europe that masting events of deciduous trees are strongly associated with the inter-annual variation of the DIN of *I. ricinus* with the expected 2-year time lag. In summary, seed production by beech trees determines the human risk of Lyme disease 2 years later.

Masting by beech trees did not influence the NIP, and this result is both in agreement and in conflict with previous studies [35, 51]. The effects of masting and rodent density on the NIP are complex and counterintuitive. Theoretical models have shown that the R_0 of tick-borne diseases depends on the ratio of nymphs to hosts [43] and on the aggregation of immature ticks on the same host, which ensures horizontal transmission of *B. burgdorferi* s.l. from infected nymphs to uninfected larvae [42]. In the year following a masting event, the rodent host population is expected to increase dramatically, but the density of infected nymphs that will feed on those rodents was determined by the conditions in the previous year (i.e., the year of the masting event when the rodent

Table 5 Model selection results for the linear models of the DIN

Rank	Model structure	*df*	logLik	AIC	ΔAIC	Weight1	Weight2	r^2
1	DIN ~ S + *Y* + *B* + RH1 + S:*Y*	11	8.1	12.3	0.0	47.0	47.0	82.5
2	DIN ~ S + *Y* + RLB + PR_{y-1} + S:*Y*	11	7.2	14.2	1.8	19.0	66.0	81.9
3	DIN ~ S + *Y* + *B* + SD1 + S:*Y*	11	6.9	14.8	2.5	14.0	80.0	81.7
4	DIN ~ S + *Y* + *B* + RH1	8	0.7	17.9	5.6	3.0	83.0	78.3
5	DIN ~ S + *Y* + *B* + S:*Y*	11	4.9	18.8	6.5	2.0	85.0	80.2
6	DIN ~ *Y* + *B* + SD1	8	0.2	19.0	6.7	2.0	87.0	77.9
7	DIN ~ S + *Y* + RLB + $T1_{y-1}$ + S:*Y*	11	4.6	19.3	7.0	1.0	88.0	80.0
8	DIN ~ S + *Y* + RLB + PR + S:*Y*	11	4.1	20.3	8.0	1.0	89.0	79.6
9	DIN ~ S + *Y* + RLB + $RH1_{y-1}$ + S:*Y*	11	4.1	20.4	8.1	1.0	90.0	79.6
10	DIN ~ S + *Y* + RLB + S:*Y*	10	2.3	20.7	8.4	1.0	91.0	78.7
11	DIN ~ S + *Y* + RLB + SD1 + S:*Y*	11	3.9	20.8	8.4	1.0	92.0	79.5
12	DIN ~ S + *Y* + RLB + $T1_{y-2}$	11	3.8	21.0	8.7	1.0	93.0	79.4
13	DIN ~ S + *Y* + RLB + S:*Y* + S:RLB	13	7.2	21.1	8.8	1.0	94.0	81.0
14	DIN ~ S + *Y* + RLB + RH1 + S:*Y*	11	3.6	21.3	9.0	1.0	95.0	79.2

Model selection results are shown for the linear models (LMs) with normal errors of the log10-transformed DIN response variable. The explanatory variables were site, year, beech masting index 2 years prior, RLB time lag, and the climate variables obtained from the weather stations and the field. The models are ranked according to their AIC. Of the 314 models in the set, only the 14 top models are shown for which the cumulative support (Weight2) is 95%. Shown for each model are the model rank (Rank), model structure (see Table 1 for the acronyms of the explanatory variables), model degrees of freedom (df), log-likelihood (logLik), AIC, difference in the AIC value from the top model (ΔAIC), model weight (Weight1), cumulative model weight (Weight2), and adjusted *r*-squared value (r^2). The results from the full model selection are shown in Additional file 1: Section 6

Table 6 Support for the 11 most important explanatory variables of the DIN

Rank	Explanatory variable of interest	Support (%)
1	Site	100.0
2	Year	100.0
3	Site:year	92.0
4	Beech mast score 2 years prior	69.1
5	RH1	50.8
6	RLB	31.2
7	PR_{y-1}	20.0
8	SD1	16.1
9	T2	2.5
10	$T1_{y-1}$	1.7
11	PR	1.2

The support for the 11 most important explanatory variables is shown from the AIC-based model selection table of the DIN. This support is calculated as the sum of the Akaike weights for all the models in the set that include that particular explanatory variable. Additional file 1: Section 6 shows the results for all the explanatory variables

density was 'normal'). Field studies have shown that when the rodent density increases relative to the density of immature ticks, the mean burden of ticks on rodent hosts decreases [75, 79, 80], which reduces horizontal transmission of *B. burgdorferi* s.l. between nymphs and larvae. Thus, masting in year y will decrease the ratio of infected nymphs to hosts in year $y+1$ and it will decrease the aggregation of immature ticks on infected hosts in year $y+1$, and both effects are expected to reduce the NIP in year $y+2$ when the DON is expected to increase dramatically. However, if the proportional increase in the DON is larger than the proportional decrease in the NIP, the DIN is still expected to increase 2 years after a masting event.

An interesting result is that the mean annual relative humidity had a negative effect on the DIN, which is mediated by the negative effect of this variable on the DON [54]. This result contradicts the general wisdom that survival of immature *Ixodes* ticks increases with relative humidity [17, 37, 81]. However, this result is not without precedent, and other studies in Europe have found a negative relationship between moisture and the abundance of *I. ricinus* nymphs [82–86]. One explanation is that humid environments are favourable for the development of entomopathogenic fungi, which can cause high mortality in *Ixodes* ticks [87, 88]. An alternative explanation is that high levels of rainfall inhibit host-seeking activity or cause flooding that reduces tick survival [17, 35].

An unexpected result was that the mean annual precipitation in the same year had a negative effect on the NIP. Increasing the mean annual precipitation in the present year by one standard deviation (e.g., 0.5 mm of precipitation) decreased the NIP on the original scale by 22.4%–24.0%. Encounters between larval ticks and vertebrate reservoir hosts and acquisition of *B. burgdorferi* s.l. during the larval blood meal are the events that determine whether a questing nymph is infected with *B. burgdorferi* s.l. in the following year. For this reason, it is difficult to imagine how precipitation in the year when the nymphs are captured could influence the NIP. Studies on *Ixodes* nymphs collected in the field have suggested that infection with *B. burgdorferi* s.l. can influence their questing behaviour and survival [89–94]. Thus, possible explanations are that precipitation increases the survival and/or the capture success *via* dragging of uninfected nymphs relative to infected nymphs.

The DIN differed among the four elevation sites (620, 740, 900 and 1073 m a.s.l.) and was inversely related to the altitudinal gradient, which agrees with previous studies [55, 57]. A mechanistic explanation is that the duration of development from one stage to the next is inversely proportional to temperature [40, 95]. At higher and colder elevations, eggs and larvae have much slower development rates than at lower and warmer elevations, which ultimately reduces the number of eggs that reach the nymphal stage [39, 96, 97]. Thus, differences in climate between the four elevation sites are expected to drive variation in the vital rates (development, survival, reproduction), which ultimately determines the observed altitudinal differences in tick density, with the low elevation site having a much higher DIN and DON compared to the top elevation site.

At the top elevation site, the decrease in tick population size was very dramatic. One explanation is the construction of recreation facilities (i.e., mountain bike trails and an adventure park) at approximately 25 m from the top elevation site mid-way through the study. This destruction of the forest habitat and the subsequent increase in the number of human visitors to the top of Chaumont Mountain, as well as the associated disturbance to the wildlife reservoir hosts, may have caused the dramatic decline over time of the *I. ricinus* tick population at the top elevation site. An alternative explanation is that repeated tick sampling over a period of 15 years decreased the tick population at the top site [63]. Field studies

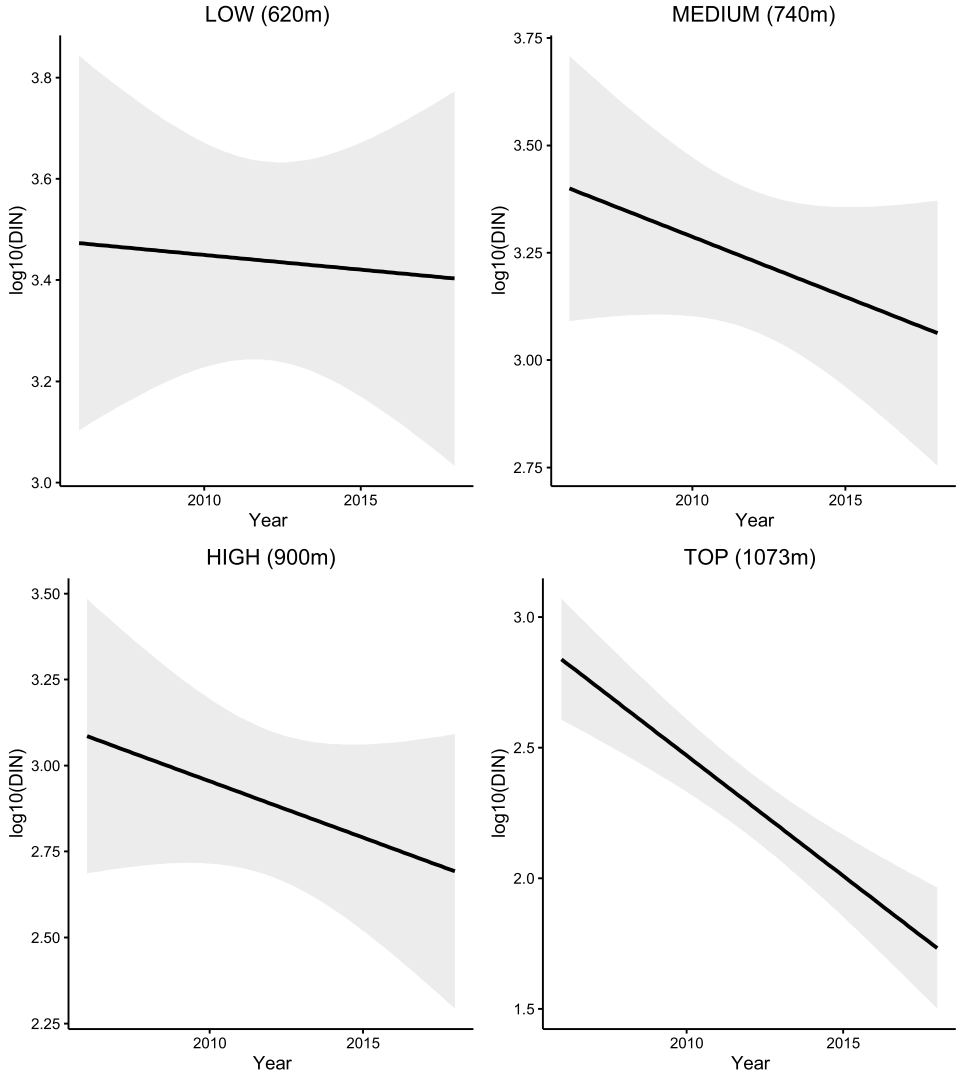

Fig. 7 Effect of year on the DIN. The parameter estimates used to calculate the effect sizes were taken from the model-averaged parameter estimates in Additional file 1: Section 6. The DIN decreased by 38.7%, 67.2%, 70.7%, and 94.6% at the low, medium, high, and top elevation sites, respectively, over the 13-year study period

typically assume that dragging removes a small fraction of the available tick population, but this assumption may not be true in habitats where tick density is already low.

The RLB time lag had a large negative effect on the NIP and a moderately negative effect on the DIN. We believe that the negative relationship between the RLB time lag and the NIP was caused by experimental error. DNA was extracted by boiling ticks in water containing NH_4OH, and the resultant DNA extractions were stored in this poor DNA storage solution for an average of 2.4 years (some for as long as 13.8 years) prior to detection of *B. burgdorferi* s.l. using RLB. We believe that the DNA in these crude DNA extractions degraded over time, which decreased the ability of the RLB to detect *B. burgdorferi* s.l. infection in the ticks. The sensitivity of the RLB blots was repeatedly tested over the course of

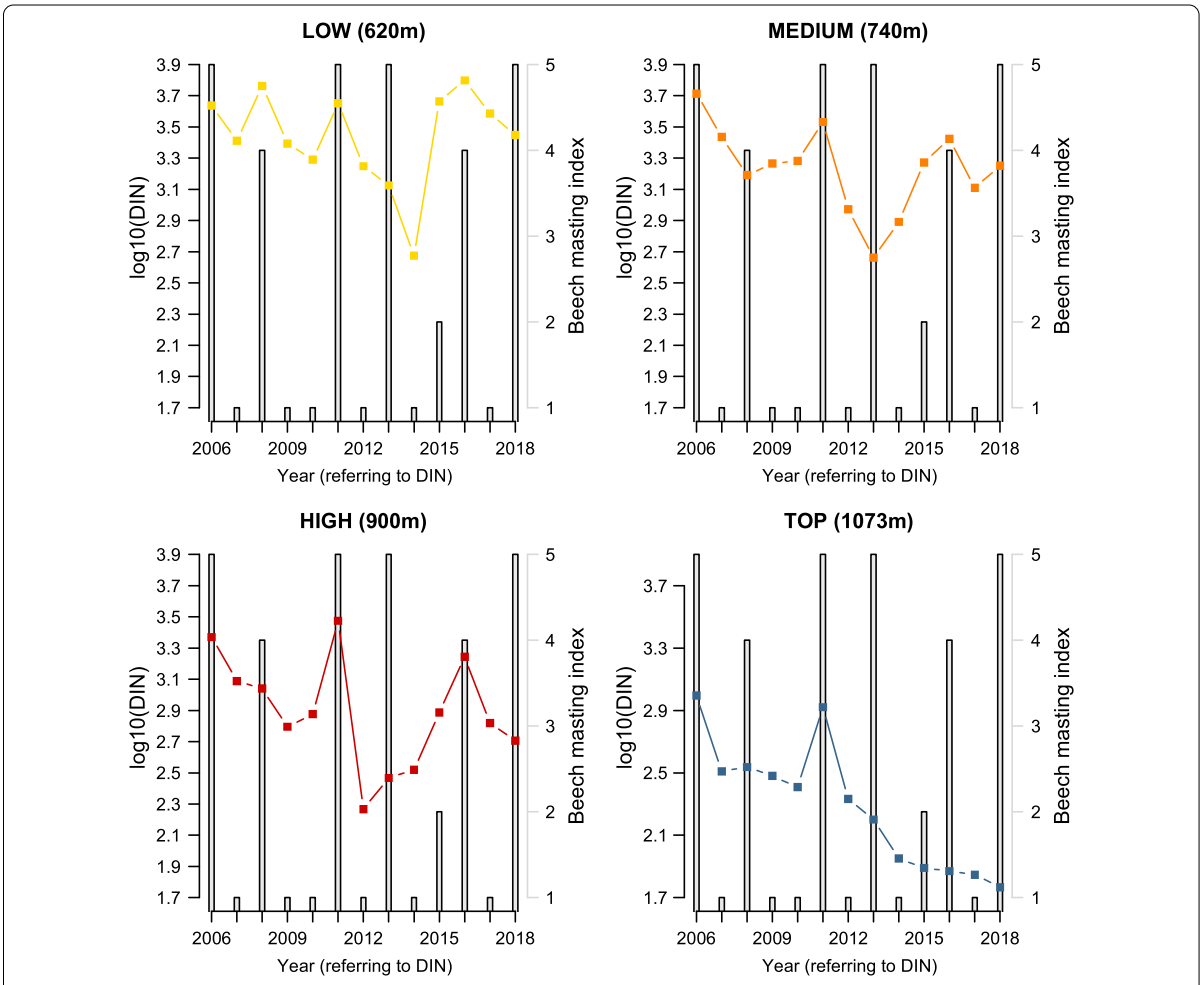

Fig. 8 The log10-transformed DIN (square points and solid lines) and the beech tree mast score 2 years prior (open bars) over the 13-year study period for each of the four elevation sites on Chaumont Mountain. The DIN values range from years 2006 to 2018, whereas the beech tree mast scores 2 years prior range from years 2004 to 2016. Years of high seed production by beech trees 2 years prior were associated with high DIN values. Beech tree mast scores of 1, 2, 3, 4, and 5 refer to very poor mast, poor mast, moderate mast, good mast, and full mast, respectively

the study by using the DNA from isolates of the six *B. burgdorferi* s.l. genospecies cultured in BSK media as positive controls. However, these isolates were grown fresh from frozen stocks when needed, and the RLB blots were therefore unable to detect the DNA degradation over time in the whole-tick DNA extractions. One solution to check for DNA degradation over time would be to repeatedly test known positive controls that are stored in the same freezers as the study samples over the duration of the study. Another solution is to process all the tick DNA extractions with respect to pathogen detection in a timely manner; for example, within a 1-year window.

One limitation of our study is that we did not collect any data on the density of vertebrate hosts at our study sites. Host blood meal analyses of unfed *I. ricinus* nymphs at our field site have shown that they obtain their larval blood meal from a variety of vertebrate hosts, including rodents, birds, carnivores and ungulates [56]. The community of vertebrate hosts plays a critical role in the ecology of *Ixodes* tick populations and their tick-borne pathogens [20, 98]. The three *Ixodes* tick stages feed on different types of vertebrate hosts; larvae and nymphs feed on small mammals and birds, whereas adult female ticks feed on ungulates [19, 20, 37, 99]. Vertebrate hosts can also differ extensively in their ability to harbor and

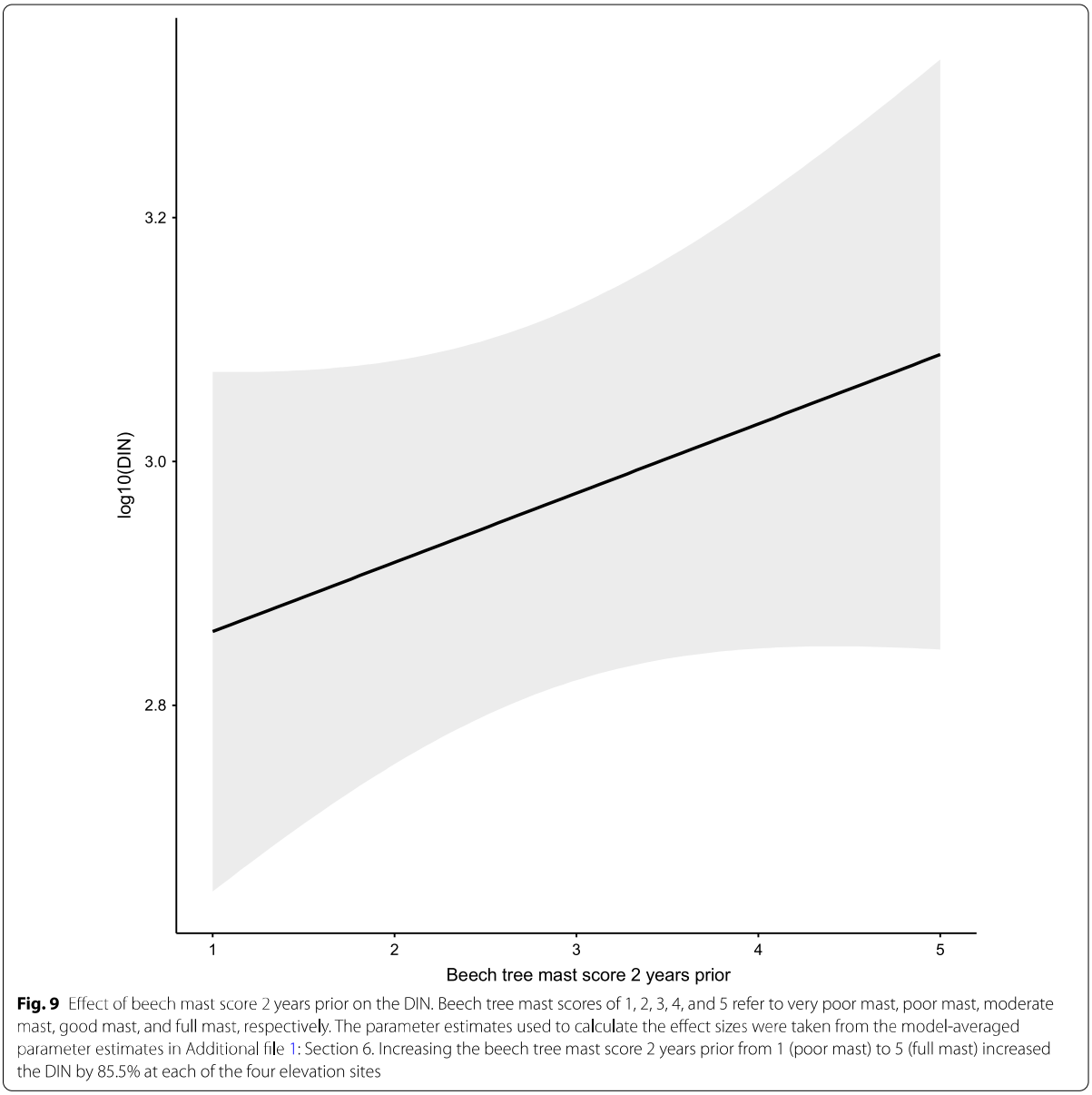

Fig. 9 Effect of beech mast score 2 years prior on the DIN. Beech tree mast scores of 1, 2, 3, 4, and 5 refer to very poor mast, poor mast, moderate mast, good mast, and full mast, respectively. The parameter estimates used to calculate the effect sizes were taken from the model-averaged parameter estimates in Additional file 1: Section 6. Increasing the beech tree mast score 2 years prior from 1 (poor mast) to 5 (full mast) increased the DIN by 85.5% at each of the four elevation sites

transmit *B. burgdorferi* s.l. infections to feeding *Ixodes* larval ticks [19, 99–102]. As mentioned previously, field studies on *I. ricinus* in Europe and on *I. scapularis* in North America have shown that the density of rodent reservoir hosts plays a critical role in determining larval feeding success, and hence the DON and the DIN in the following year [35, 36, 50–52, 75, 76]. In the present study, we used the beech masting index as an indirect estimate of the abundance of small vertebrate hosts available to feed the larval ticks the following year. However, data on the vertebrate host community are the missing link in this study and would have undoubtedly enhanced the ability of our models to explain inter-annual variation in the DON, NIP and DIN.

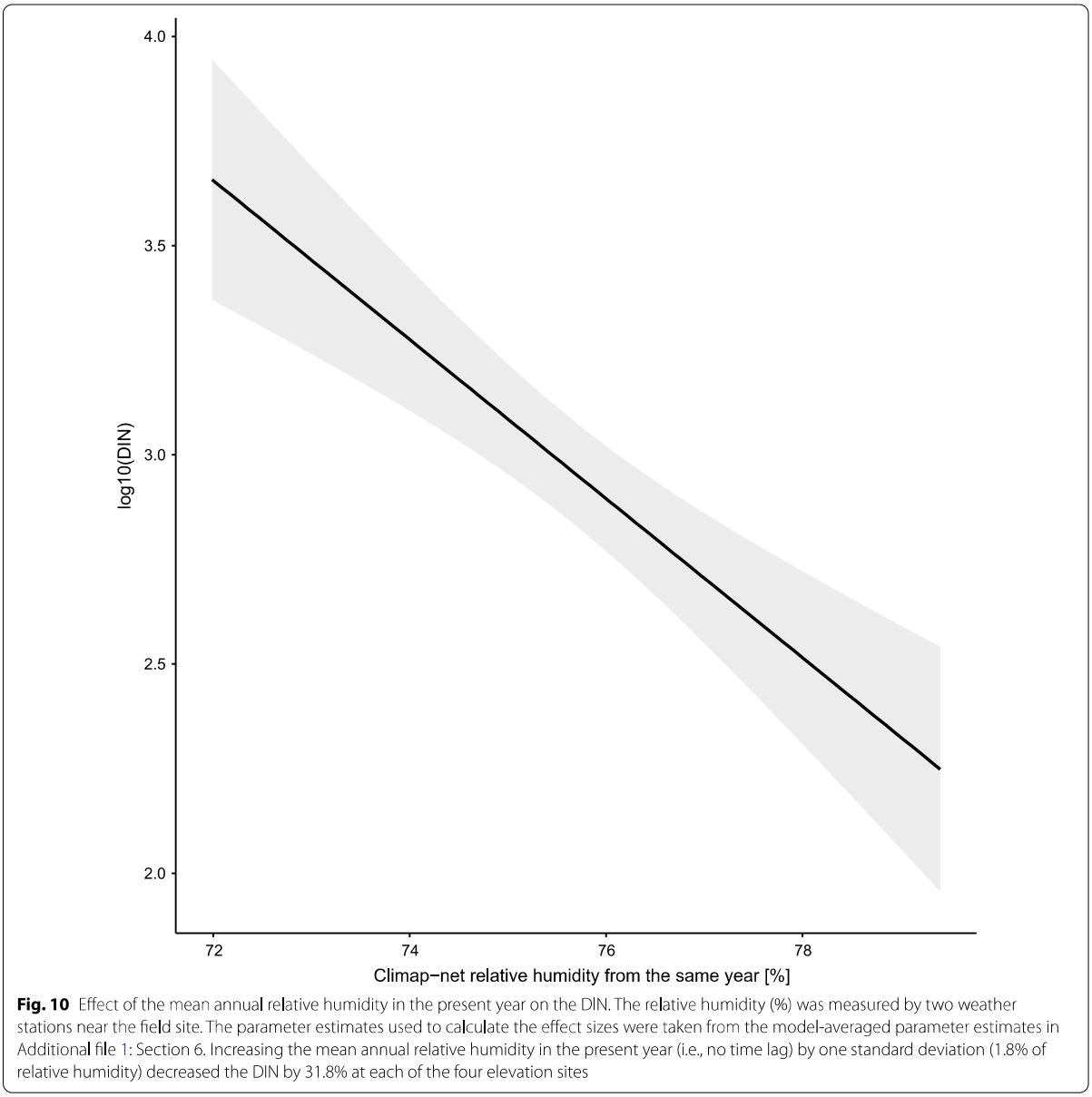

Fig. 10 Effect of the mean annual relative humidity in the present year on the DIN. The relative humidity (%) was measured by two weather stations near the field site. The parameter estimates used to calculate the effect sizes were taken from the model-averaged parameter estimates in Additional file 1: Section 6. Increasing the mean annual relative humidity in the present year (i.e., no time lag) by one standard deviation (1.8% of relative humidity) decreased the DIN by 31.8% at each of the four elevation sites

Conclusions

In conclusion, we found that the NIP decreased by 78% over the study period at Chaumont Mountain. We also found that the DIN decreased over the study period at all four elevation sites, but the decrease was only significant at the top elevation. The RLB time lag had a large negative effect on the NIP and a moderately negative effect on the DIN. Beech masting 2 years prior was strongly and positively correlated with inter-annual variation in the DIN. This is the first long-term study in Europe to provide evidence that seed production by deciduous trees influences the density of nymphs infected with *B. burgdorferi* s.l.. Public health officials in Europe should be aware that masting by deciduous trees is an important predictor of the risk of Lyme borreliosis.

Abbreviations
AIC: Akaike information criterion; AIP: Adult infection prevalence; CAD: Cumulative adult density; CND: Cumulative nymph density; DIA: Density of infected adults; DIN: Density of infected nymphs; DOA: Density of adults; DON: Density of nymphs; GLMM: Generalized linear mixed effects model; LM: Linear model; NIP: Nymphal infection prevalence; RH: Relative humidity; RLB: Reverse line blot; SD: Saturation deficit.

Supplementary Information

The online version contains supplementary material available at https://doi.org/10.1186/s13071-021-04646-0.

Additional file 1: Section 1. Interpolation of the Climap-net climate data. **Section 2.** Correlation between two measures of nymph density. **Section 3.** Assumptions of the statistical methods. **Section 4.** Full statistical analysis of the adult infection prevalence (AIP) and density of infected adults (DIA) for the restricted 13-year period of the study (2006–2018). **Section 5.** Full statistical analysis of the nymphal infection prevalence (NIP) for the restricted 13-year period of the study (2006–2018). **Section 6.** Full statistical analysis of the density of infected nymphs (DIN) for the restricted 13-year period of the study (2006–2018).

Additional file 2: Table S1. Raw data used for all statistical analyses.

Acknowledgements
We would like to thank Lise Gern for her financial support and for generously giving us these data. This study was part of the PhD thesis of Cindy Bregnard.

Authors' contributions
OR collected the ticks and the meteorological data in the field, performed the molecular work, and managed the data. CB and MJV analyzed the data and wrote the manuscript. All authors read and approved the final manuscript.

Funding
This study was supported by grants obtained by Lise Gern from the Swiss National Science Foundation: FN 32-57098.99, FN 3200B0-100657, FN 320000-113936 and FN 310030-127064 and by grants obtained by Lise Gern from the Federal Office of Public Health National Reference Center: 2009/10 (Projekt (911) 316) and 2011/13 (11.006911/304.0001-707). The doctoral salary of Cindy Bregnard was supported by the University of Neuchâtel. This research was also supported by two grants awarded to Maarten J. Voordouw, a Discovery Grant from the Natural Sciences and Engineering Research Council of Canada (RGPIN-2019-04483) and an Establishment Grant from the Saskatchewan Health Research Foundation (4583).

Availability of data and materials
The raw data for this study are stored in the Additional file 2. The climate data are available from the Climap-net database of the Federal Office for Meteorology and Climatology (http://www.meteosuisse.admin.ch/home/service-et-publications/conseil-et-service/portail-de-donnees-dedie-aux-specialistes.html). The MASTREE database is available in the Ecology - Ecological Society of America repository (http://onlinelibrary.wiley.com/doi/10.1002/ecy.1785/suppinfo).

Declarations

Ethics approval and consent to participate
Not applicable.

Consent for publication
Not applicable.

Competing interests
The authors declare that they have no competing interests.

Author details
[1] Laboratory of Ecology and Evolution of Parasites, Institute of Biology, University of Neuchâtel, Neuchâtel, Switzerland. [2] Laboratory of Ecology and Epidemiology of Parasites, Institute of Biology, University of Neuchâtel, Neuchâtel, Switzerland. [3] Department of Veterinary Microbiology, Western College of Veterinary Medicine, University of Saskatchewan, Saskatoon, Canada.

Received: 3 November 2020 Accepted: 16 February 2021
Published online: 20 March 2021

References

1. Jongejan F, Uilenberg G. The global importance of ticks. Parasitology. 2005;129:3–14.
2. Rosenberg R, Lindsey N, Fischer M, Gregory C, Hinckley A, Mead P, et al. Vital signs: trends in reported vectorborne disease cases—United States and territories, 2004–2016. MMWR Morb Mortal Wkly Rep. 2018;67:1–6.
3. Lindgren E, Tälleklint L, Polfeldt T. Impact of climatic change on the northern latitude limit and population density of the disease-transmitting European tick *Ixodes ricinus*. Environ Health Perspect. 2000;108:119–23.
4. Jaenson TGT, Jaenson DG, Eisen L, Petersson E, Lindgren E. Changes in the geographical distribution and abundance of the tick *Ixodes ricinus* during the past 30 years in Sweden. Parasites Vectors. 2012;5:8.
5. Ogden NH, Lindsay LR, Morshed M, Sockett PN, Artsob H. The emergence of Lyme disease in Canada. CMAJ. 2009;180:1221–4.
6. Gasmi S, Ogden NH, Lindsay LR, Burns S, Fleming S, Badcock J, et al. Surveillance for Lyme disease in Canada: 2009–2015. Can Commun Dis Rep. 2017;43:194–9.
7. Brownstein JS, Holford TR, Fish D. Effect of climate change on Lyme disease risk in North America. EcoHealth. 2005;2:38–46.
8. Medlock J, Leach S. Impact of climate change on vector-borne disease in the UK. Lancet. 2015;15:159–99.
9. Parham PE, Waldock J, Christophides GK, Hemming D, Agusto F, Evans KJ, et al. Climate, environmental and socio-economic change: weighing up the balance in vector-borne disease transmission. Philos Trans R Soc Lond B Biol Sci. 2015;370:20130551.
10. Barbour AG, Fish D. The biological and social phenomenon of Lyme disease. Science. 1993;260:1610–6.
11. Wood CL, Lafferty KD. Biodiversity and disease: a synthesis of ecological perspectives on Lyme disease transmission. Trends Ecol Evol. 2013;28:239–47.
12. Randolph SE. Tick-borne encephalitis incidence in central and eastern Europe: consequences of political transition. Microb Infect. 2008;10:209–16.
13. Sumilo D, Asokliene L, Bormane A, Vasilenko V, Golovljova I, Randolph SE. Climate change cannot explain the upsurge of tick-borne encephalitis in the Baltics. PLoS ONE. 2007;2:e500.
14. Godfrey ER, Randolph SE. Economic downturn results in tick-borne disease upsurge. Parasites Vectors. 2011;4:35.
15. Diuk-Wasser MA, Hoen AG, Cislo P, Brinkerhoff R, Hamer SA, Rowland M, et al. Human risk of infection with *Borrelia burgdorferi*, the Lyme disease agent, in eastern United States. Am J Trop Med Hyg. 2012;86:320–7.
16. Mysterud A, Stigum V, Seland I, Herland A, Easterday WR, Jore S, et al. Tick abundance, pathogen prevalence, and disease incidence in two contrasting regions at the northern distribution range of Europe. Parasites Vectors. 2018;11:309.
17. Kilpatrick A, Dobson A, Levi T, Salkeld D, Swei A, Ginsberg HS, et al. Lyme disease ecology in a changing world: consensus, uncertainty and critical gaps for improving control. Philos Trans R Soc Lond B Biol Sci. 2017;372:20160117.
18 Gern L, Humair PF. Ecology of *Borrelia burgdorferi* sensu lato in Europe. In: Gray JS, Kahl O, Lane RS, Stanek G, editors. Lyme borreliosis: biology, epidemiology and control. Wallinford: CABI International; 2002. p. 149–74.
19. Gern L, Estrada-Peña A, Frandsen F, Gray JS, Jaenson TGT, Jongejan F, et al. European reservoir hosts of *Borrelia burgdorferi* sensu lato. Zentralbl Bakteriol B. 1998;287:196–204.
20. Mannelli A, Bertolotti L, Gern L, Gray J. Ecology of *Borrelia burgdorferi* sensu lato in Europe: transmission dynamics in multi-host systems,

influence of molecular processes and effects of climate change. FEMS Microbiol Rev. 2012;36:837–61.
21. van Duijvendijk G, Coipan C, Wagemakers A, Fonville M, Ersöz J, Oei A, et al. Larvae of *Ixodes ricinus* transmit *Borrelia afzelii* and *B. miyamotoi* to vertebrate hosts. Parasites Vectors. 2016;9:97.
22. Rollend L, Fish D, Childs JE. Transovarial transmission of Borrelia spirochetes by *Ixodes scapularis*: a summary of the literature and recent observations. Ticks Tick Borne Dis. 2013;4:46–51.
23. Matuschka FR, Schinkel TW, Klug B, Spielman A, Richter D. Failure of *Ixodes* ticks to inherit *Borrelia afzelii* infection. Appl Environ Microbiol. 1998;64:3089–91.
24. Anderson JF, Magnarelli LA. Biology of ticks. Infect Dis Clin North Am. 2008;22:195–215.
25. Gray JS, Kahl O, Janetzki C, Stein J. Studies on the ecology of Lyme disease in a deer forest in County Galway, Ireland. J Med Entomol. 1992;29:915–20.
26. Huang C-I, Kay SC, Davis S, Tufts DM, Gaffett K, Tefft B, et al. High burdens of *Ixodes scapularis* larval ticks on white-tailed deer may limit Lyme disease risk in a low biodiversity setting. Ticks Tick Borne Dis. 2019;10:258–68.
27. Tälleklint L, Jaenson TGT. Relationship between *Ixodes ricinus* density and prevalence of infection with Borrelia-like spirochetes and density of infected ticks. J Med Entomol. 2014;33:805–11.
28. Ostfeld RS. Lyme disease: the ecology of a complex system. Oxford: Oxford University Press USA; 2011.
29. Stafford KC 3rd, Cartter ML, Magnarelli LA, Ertel SH, Mshar PA. Temporal correlations between tick abundance and prevalence of ticks infected with *Borrelia burgdorferi* and increasing incidence of Lyme disease. J Clin Microbiol. 1998;36:1240–4.
30. Mather TN, Nicholson MC, Donnelly EF, Matyas BT. Entomologic index for human risk of Lyme disease. Am J Epidemiol. 1996;144:1066–9.
31. Ostfeld RS, Keesing F, Schauber EM, Schmidt KA. Ecological context of Lyme disease: biodiversity, habitat fragmentation, and risk of infection. In: Conservation medicine: ecological health in practice. New York: Oxford University Press; 2002. p. 207–19.
32. Gray JS. The development and seasonal activity of the tick *Ixodes ricinus*: a vector of Lyme borreliosis. Rev Med Vet Entomol. 1991;79:323–33.
33 Gray JS, Kahl O, Lane RS, Levin M, Tsao J. Diapause in ticks of the medically important *Ixodes ricinus* species complex. Ticks Tick Borne Dis. 2016;7:992–1003.
34. Korenberg EI. Seasonal population dynamics of Ixodes ticks and tick-borne encephalitis virus. Exp Appl Acarol. 2000;24:665–81.
35. Ostfeld RS, Canham CD, Oggenfuss K, Winchcombe RJ, Keesing F. Climate, deer, rodents, and acorns as determinants of variation in Lyme-disease risk. PLoS Biol. 2006;4:e145.
36. Krawczyk AI, van Duijvendijk GLA, Swart A, Heylen D, Jaarsma RI, Jacobs FHH, et al. Effect of rodent density on tick and tick-borne pathogen populations: consequences for infectious disease risk. Parasites Vectors. 2020;13:34.
37. Gray JS. Review: the ecology of ticks transmitting Lyme borreliosis. Exp Appl Acarol. 1998;22:249–58.
38. Stanek G, Wormser GP, Gray J, Strle F. Lyme borreliosis. Lancet. 2012;379:461–73.
39. Randolph SE. Tick ecology: processes and patterns behind the epidemiological risk posed by ixodid ticks as vectors. Parasitology. 2004;129:37–65.
40. Ogden NH, Lindsay LR, Beauchamp G, Charron D, Maarouf A, O'Callaghan CJ, et al. Investigation of relationships between temperature and developmental rates of tick *Ixodes scapularis* (Acari: Ixodidae) in the laboratory and field. J Med Entomol. 2004;41:622–33.
41. Gray JS, Dautel H, Estrada-Peña A, Kahl O, Lindgren E. Effects of climate change on ticks and tick-borne diseases in Europe. Interdiscip Perspect Infect Dis. 2009;2009:593232.
42. Ogden NH, Tsao JI. Biodiversity and Lyme disease: dilution or amplification? Epidemics. 2009;1:196–206.
43. Randolph SE. Ticks are not insects: consequences of contrasting vector biology for transmission potential. Parasitol Today. 1998;14:186–92.
44. Clotfelter E, Pedersen A, Cranford J, Ram N, Snajdr E, Nolan V, et al. Acorn mast drives long-term dynamics of rodent and songbird populations. Oecologia. 2008;154:493–503.
45. Schnurr JL, Ostfeld RS, Canham CD. Direct and indirect effects of masting on rodent populations and tree seed survival. Oikos. 2002;96:402–10.
46. Drobyshev I, Niklasson M, Mazerolle MJ, Bergeron Y. Reconstruction of a 253-year long mast record of European beech reveals its association with large scale temperature variability and no long-term trend in mast frequencies. Agric For Meteorol. 2014;192:9–17.
47. Drobyshev I, Övergaard R, Saygin I, Niklasson M, Hickler T, Karlsson M, et al. Masting behaviour and dendrochronology of European beech (*Fagus sylvatica* L.) in southern Sweden. For Ecol Manag. 2010;259:2160–71.
48. Piovesan G, Adams JM. Masting behaviour in beech: linking reproduction and climatic variation. Can J Bot. 2001;79:1039–47.
49. Övergaard R, Gemmel P, Karlsson M. Effects of weather conditions on mast year frequency in beech (*Fagus sylvatica* L.) in Sweden. Forestry. 2007;80:555–65.
50. Ostfeld RS, Levi T, Keesing F, Oggenfuss K, Canham CD. Tick-borne disease risk in a forest food web. Ecology. 2018;99:1562–73.
51. Ostfeld RS, Schauber EM, Canham CD, Keesing F, Jones CG, Wolff JO. Effects of acorn production and mouse abundance on abundance and *Borrelia burgdorferi* infection prevalence of nymphal *Ixodes scapularis* ticks. Vector Borne Zoonotic Dis. 2001;1:55–63.
52. Schauber EM, Ostfeld RS, Evans J, Andrew S. What is the best predictor of annual Lyme disease incidence: weather, mice, or acorns? Ecol Appl. 2005;15:575–86.
53. Brugger K, Walter M, Chitimia-Dobler L, Dobler G, Rubel F. Forecasting next season's *Ixodes ricinus* nymphal density: the example of southern Germany 2018. Exp Appl Acarol. 2018;75:281–8.
54. Bregnard C, Rais O, Voordouw MJ. Climate and tree seed production predict the abundance of the European Lyme disease vector over a 15-year period. Parasit Vectors. 2020;13:408.
55. Jouda F, Perret JL, Gern L. *Ixodes ricinus* density, and distribution and prevalence of *Borrelia burgdorferi* sensu lato infection along an altitudinal gradient. J Med Entomol. 2004;41:162–9.
56. Morán Cadenas F, Rais O, Humair PF, Douet V, Moret J, Gern L. Identification of host bloodmeal source and *Borrelia burgdorferi* sensu lato in field-collected *Ixodes ricinus* ticks in Chaumont (Switzerland). J Med Entomol. 2007;44:1109–17.
57. Morán Cadenas F, Rais O, Jouda F, Douet V, Humair PF, Moret J, et al. Phenology of *Ixodes ricinus* and infection with *Borrelia burgdorferi* sensu lato along a North- and South-facing altitudinal gradient on Chaumont Mountain, Switzerland. J Med Entomol. 2007;44:683–93.
58. Morán Cadenas F, Schneider H, Lommano E, Burri C, Moret J, Gern L. A comparison of two DNA extraction approaches in the detection of *Borrelia burgdorferi* sensu lato from live *Ixodes ricinus* ticks by PCR and reverse line blotting. Vector Borne Zoonotic Dis. 2007;7:555–62.
59. Burri C, Morán Cadenas F, Douet V, Moret J, Gern L. *Ixodes ricinus* density and infection prevalence of *Borrelia burgdorferi* sensu lato along a north-facing altitudinal gradient in the Rhône Valley (Switzerland). Vector Borne Zoonotic Dis. 2007;7:50–8.
60. Berret J, Voordouw MJ. Lyme disease bacterium does not affect attraction to rodent odour in the tick vector. Parasites Vectors. 2015;8:249.
61. Durand J, Jacquet M, Paillard L, Rais O, Gern L, Voordouw MJ. Cross-immunity and community structure of a multiple-strain pathogen in the tick vector. Appl Environ Microbiol. 2015;81:7740–52.
62. Randolph SE, Storey K. Impact of microclimate on immature tick-rodent host interactions (Acari: Ixodidae): implications for parasite transmission. J Med Entomol. 1999;36:741–8.
63. Perret JL, Guigoz E, Rais O, Gern L. Influence of saturation deficit and temperature on *Ixodes ricinus* tick questing activity in a Lyme borreliosis-endemic area (Switzerland). Parasitol Res. 2000;86:554–7.
64. Bogdziewicz M, Kelly D, Thomas PA, Lageard JG, Hacket-Pain A. Climate warming disrupts mast seeding and its fitness benefits in European beech. Nat Plants. 2020;6:88–94.
65. Ascoli D, Maringer J, Hacket-Pain A, Conedera M, Drobyshev I, Motta R, et al. Two centuries of masting data for European beech and Norway spruce across the European continent. Ecology. 2017;98:1473.
66. Eisen RJ, Eisen L, Castro MB, Lane RS. Environmentally related variability in risk of exposure to Lyme disease spirochetes in northern California: effect of climatic conditions and habitat type. Environ Entomol. 2003;32:1010–8.

67. R Development Core Team. R: a language and environment for statistical computing. Vienna: R Foundation for Statistical Computing. 2013.
68. Ostfeld RS, Jones CG, Wolff JO. Of mice and mast. Bioscience. 1996;46:323–30.
69. Wolff JO. Population fluctuations of mast-eating rodents are correlated with production of acorns. J Mammal. 1996;77:850–6.
70. Jones CG, Ostfeld RS, Richard MP, Schauber EM, Wolff JO. Chain reactions linking acorns to gypsy moth outbreaks and Lyme disease risk. Science. 1998;279:1023–6.
71. Ostfeld RS, Keesing F. Pulsed resources and community dynamics of consumers in terrestrial ecosystems. Trends Ecol Evol. 2000;15:232–7.
72. Pucek Z, Jędrzejewski W, Jędrzejewska B, Pucek M. Rodent population dynamics in a primeval deciduous forest (Białowieża National Park) in relation to weather, seed crop, and predation. Acta Theriol. 1993;38:199–232.
73. McShea WJ. The influence of acorn crops on annual variation in rodent and bird populations. Ecology. 2000;81:228–38.
74. Jensen TS. Seed production and outbreaks of non-cyclic rodent populations in deciduous forests. Oecologia. 1982;54:184–92.
75. Perez G, Bastian S, Agoulon A, Bouju A, Durand A, Faille F, et al. Effect of landscape features on the relationship between *Ixodes ricinus* ticks and their small mammal hosts. Parasites Vectors. 2016;9:20.
76. Hofmeester TR, Jansen PA, Wijnen HJ, Coipan EC, Fonville M, Prins HHT, et al. Cascading effects of predator activity on tick-borne disease risk. Proc Royal Soc B. 1859;2017(284):20170453.
77. Bogdziewicz M, Szymkowiak J. Oak acorn crop and Google search volume predict Lyme disease risk in temperate Europe. Basic Appl Ecol. 2016;17:300–7.
78. Tkadlec E, Václavík T, Široký P. Rodent host abundance and climate variability as predictors of tickborne disease risk 1 year in advance. Emerg Infect Dis. 2019;25:1738.
79. Brunner JL, Ostfeld RS. Multiple causes of variable tick burdens on small-mammal hosts. Ecology. 2008;89:2259–72.
80. Schmidt K, Ostfeld RS, Schauber EM. Infestation of *Peromyscus leucopus* and *Tamias striatus* by *Ixodes scapularis* (Acari: Ixodidae) in relation to the abundance of hosts and parasites. J Med Entomol. 1999;36:749–57.
81. Rodgers SE, Zolnik CP, Mather TN. Duration of exposure to suboptimal atmospheric moisture affects nymphal blacklegged tick survival. J Med Entomol. 2007;44:372–5.
82. Hubálek Z, Halouzka J, Juricova Z. Host-seeking activity of ixodid ticks in relation to weather variables. J Vector Ecol. 2003;28:159–65.
83 Schwarz A, Maier WA, Kistemann T, Kampen H. Analysis of the distribution of the tick *Ixodes ricinus* L. (Acari: Ixodidae) in a nature reserve of western Germany using geographic information systems. Int J Hyg Environ Health. 2009;212:87–96.
84. Li S, Heyman P, Cochez C, Simons L, Vanwambeke SO. A multi-level analysis of the relationship between environmental factors and questing *Ixodes ricinus* dynamics in Belgium. Parasites Vectors. 2012;5:149.
85. James M, Bowman A, Forbes K, Lewis F, McLeod J, Gilbert L. Environmental determinants of *Ixodes ricinus* ticks and the incidence of *Borrelia burgdorferi* sensu lato, the agent of Lyme borreliosis, in Scotland. Parasitology. 2012;140:1–10.
86. Kiewra D, Kryza M, Szymanowski M. Influence of selected meteorological variables on the questing activity of *Ixodes ricinus* ticks in Lower Silesia, SW Poland. J Vector Ecol. 2014;39:138–45.
87. Benjamin MA, Zhioua E, Ostfeld RS. Laboratory and field evaluation of the entomopathogenic fungus *Metarhizium anisopliae* (Deuteromycetes) for controlling questing adult *Ixodes scapularis* (Acari: Ixodidae). J Med Entomol. 2002;39:723–8.
88. Hartelt K, Wurst E, Collatz J, Zimmermann G, Kleespies RG, Oehme RM, et al. Biological control of the tick *Ixodes ricinus* with entomopathogenic fungi and nematodes: preliminary results from laboratory experiments. Int J Med Microbiol. 2008;298:314–20.
89. Herrmann C, Gern L. Survival of *Ixodes ricinus* (Acari: Ixodidae) under challenging conditions of temperature and humidity is influenced by *Borrelia burgdorferi* sensu lato infection. J Med Entomol. 2010;47:1196–204.
90. Herrmann C, Gern L. Do the level of energy reserves, hydration status and Borrelia infection influence walking by *Ixodes ricinus* (Acari: Ixodidae) ticks? Parasitology. 2012;139:330–7.
91. Herrmann C, Gern L. Survival of *Ixodes ricinus* (Acari: Ixodidae) nymphs under cold conditions is negatively influenced by frequent temperature variations. Ticks Tick Borne Dis. 2013;4:445–51.
92. Herrmann C, Gern L. Search for blood or water is influenced by *Borrelia burgdorferi* in *Ixodes ricinus*. Parasites Vectors. 2015;8:6.
93. Herrmann C, Voordouw MJ, Gern L. *Ixodes ricinus* ticks infected with the causative agent of Lyme disease, *Borrelia burgdorferi* sensu lato, have higher energy reserves. Int J Parasitol. 2013;43:477–83.
94. Lefcort H, Durden LA. The effect of infection with Lyme disease spirochetes (*Borrelia burgdorferi*) on the phototaxis, activity, and questing height of the tick vector *Ixodes scapularis*. Parasitology. 1996;113(Pt 2):97–103.
95. Randolph SE, Green RM, Hoodless AN, Peacey MF. An empirical quantitative framework for the seasonal population dynamics of the tick *Ixodes ricinus*. Int J Parasitol. 2002;32:979–89.
96. Ogden NH, Bigras-Poulin M, O'Callaghan CJ, Barker IK, Lindsay LR, Maarouf A, et al. A dynamic population model to investigate effects of climate on geographic range and seasonality of the tick *Ixodes scapularis*. Int J Parasitol. 2005;35:375–89.
97. Eisen RJ, Eisen L, Ogden NH, Beard CB. Linkages of weather and climate with *Ixodes scapularis* and *Ixodes pacificus* (Acari: Ixodidae), enzootic transmission of *Borrelia burgdorferi*, and Lyme disease in North America. J Med Entomol. 2016;53:250–61.
98. Pfäffle M, Littwin N, Muders SV, Petney TN. The ecology of tick-borne diseases. Int J Parasitol. 2013;43:1059–77.
99. Hofmeester T, Coipan E, Van Wieren S, Prins H, Takken W, Sprong H. Few vertebrate species dominate the *Borrelia burgdorferi* sl life cycle. Environ Res Lett. 2016;11:043001.
100. LoGiudice K, Duerr ST, Newhouse MJ, Schmidt KA, Killilea ME, Ostfeld RS. Impact of host community composition on Lyme disease risk. Ecology. 2008;89:2841–9.
101. LoGiudice K, Ostfeld RS, Schmidt KA, Keesing F. The ecology of infectious disease: effects of host diversity and community composition on Lyme disease risk. Proc Natl Acad Sci USA. 2003;100:567–71.
102 Tälleklint L, Jaenson T. Transmission of *Borrelia burgdorferi* s.l. from mammal reservoirs to the primary vector of Lyme borreliosis, *Ixodes ricinus* (Acari: Ixodidae), in Sweden. J Med Entomol. 1994;31:880–6.

Publisher's Note

6 Chapter 3

Beech tree masting explains the inter-annual variation in the fall and spring peaks of Ixodes ricinus ticks with different time lags

Cindy Bregnard[1], Olivier Rais[2, 3], Coralie Herrmann[3], Olaf Kahl[4], Katharina Brugger[5], and Maarten J. Voordouw[1, 6*]

[1] Laboratory of Ecology and Evolution of Parasites, Institute of Biology, University of Neuchâtel, Neuchâtel, Switzerland

[2] Laboratory of Ecology and Epidemiology of Parasites, Institute of Biology, University of Neuchâtel, Neuchâtel, Switzerland

[3] Laboratory of Eco-Epidemiology of Parasites, Institute of Biology, University of Neuchâtel, Neuchâtel, Switzerland

[4] tick-radar GmbH, 10555 Berlin, Germany

[5] Unit for Veterinary Public Health and Epidemiology, University of Veterinary Medicine Vienna, Veterinärplatz 1, 1210 Vienna, Austria

[6] Department of Veterinary Microbiology, Western College of Veterinary Medicine, University of Saskatchewan, Saskatoon, Canada

Submitted April 22, 2021 in Parasites & Vectors.

Beech tree masting explains the inter-annual variation in the fall and spring peaks of *Ixodes ricinus* ticks with different time lags

Authors: Cindy Bregnard[1], Olivier Rais[2, 3], Coralie Herrmann[3], Olaf Kahl[4], Katharina Brugger[5], and Maarten J. Voordouw[1, 6*]

[1] Laboratory of Ecology and Evolution of Parasites, Institute of Biology, University of Neuchâtel, Neuchâtel, Switzerland
[2] Laboratory of Ecology and Epidemiology of Parasites, Institute of Biology, University of Neuchâtel, Neuchâtel, Switzerland
[3] Laboratory of Eco-Epidemiology of Parasites, Institute of Biology, University of Neuchâtel, Neuchâtel, Switzerland
[4] tick-radar GmbH, 10555 Berlin, Germany
[5] Unit for Veterinary Public Health and Epidemiology, University of Veterinary Medicine Vienna, Veterinärplatz 1, 1210 Vienna, Austria
[6] Department of Veterinary Microbiology, Western College of Veterinary Medicine, University of Saskatchewan, Saskatoon, Canada

*Corresponding author
CB: cindy.bregnard@unine.ch
OR: olivier.rais@unine.ch
CH: herrmann.coralie@gmail.com
OK: olaf.kahl@berlin.de
KB: katharina.brugger@vetmeduni.ac.at
MJV: maarten.voordouw@usask.ca

ABSTRACT

Background: The tick *Ixodes ricinus* is an important vector of tick-borne diseases including Lyme borreliosis. In continental Europe, the nymphal stage of *I. ricinus* often has a bimodal phenology with a large spring/early summer peak and a smaller fall peak. While there is consensus about the origin of the spring nymphal peak, there are two alternative hypotheses for the fall nymphal peak, direct development versus diapause development. These two hypotheses make different predictions about the time lags of the correlations between the spring peak, the fall peak, and seed production (masting) by deciduous trees.

Methods: To determine which hypothesis is most important for explaining the fall peak, we used data from a long-term surveillance study (15 years) on the density of *I. ricinus* nymphal ticks at 4 different elevation sites in an area of Switzerland that is endemic for Lyme borreliosis, and long-term data on the mast of the European beech tree from the literature.

Results: *I. ricinus* nymphs had a bimodal phenology at the three lower elevation sites, but a unimodal phenology at the top elevation site. At the lower elevation sites, the density of nymphs (DON) in the fall was strongly correlated with the DON in the spring of the following year. The inter-annual variation in the densities of *I. ricinus* nymphs in the fall and spring were best explained by a 1-year versus a 2-year time lag with the beech tree masting index. Fall nymphs had higher fat content and are younger than spring nymphs. All of these observations are consistent with the direct development hypothesis for the fall peak of *I. ricinus* nymphs at our study site. Our study provides new insight into the complex bimodal phenology of this important disease vector.

Conclusion: Public health officials in Europe should be aware that following a strong mast year, the DON will increase 1 year later in the fall and 2 years later in the spring and summer. Population ecology studies of *I. ricinus* should consider that the spring and fall peak in the same calendar year represent different generations of ticks.

KEYWORDS: Beech tree, Climate, *Ixodes ricinus*, *Fagus sylvatica*, phenology, Tick population ecology

INTRODUCTION

The incidence of tick-borne diseases is increasing in Europe and North America [1-7]. In large parts of Europe, the hard tick *Ixodes ricinus* is an important vector of a variety of tick-borne diseases including Lyme borreliosis and tick-borne encephalitis [8, 9]. This tick species consists of three motile stages, larva, nymph, and adult, that must obtain a blood meal from a vertebrate host to moult into the next stage (or produce eggs in the case of adult female ticks). The population ecology of *I. ricinus* is complicated by a number of factors. First, *I. ricinus* can feed on a wide variety of vertebrate hosts (e.g., lizards, rodents, birds, carnivores, ungulates), for which the population density is often unknown [10, 11]. Second, the life cycle takes several years to complete, which introduces time lags [12-14]. For example, the density of nymphs in year *y* depends on the feeding success of the larvae in year *y*-1, which depends on the ratio of larvae to vertebrate reservoir hosts in year *y*-1 [15, 16]. Third, the existence of diapause as an adaptation to surviving cold winters can split the same cohort of ticks into groups that are active at different times of the year [17-19]. Uncertainty about the origin of these groups complicates our ability to model the underlying ecological factors and appropriate time lags that drive inter-annual variation in tick abundance.

Long-term studies have shown that a combination of abiotic and biotic factors drive inter-annual variation in tick abundance. *Ixodes* ticks spend more than 99% of their life cycle off the host, where they are exposed to changes in temperature and precipitation [17, 20]. The life history traits of *Ixodes* ticks, such as development rates and survival rates, are highly sensitive to temperature and relative humidity (RH) [17, 21-23]. Tick population ecology is also highly sensitive to the abundance of vertebrate hosts because all tick stages must blood feed to graduate to the next stage in the life cycle [24, 25]. Small mammals (e.g., rodents) are an important but variable source of food for immature ticks (larvae and nymphs); rodent populations often exhibit inter-annual fluctuations due to variation in their food supply [26-31]. Studies on *I. ricinus* in Europe and on *I. scapularis* in North America have shown that inter-annual variation in seed production by deciduous trees drives inter-annual variation in the density of nymphs 2 years later; this relationship is mediated by rodents that feed on the tree seeds and provide blood meals for the larvae [12, 14, 15, 32-36]. In summary, masting in the fall of year *y*-2 enhances rodent density and larval feeding success in the spring and summer of year *y*-1, which increases the density of nymphs in year *y*.

I. ricinus has a distinct seasonal activity pattern (phenology) that allows them to search for vertebrate hosts (a behaviour called questing) when abiotic conditions (temperature and humidity) are favourable. Diapause is a critical adaptation that allows ticks (and other

arthropods) to overwinter in an inactive state and thereby avoid cold winter temperatures. Behavioural diapause is the suppression of host-seeking activity by unfed ticks in the fall in anticipation of unfavourable winter conditions. Developmental diapause is the cessation of development by engorged ticks in the fall to enhance overwinter survival [37]. Both types of diapause are driven by changes in photoperiod (the most reliable predictor of seasonal change) and both are important for structuring the phenology of *I. ricinus* ticks [19, 21], which varies widely among geographic locations [17-19, 38, 39]. In some parts of Europe, nymphs and adult ticks exhibit a unimodal phenology where questing activity peaks in late spring or early summer and ends in the fall (Table 1) [40-44]. In central Europe, the most common phenology is bimodal with a large peak of activity in spring/early summer and a smaller peak of activity in fall (Table 1) [19].

The two alternative explanations for this bimodal phenology of questing *I. ricinus* nymphs are the developmental diapause hypothesis and the direct development hypothesis (Figure 1) [19, 38, 42, 43, 45-47]. The developmental diapause hypothesis (Figure 1) suggests that the timing of the larval blood meal splits the larval cohort into two groups of nymphs that are active in the spring and fall of the following year [18, 19]. Larvae that obtain their blood meal in early summer, moult into unfed nymphs, enter behavioural diapause in fall, overwinter as unfed nymphs, and quest the following spring. In contrast, larvae that obtain their blood meal in late summer or early fall, enter developmental diapause, overwinter as engorged larvae, complete their development the following summer, and quest the following fall [19]. The direct development hypothesis (Figure 1) suggests that the timing of the larval blood meal splits the larval cohort into two groups of nymphs that are active in the fall of that year and the spring of the following year [18, 19]. Larvae that obtain their blood meal in early summer, moult into unfed nymphs, and quest that same fall. In contrast, larvae that obtain their blood meal in late summer or early fall, moult into unfed nymphs, enter behavioural diapause, and quest the following spring [19]. In both hypotheses, there is a 1-year time lag between larval feeding and the spring nymphal peak. The critical distinction between these two hypotheses is the time lag between larval feeding and the fall nymphal peak, which is 1 year for the developmental diapause hypothesis and 0 years for the direct development hypothesis. To date, it is not clear which of these two hypotheses is more important for explaining the fall peak of *I. ricinus* nymphs.

In addition to influencing the vital rates (development, survival, and reproduction) and the seasonal phenology, the climate also influences tick questing behaviour, which in turn determines the probability that ticks are captured by common tick sampling methods (e.g.,

dragging). Thus, while the seasonal phenology in central Europe dictates that questing nymphs are most abundant in spring or early summer, the questing activity of nymphs on any given day in spring depends on the weather [21, 48, 49]. Field plot experiments have shown that the percentage of ticks that are actively questing depends on the weather [39, 50]. Questing activity is generally determined by the water balance regulation, which is affected by both temperature and relative humidity [51-53]. In summary, variation in the abundance of questing ticks at any given time depends on three separate mechanisms: (1) time-lagged ecological factors that influence the vital rates, (2) photoperiod-dependent diapause that determines the broad seasonal activity patterns of questing ticks, and (3) daily weather conditions interacting with the tick water balance that determine whether ticks will quest or not on that day. Separating these different mechanisms, which operate on different temporal scales, is not an easy task.

We have previously used a long-term data set (15 years) on the questing abundance of *I. ricinus* ticks at four different elevations on a mountain in western Switzerland to investigate the ecological factors that influence the inter-annual variation in the density of questing nymphs (DON) and the density of questing nymphs infected with the causative agents of Lyme borreliosis (DIN) [12, 36]. The most important finding in these two studies was that inter-annual variation in the DON and the DIN was strongly associated with inter-annual variation in the production of seeds by European beech trees 2 years prior. For these two studies, we analysed the annual abundance of nymphs for the calendar year (January 1 to December 31). This approach assumes that the spring and fall peaks of questing nymphs in the same calendar year are both governed by the same ecological factors and time lags. This assumption is correct for the developmental diapause hypothesis, but incorrect for the direct development hypothesis. Another limitation of our previous study was that we investigated a highly limited set of climate variables calculated as annual means for either the current year or the previous year. In contrast, numerous studies suggest that season rather than calendar year is the relevant time scale over which climate variables influence the population ecology of *Ixodes* ticks [13, 54]. By dividing the calendar year into different seasons, we are increasing the temporal resolution at which our climate variables can explain inter-annual variation in tick abundance.

In the present study, we build on our previous modelling efforts of the same data set to investigate three objectives. First, determine whether the developmental diapause hypothesis or the direct development hypothesis is better at explaining inter-annual variation in the fall peak of nymphs. Second, determine whether seasonal climate means are better than annual climate means at predicting inter-annual variation in the density of nymphs, and which seasonal climate variables are important. Third, determine whether we can use generalized additive models

(GAMs) to model the complex bimodal seasonal phenology of *I. ricinus* nymphs and whether this approach yields additional insights into the factors that explain seasonal variation in questing tick abundance.

METHODS

Study location: The study was conducted on the south-facing slope of Chaumont Mountain, which is part of the Jura mountains, and is in the canton of Neuchâtel, in western Switzerland. Four tick sampling sites, referred to as low, medium, high, and top, were established at elevations of 620, 740, 900, and 1073 m above sea level (ASL), respectively, and have been described previously [43, 55, 56]. There is logging in the area, and there are hiking trails and recreation areas for the public. The forest on Chaumont Mountain is mainly composed of European beech (*Fagus sylvatica*; 28.6%), Norway spruce (*Picea abies*; 28.5%), European silver fir (*Abies alba*; 20.4%), sycamore maple (*Acer pseudoplatanus*; 5.9%), European ash (*Fraxinus excelsior*; 3.7%), Scots pine (*Pinus sylvestris*; 2.3%), sessile oak (*Quercus petraea*; 2.3%), willow (*Salix* spp.; 2.1%), common whitebeam (*Sorbus aria*; 1.6%), and European hornbeam (*Carpinus betulus*; 1.0%) [57].

Sampling *I. ricinus* ticks in the field: Questing *I. ricinus* nymphs and adult ticks were collected monthly over a period of 15 years (January 2004 to December 2018) at each of the four elevation sites. The sampling protocol has been described previously [55]. Briefly, a 1-m^2 cotton flag was dragged over the ground along a fixed transect with a length of 100 m (low elevation) or 120 m (other elevations). The flag was inspected every 20 m and nymphs and adult ticks were counted separately and placed in collection vials. This method of tick collection targets questing ticks and removes them from the environment; these removed ticks cannot be encountered on future sampling occasions and they cannot contribute to future tick population growth. The same person (Olivier Rais) conducted all 720 transects (4 elevations*15 years*12 months = 720 transects). No dragging was performed on days when there was snow on the ground (hereafter referred to as snow days). Over the study period, a total of 34 snow days occurred, which resulted in missing data for 136 transects.

Field-collected climate variables: Temperature (units are °C) and relative humidity (RH; units are %) were recorded at 60 cm above ground at one moment in time on the day of tick collection (usually between 10:00 am and 2:00 pm) at each tick sampling site using a thermohygrometer (Model 615, Testo SA, Lonay, Switzerland). Thus, for each combination of

elevation and year, we had a total of 12 field-collected measurements of temperature and RH. The saturation deficit (SD) is a measure of the drying power of the atmosphere (units are mm of mercury) and is calculated using temperature (T; units are °C) and RH (units are %) as follows: $SD = (1 - RH/100) * 4.9463 * e^{0.0621T}$ [42, 58]. The accuracy of our field-collected climate data was confirmed by comparing them to the weather station data [12].

Weather station climate variables: We also obtained climate data from the CLIMAP-net database of the Federal Office of Meteorology and Climatology MeteoSwiss. Two weather stations close to our study site are in Neuchâtel at 485 m ASL (WMO number = 06604) and in Chaumont at 1136 m ASL (WMO number = 06608). These weather stations sample the temperature and RH every hour, and the total precipitation each day at 200 cm above ground. We used the daily mean temperature (average of the 24 measurements per day), the daily mean RH (average of the 24 measurements per day), and the daily total precipitation (rain, snow). Thus, for each year, we had a total of 365 weather station measurements of these three climate variables. The SD was calculated as previously described. For each of the four elevation sites, we calculated site-specific climate variables by interpolating the data between the two weather stations (Additional file 1: Section 1).

Data on inter-annual variation in tree masting: We previously demonstrated that the abundance of *I. ricinus* ticks depends on the seed production of deciduous trees [12, 36]. The seeds or fruit of forest trees (e.g., acorns of oak trees or the beech nuts of beech trees) are often referred to as mast. The annual production of mast by a population of trees in an area occurs in the fall and is highly variable among years [59]. The MASTREE database contains data on masting (or seed production) for many locations in Europe from year 1982 to year 2016 for two tree species, European beech (*Fagus sylvatica*) and Norway spruce (*Picea abies*) [60]. In this database, the mast intensity is classified into five classes: 1, 2, 3, 4, and 5, which refer to very poor mast, poor mast, moderate mast, good mast, and full mast, respectively [60]. We used the MASTREE database [60] to obtain masting data for the European beech and Norway spruce for the canton of Neuchâtel for the years of our study. These two species of tree account for 57.1% of the trees at our study location.

Fat content of *I. ricinus* nymphs collected in the spring and fall: Fat is a non-renewable source of energy derived from each blood meal that ticks use to quest for hosts and to maintain their water balance [58, 61, 62]. As *I. ricinus* feeds once per life stage and has no other energy

sources between blood meals, their fat content is an index of their current age and future longevity in the unfed state [40, 45, 58]. In a previous study on the *I. ricinus* population at our field site, we had collected nymphs in the spring and fall of 2010 and measured their fat content [63]. In the present study, we compared the fat content between the spring and fall nymphs. The direct development hypothesis predicts that the fall nymphs are younger and should therefore have a higher fat content compared to the spring nymphs (~3 months versus ~9 months since the larval blood meal). In contrast, the diapause development hypothesis predicts that the fall nymphs are older and should therefore have a lower fat content compared to the spring nymphs.

Statistical methods

The MASTREE database contains data on masting from year 1982 to year 2016, whereas our tick surveillance study ran from January 2004 to December 2018. We therefore had the beech masting scores one year prior for the DON in 2017 but not for the DON in 2018. For this reason, the statistical analyses are restricted to a 14-year period (2004 to 2017).

The density of nymphs (DON): The density of nymphs (DON) is a measure of the monthly abundance of questing nymphs per 100 m^2. The density of infected nymphs (DIN) is the number of questing nymphs infected with *B. burgdorferi* sl per 100 m^2. Over the 14-year study period that was covered by the MASTREE database, estimates of the DON and DIN were obtained from 558 fixed monthly transects (4 elevations * 14 years * 12 months = 672 transects; 114 missing transects due to snow and other reasons; 672 transects – 114 transects = 558 transects). The transects on the snow days were coded as missing data.

Definition of the spring nymphal peak and the fall nymphal peak: Previous work on the abundance of questing *I. ricinus* nymphs at Chaumont Mountain and at other nearby sites have shown a bimodal phenology with a large peak of the DON in the spring and a smaller peak of the DON in the fall [42, 43, 49, 50, 55]. To test which variables are best at explaining inter-annual variation in the spring and fall peaks of the DON, a date must be chosen to separate these two groups of nymphs. We decided that the spring peak included the nymphs sampled from January 1 to August 31, whereas the fall peak included the nymphs sampled from September 1 to December 31. This date was chosen because the DON reached a minimum at this time.

Weather on the day of tick sampling: To investigate if the weather influenced nymphal questing activity, we used the field-measured weather data on the day of tick sampling. An important advantage of the field-measured data compared to the weather station data was that they are specific for each of the four elevation sites. We did not use the field-measured weather data to calculate annual or seasonal means because there were not enough data (i.e., only 12 measurements per calendar year at each site).

Annual and seasonal mean climate variables: Life history traits (development, survival, reproduction) of tick populations depend on abiotic factors such as temperature, RH, SD, and precipitation (rain, snow). A great unknown is the relevant time frame over which these abiotic climate variables affect the vital rates of tick populations. For example, the DON in the spring might depend on the climate conditions of the previous winter (e.g., overwinter survival of nymphs), or on the climate conditions of the previous summer, which would influence the rates at which larvae obtain and digest their blood meals, and moult into nymphs. In our previous studies on inter-annual variation in the DON and DIN [12, 36], we calculated annual means for the climate variables that were based on a 12-month calendar year. However, many steps in the tick life cycle happen over shorter time scales; for example, engorged larvae take ~ 6 to 8 weeks to moult into nymphs at room temperature [64]. Thus, the life history traits of tick populations may depend on climate variables that are operating over shorter temporal windows (e.g., seasons rather than years). We therefore calculated mean seasonal climate variables for each of the 12 seasons (3 years * 4 seasons per year = 12 seasons) that preceded and encompassed the year of tick collection (Figure 2). The seasonal means for the winter, spring, summer, and fall were calculated as follows: December 1 (e.g., previous year) to February 28/29, March 1 to May 31, June 1 to August 31, and September 1 to November 30. As time lags are important in tick ecology, we calculated our annual mean climate variables and seasonal mean climate variables in the present year, the previous year, or two years prior (Figure 2). Thus, for each climate variable, there were a total of 12 seasonal means (3 years * 4 seasons per year = 12) and 3 annual means. The exception was the annual snow fall (units of cm) which was calculated over the time from October 1 (e.g., previous year) to May 31.

Annual beech masting score: Previous studies have shown that there is a 2-year time lag between masting events and the annual DON and the annual DIN [12, 14, 35, 36]. Our recent analyses of the same data showed that inter-annual variation in the DON and the DIN was strongly associated with the mast scores 2 years prior of European beech but not Norway spruce

[12, 36]. Upon further reflection, we realized that while the 2-year time lag is true for the spring peak it may not be true for the fall peak. The developmental diapause hypothesis and the direct development hypothesis predict that the time lag between the beech masting score and the fall peak of nymphs should be 2 years versus 1 year, respectively. To test these two hypotheses, we created three different explanatory variables, $BM_{2/2}$, $BM_{1/1}$, and $BM_{2/1}$, for the beech masting (BM) score. $BM_{2/2}$ assumes there is a 2-year time lag between BM and the spring and fall peaks of nymphs. $BM_{1/1}$ assumes there is a 1-year time lag between BM and the spring and fall peaks of nymphs. $BM_{2/1}$ assumes there is a 2-year time lag and a 1-year time lag between BM and the spring and fall peak, respectively. $BM_{2/2}$ is consistent with the developmental diapause hypothesis, $BM_{2/1}$ is consistent with the direct development hypothesis, and $BM_{1/1}$ is not consistent with either hypothesis.

The monthly DON was analysed using generalized additive models (GAMs): We used generalized additive models (GAMs) with extra-binomial errors to model the non-linear bimodal seasonal phenology of the monthly DON, which represent count data. GAMs are like generalized linear models, but an important difference is that smoother functions are used to model the response variable as a non-linear function of one or more explanatory variables. The smoother functions are non-parametric (they are like moving average functions) and can be used to fit any complex curve and this flexibility is a great strength of the GAM approach. A weakness is that there are no parameter estimates for the explanatory variables that are modelled with the smoother functions, which makes model interpretation more difficult.

Parametric versus non-parametric functions of explanatory variables: The major motivation for using GAMS was to capture the bimodal non-linear seasonal phenology of the DON over the calendar year. We compared the ability of smoother functions of calendar day, temperature, RH, and SD to capture this seasonal phenology. We also used the smoother function as a tool to investigate which explanatory variables were important for explaining variation in the DON without having to specify the nature of the relationship. However, if the relationship between the DON and an explanatory variable was obviously linear or quadratic, then we replaced the non-parametric smoother function of this explanatory variable with a parametric function because model interpretation is easier for simple parametric functions compared to complex non-parametric functions.

Variables used to model the DON: The explanatory variables that were investigated included elevation site (4 levels: low, medium, high, top), the covariate year (rescaled as 1, 2, 3, …, 14), the covariate day (rescaled as 1, 2, 3, …, 365), the covariate beech mast score (range: 1 to 5), the field-collected climate variables of temperature (t), relative humidity (rh), and saturation deficit (sd) on the day of tick sampling, and the mean annual and mean seasonal climate variables obtained from the weather stations for temperature (T), RH, SD, precipitation (PR), and annual snow fall (SN). For beech mast score there were three different types of variables, $BM_{2,2}$, $BM_{1,1}$, and $BM_{2,1}$, as previously discussed. For 4 climate variables (T, RH, SD, PR), there were 3 annual means and 12 seasonal means; for annual SN there were 3 annual means. The 72 explanatory variables and their acronyms are listed in Table 2.

Count data and extra-binomial errors: As the DON represents count data (number of nymphs per 100 m^2), we initially used the Poisson distribution to model the residual errors. The residuals from these models were highly overdispersed; the ratio of the residual deviance (7025) to the residual degrees of freedom (500) was > 1 (7025/500 = 14.05). This problem of overdispersion was solved by using the negative binomial distribution to model the residual errors; the residuals from these models were no longer overdispersed (517/514 = 1.01). Parameter estimates from models with Poisson errors (or extra-binomial errors) are reported on a log scale. Thus, the exponential function must be applied to the parameter estimates to determine the effect size of the explanatory variables on the DON on the original scale.

Models with Poisson errors (or extra-binomial errors) analyse count data, which are integers. However, the monthly DONs were not always integers because they had been measured over a transect area of 120 m^2 before being standardized to an area of 100 m^2. These non-integer DON values had to be rounded to the nearest integer to run GAMs with Poisson errors (or extra-binomial errors).

Scaling of the explanatory climate variables: All the annual and seasonal climate variables were transformed to z-scores with a mean of 0 and a standard deviation of 1. This transformation facilitates the comparison of slopes between climate variables measured in different units. One problem with modelling the response variable as a quadratic relationship of the explanatory variable is the strong collinearity between the linear and quadratic terms of the explanatory variable. To solve this problem, we transformed the explanatory variables using the *poly()* function in R so that the linear and quadratic terms were orthogonal to each other.

Model selection approach: To identify the best model, we used a model selection approach based on the Akaike information criterion (AIC). Models were ranked according to their AIC values, and the Akaike weights, which indicate the percent support, were calculated for each model. We used the Akaike weights to calculate the model-averaged parameter estimates and their 95% confidence intervals (CIs). For the generalized additive models that analysed the DON, we assessed the goodness of fit for the best model from the model selection table (Additional file 1: Section 2).

Statistical software: We used R version 4.0.3 for all statistical analyses [65]. We used the *gam()* function in the mgcv package to run the GAMs [66]. We used the *poly()* function in the base package to rescale the linear and quadratic terms of each explanatory climate variable to avoid problems with collinearity. We used the *mod.sel()* function and the *model.av()* function in the MuMIn package to create the model selection tables and the model-averaged parameter estimates [67]. We used the *ggplot()* function in the ggplot2 package to create the graphs that show the effect sizes of the explanatory variables [68].

RESULTS

Mean monthly DON at each of the four elevation sites: The mean monthly DON was inversely related to the altitudinal gradient; it was highest at the low elevation site and lowest at the top elevation site (Table 3; Additional file 1: Section 3). The mean monthly DON at the low, medium, high, and top elevation sites was 74.4, 61.4, 42.7, and 10.6 nymphs per 100 m^2, respectively (Table 3). If the low elevation site is set as the reference, the mean monthly DON at the medium, high, and top elevation sites were 19.3%, 41.2%, and 87.1% lower, respectively (Table 3; Additional file 1: Section 3). These estimates of the mean DON do not consider the effects of any other explanatory variables.

***I. ricinus* nymphs have a bimodal phenology on Chaumont Mountain:** The seasonal changes in the DON over the calendar year at the four elevation sites clearly showed a bimodal phenology with a large peak of the DON in the spring and a smaller peak of the DON in the fall (Figure 3). This bimodal phenology of the nymphs was observed at the low, medium, and high elevation sites, but not at the top elevation site where the phenology was characterized by a single peak in the spring. For each of the four elevation sites, we compared the size of the spring and fall nymphal peaks by calculating the area under the curve of the seasonal phenology (Table 4). Expressed as a percent of the total, the fall peak at the low, medium, high, and top elevation

sites was 14.9%, 11.5%, 12.5%, and 5.5%, respectively. Thus, the fall peak was largest for the low site and smallest for the top site. Interestingly, the spring peak occurred in April for the low site whereas it occurred in May at the medium, high, and top elevation sites.

Under the direct development hypothesis, we predict that the fall peak in year *y*-1 will be strongly correlated with the spring peak in year *y*. In contrast, under the diapause development hypothesis, we predict that the fall peak in year *y* should be strongly correlated with the spring peak in year *y*. To compare these two competing hypotheses, we created scatter plots of the fall peak versus the spring peak with different time lags and calculated the Pearson correlation coefficient. The fall peak in year *y*-1 was strongly correlated with the spring peak in year *y* for the low elevation site (Figure 4; $r = 0.866$, $p = 0.0001$) and the medium elevation site (Figure 4; $r = 0.730$, $p = 0.005$). In contrast, the fall peak and the spring peak in the same calendar year were not correlated (Additional file 1: Section 4). These results support the direct development hypothesis and provide strong evidence that the fall peak and spring peak that bookend the same winter represent the same generation of ticks.

We found that the bimodal non-linear phenology of the DON was best captured using GAMs that contained a non-parametric smoother function of the calendar day rather than temperature, relative humidity, or saturation deficit. Visual inspection shows that the values predicted by this smoother function of calendar day re-created the bimodal non-linear phenology of the DON (Additional file 1: Section 5).

Sequential modelling approach: To determine the best model for explaining variation in the monthly DON over the 14 years of the study (2004 to 2017) at the four elevation sites on Chaumont Mountain, we used a sequential modelling approach (Additional file 1: Section 6). We used our previous work on the same data set as starting point [12, 36]. We compared more than 639 GAMs that modelled the DON as a function of the various explanatory variables using AIC-based model selection (Additional file 1: Section 6). Our sequential modelling approach led us to a set of 13 models that are presented in Table 5.

Inter-annual variation in the fall and spring peaks of the DON are explained by different masting years: To investigate which of the 3 beech masting variables, $BM_{2/2}$, $BM_{1/1}$, $BM_{2/1}$, was best at explaining the inter-annual variation in the spring and fall nymphal peaks, we compared their performance on a common background model (i.e., model 1 in Table 5). The best model contained the masting explanatory variable $BM_{2/1}$, and had an AIC score of 4344.1, a support of 100.0%, and an r^2 value of 71.4%. In contrast, the models containing $BM_{2/2}$ and

$BM_{1/1}$ had AIC scores of 4481.3 and 4510.4 (ΔAIC with $BM_{2/1}$ was 137.2 and 166.3), no support, and r^2 values of 64.6% and 60.3%, respectively (Additional file 1: Section 7). A comparison of the model weights found that the support for the model with $BM_{2/1}$ was nonillion times greater (1*10^30) compared to the model with $BM_{2/2}$. Thus, the inter-annual variation in the spring and fall nymphal peaks are best explained by masting events that occurred 2 years prior and 1 year prior, respectively, which suggests that these two populations of nymphs are from different cohorts (i.e., born in different calendar years). This result provides strong evidence for the direct development hypothesis of the origin of the fall peak of nymphs.

AIC-based model selection analysis of the best model: The model selection table for all 13 models is presented in Table 5. For the monthly DON, the best model had a support of 98.0%, explained 71.4% of the variation in the DON, and contained the explanatory variables of site (partial r^2 = 13.8%), year (partial r^2 = 6.6%), site:year interaction (partial r^2 = 7.6%), beech mast score with different time lags for spring and fall peak ($BM_{2/1}$; partial r^2 = 16.0%), quadratic function of the temperature on the day of tick sampling (t and t^2; partial r^2 = 1.4%), quadratic function of the weather station mean seasonal SD of the summer in the present year (SD_{S0}, SD_{S0}^2, site:SD_{S0}, and site:SD_{S0}^2; partial r^2 = 4.3%), and the smoothed function of the calendar day for each of the four elevation sites (partial r^2 = 32.1%; Table 5).

The support for the 11 most important individual explanatory variables is shown in Table 6 and was as follows: site (100.0%), year (100.0%), site:year interaction (100.0%), beech mast score with different time lags for spring and fall peak ($BM_{2/1}$; 100.0%), temperature on the day of tick sampling (support is 100.0% for both t and t^2), smoothed function of the calendar day (100.0%), weather station mean seasonal SD of the summer in the present year (support is 97.8% to 97.9% for SD_{S0}, SD_{S0}^2, site:SD_{S0} interaction, and the site:SD_{S0}^2 interaction). None of the other explanatory variables had a support > 2.0% (Additional file 1: Section 8).

Parameter estimates for the explanatory variables: To determine the effect of the explanatory variables on the DON, we present the parameter estimates on the log scale (and their 95% confidence intervals; Table 7). We also back calculated the effect sizes of the explanatory variables on the DON on the original scale with respect to the following reference conditions: the site was low elevation, the year was 2004, and the beech tree mast index was 1. For simplicity, we present the parameter estimates from the top model (model 1 in Table 5), but we note that they are similar to the model-averaged parameter estimates (Additional file 1: Section 8).

The interaction between elevation site and year indicated that the change in the DON over time differed between the four elevation sites (Figure 5; Table 7). Over the 14-year period (2004–2017), the DON increased at the low elevation (slope = 0.056 per year, s.e. = 0.014, $p < 0.001$), and medium elevation (Medium – Low contrast of the slope = −0.035, s.e. = 0.020, $p = 0.073$) sites, but decreased at the high elevation (High – Low contrast of the slope = −0.091, s.e. = 0.019, $p < 0.001$), and top elevation (Top – Low contrast of the slope = −0.142, s.e. = 0.022, $p < 0.001$) sites. Over the 14-year period (2004–2017), the DON increased by 119.0% and 34.2% at the low and medium elevation sites but decreased by 38.7% and 70.0% at the high and top elevation sites, respectively (Figure 5).

The beech mast score with different time lags (2 years versus 1 year) for the spring and fall peak ($BM_{2/1}$) had a positive and significant effect on the DON (slope = 0.232 per class, s.e. = 0.017, $p < 0.001$; Figure 6; Table 7). Increasing the beech mast score from 1 (poor mast) to 5 (full mast) increased the DON by 152.9% at each of the four elevation sites on Chaumont Mountain (Figure 6).

The slope of the linear effect of the field-measured temperature (i.e., the temperature measured on the day of tick sampling) on the DON was positive and significant (slope = 9.616 per °C, s.e. = 1.229, $p < 0.001$; Figure 7; Table 7), indicating that the DON increased with temperature over the range of observed values (−5°C to 30°C). The slope of the quadratic effect of the field-measured temperature on the DON was negative and significant (slope = −8.822, s.e. = 0.927, $p < 0.001$; Figure 7; Table 7) indicating that the DON plateaued once the field-measured temperature reached ~ 30°C.

The SD_{S0} is the mean SD during the summer (1 June to 31 August) of the same year as the DON (i.e., no time lag). Thus, the SD_{S0} represents the SD during the last 3 months of the spring nymphal peak, just before the start of the fall peak. The significant interaction between elevation site and SD_{S0} indicates that the relationship between the DON and the SD_{S0} differed between the four elevation sites (Figure 8; Table 7). The relationship between the DON and the SD_{S0} was positive linear at the low and high elevation sites, and negative quadratic at the medium and top elevation sites. At the medium and top elevation sites, the DON decreased once the SD_{S0} reached ~ 5.5 mmHg and ~ 4.0 mmHg, respectively.

In summary, the DON had a bimodal phenology at the low, medium, and high elevation sites and a unimodal phenology at the top elevation site. The DON increased over time at the low and medium elevation sites, whereas it decreased at the high and top elevation sites. The DON increased significantly with beech masting index and the time lag differed between the two nymphal peaks with a 2-year time lag for the spring peak and a 1-year time lag for the fall

peak. This result provides strong evidence that the spring and fall nymphal peaks are distinct cohorts that are born in different years, which supports the direct development hypothesis and not the developmental diapause hypothesis. The DON increased with the field-measured temperature but reached a plateau at 30°C. Finally, the relationship between the DON and the seasonal SD of the summer in year *y* (SD_{S0}) was positive linear at the low and high elevation sites, and negative quadratic at the medium and top elevation sites.

Fall nymphs have higher fat content than the spring nymphs: We compared the log10-transformed fat content between the *I. ricinus* nymphs collected in the fall of 2010 and the nymphs collected in the spring of 2010 using a two independent samples t-test. The mean fat content of the fall nymphs (n = 40; 9.3 ug; 95% CI = 7.0 to 12.4) was 76.1% higher than that of the spring nymphs (n = 40; 5.3 ug; 95% CI = 4.0 to 7.1), and this difference was significant (Figure 9; t = 2.653, df = 68.003, p = 0.010). This result suggests that the fall nymphs are younger than the spring nymphs, which is consistent with the direct development hypothesis.

DISCUSSION

Given the importance of *I. ricinus* as a disease vector, forecasting the density of ticks questing for hosts is important for managing the risk of tick-borne diseases [12, 13, 35, 36, 69-71]. In Europe, there is much interest to determine which ecological factors are influencing the seasonal and inter-annual abundance of *I. ricinus* ticks [12, 35]. In continental Europe, *I. ricinus* nymphs have a bimodal seasonal phenology with a large spring peak followed by a smaller fall peak. There are at least two alternative hypotheses to explain the fall peak of nymphs: direct development and diapause development. We provide multiple lines of evidence that the fall peak is best explained by the direct development hypothesis at our field site in Switzerland. The fall peak of nymphs does not occur at our top elevation site because summer temperatures do not permit direct development of engorged larvae into nymphs. The fall peak in year *y*-1 is strongly correlated with the spring peak in year *y*, indicating that they represent the same tick generation. Inter-annual variation in the fall peak is best explained by a 1-year time lag with beech masting compared to the standard 2-year time lag for the spring peak. Fall nymphs have higher fat content than spring nymphs indicating that they are younger. All of these results are consistent with the direct development hypothesis and they are inconsistent with the diapause development hypothesis, as we explain in more detail below.

The *I. ricinus* nymphs at Chaumont Mountain have a bimodal phenology: The seasonal phenology of *I. ricinus* nymphs at Chaumont Mountain is bimodal where a large spring peak is followed by a smaller fall peak. This bimodal phenology occurred at the three lower elevation sites, whereas a unimodal phenology with a single large peak in the spring occurred at the top elevation site (Figure 3), and this discrepancy is consistent with the direct development hypothesis. The mean field-measured temperature in the spring and summer at the top elevation site is 5.4°C colder compared to the low elevation site. The result is that at the top site, tick development rates are slower, engorged larvae rarely (if ever) undergo direct development to questing nymphs in the same calendar year, and there is no fall peak of nymphs. Across Europe, we expect *I. ricinus* populations to have bimodal phenologies where longer, warmer summers facilitate direct development of engorged larvae into unfed nymphs in the summer so that they have enough time to quest and create the fall nymphal peak that same year (Table 1). In contrast, we expect unimodal phenologies to occur at northern latitudes or at high elevation sites (Table 1) where lower temperatures during the summer do not allow engorged larvae to complete their development from engorged larvae to unfed nymphs and quest in the same calendar year [40, 45, 72].

Our study also found that *I. ricinus* nymphs started questing earlier at the low elevation site (April) compared to the medium, high, and top elevation sites (May), and this result is probably also true for the larvae. Thus, larvae at the low site start questing earlier, which means that they have more time to complete their larvae-to-nymph moult and at faster development rates due to the elevated summer temperatures compared to larvae at the top elevation site. All these differences combine to create a fall nymphal peak that is prominent at the low elevation site and absent at the top elevation site, and this altitudinal gradient in phenology is consistent with the direct development hypothesis.

One cohort of larvae occurs in two different calendar years: A striking result of our study is the strong correlation between the fall nymphal peak in year *y*-1 and the spring nymphal peak in year *y* at both the low and medium elevation sites (Figure 4). In contrast, there is no correlation between the spring peak and the fall peak in the same calendar year (Additional file 1: Section 4). These results are consistent with the direct development hypothesis and they are not consistent with the diapause development hypothesis (Figure 2). Under the direct development hypothesis, the larvae that obtain an early larval blood meal and/or that develop fast in year *y*-1, will quest as nymphs in the fall of year *y*-1, whereas the larvae that obtain a late larval blood meal and/or that develop slow, will overwinter as unfed nymphs and quest in the

spring of year *y*. Under the direct development hypothesis, the tick year starts in the fall of year *y*-1 and ends in the summer of year *y* and it does not correspond to the calendar year. Studies that analyse inter-annual variation in the density of *I. ricinus* typically calculate a cumulative DON for the calendar year [12, 35, 36, 44, 49]. The present study shows that this approach is wrong when the fall peak and the spring peak in the same calendar year are two different cohorts of ticks. Researchers studying *I. ricinus* populations with a bimodal phenology should be aware that the fall nymphal peak and the spring nymphal peak that bookend the winter may be part of the same cohort of nymphs.

Beech masting has different time lags with the spring and fall nymphs: An important result is the strong and positive association between the beech masting score ($BM_{2/1}$) and the density of *I. ricinus* nymphs in the spring (Figure 6). For the spring peak, the consensus is that it consists of larvae that obtained their blood meal the previous spring and summer, moulted into nymphs in the summer (Kahl, 1989), entered behavioural diapause, overwintered as unfed nymphs, and quested the following spring [19, 45, 46]. We expect a 2-year time lag between beech masting and the spring nymphal peak because masting in the fall of year *y*-2 increases the density of mice and larval feeding success in the spring and summer of year *y*-1, which in turn increases the DON in the spring of year *y*. Studies in North America and Europe have shown that the masting events of deciduous trees can drive inter-annual variation in the DON and DIN of *Ixodes* nymphs with a 2-year time lag [14, 32, 33, 35]. We had previously shown using the same data from the present study that the beech masting score 2 years prior was highly significantly associated with inter-annual variation in the DON and DIN [12, 36]. In these studies, we had incorrectly assumed that the spring peak and fall peak that bookend the summer and occur in the same calendar year represent the same cohort of nymphs [12, 36]. Our previous studies found a strong association between beech masting 2 years prior and the cumulative DON because the spring peak is typically 6 to 7 times larger than the fall peak. Nevertheless, our decision to combine the spring and fall peak of the same calendar year into a single estimate of the annual DON and DIN was incorrect [12, 36].

The novel aspect of the present study is that our analysis of the bimodal phenology of the DON shows that the spring peak and the fall peak of the same calendar year represent different cohorts of nymphs. Inter-annual variation in the spring peak and fall peak was best predicted by the beach masting index 2 years prior and 1 year prior, respectively. This result provides strong evidence for the direct development hypothesis [38, 42, 43, 45, 46] which predicts a 1-year time lag between beech masting and the fall nymphal peak; masting in year *y*-

1 increases the density of mice and larval feeding success in year *y*, which in turn increases the DON in the fall of year *y*. In contrast, the developmental diapause hypothesis [19, 45, 46] predicts a 2-year time lag between beech masting and the fall nymphal peak; masting in year *y*-2 increases the density of mice and larval feeding success in year *y*-1, but larvae that obtain their blood meal in late summer have to overwinter as engorged larvae, moult into unfed nymphs the following summer, and quest in the fall of year *y*. A seminal review on diapause in *Ixodes* ticks presented both hypotheses, but appeared to favour the developmental diapause hypothesis over the direct development hypothesis [19]. In contrast, we found that the direct development hypothesis for the fall peak of *I. ricinus* nymphs had 100% support whereas the developmental diapause hypothesis had 0% support.

Differences in fat content between spring and fall nymphs support the direct development hypothesis: The direct development hypothesis predicts that the fall nymphs are younger compared to the spring nymphs (~3 months versus ~9 months since the larval blood meal), which agrees with studies comparing the fat content between these two types of nymphs in our study area and elsewhere [45, 63]. In the present re-analysis of the fat content of field-collected *I. ricinus* nymphs at our study location (Figure 9), we found that the fall nymphs had 76% more fat content than the spring nymphs [63], and studies in the UK have found a similar pattern [45]. This phenomenon can be explained by the direct development hypothesis; fall nymphs obtained their larval blood meal earlier that summer and their fat content is high because they are young (~3 months since the larval blood meal) with less time to burn their fat reserves. In contrast, spring nymphs obtained their larval meal the previous summer and their fat content is low because they are older (~9 months since the larval blood meal) with more time to burn their fat reserves. Thus, the finding that fall nymphs have higher fat reserves than spring nymphs is consistent with our discovery of 1-year and 2-year time lags for the fall and spring peak, and both these results support the direct development hypothesis.

Some studies have suggested a third explanation for the fall peak of *I. ricinus* nymphs. The summer quiescence hypothesis proposes that nymphal questing activity decreases in the late summer because the nymphs are hiding in the leaf litter from unfavourable conditions (high temperatures and low RH) and waiting to resume their questing activity in the fall when conditions are more favourable [18, 42]. We disagree with this hypothesis for two reasons. First, if the spring and fall peak are from the same cohort then the fall nymphs are older and should have lower fat content than the spring nymphs, but this is not the case [45, 63]. Second, if the spring and fall nymphs are from the same cohort then they should have the same time lag with

the masting index, but this was not the case in our study. In summary, our study does not support the summer quiescence hypothesis.

Effect of weather on the questing behaviour of *I. ricinus* nymphs: Our study found that the field-measured temperature on the day of tick sampling was positively correlated with the density of questing nymphs (Figure 7), which agrees with other studies in Europe [39, 73-76]. These studies suggest that for any given date, warmer temperatures increase the percentage of nymphs questing for hosts (i.e., increased nymphal activity levels), which in turn, increase the number of questing nymphs captured by drag sampling. *I. ricinus* becomes active above a minimum threshold temperature and questing activity increases with temperature up to some maximum value. While these threshold temperatures are expected to vary among tick populations from different geographical locations, a previous study at our field location suggested that the maximum threshold value was 24°C [42], whereas the present study found that this threshold was 30°C. *I. ricinus* is also sensitive to desiccation during questing [17], and they make repeated return trips to the litter layer where they can rehydrate and maintain their water balance [51, 52, 77]. For this reason, ticks prefer to quest under cool and humid conditions (i.e., low SD) [48, 78] and they reduce their questing activity in hot and dry conditions (i.e., high SD) [42, 50, 58, 79, 80]. Our observation that the DON plateaued at ~30°C in our study (Figure 7) suggests that *I. ricinus* nymphs at our study site avoid questing at hot (and presumably dry) conditions.

Effect of climate variables on the population ecology of *I. ricinus* ticks: Climate variables can influence tick population ecology via their effects on the vital rates (development, survival, reproduction). An interesting result of our study was that the seasonal climate variables were much more important than the annual climate variables at explaining the inter-annual variation in the DON. Our previous work found that annual climate variables (e.g., mean annual relative humidity and mean annual precipitation) were important for explaining the inter-annual variation in the DON or DIN [12, 36], but these studies did not investigate seasonal means. The present study is better because it compares climate variables operating at different temporal scales (i.e., annual versus seasonal). Many steps in the tick life cycle happen over short time scales suggesting that the critical climate variables operate over seasons rather than years. Researchers have addressed this issue by investigating a wide variety of durations and time lags [13, 49, 81]. For example, a 14-year study in Switzerland averaged the climate variables over different time intervals (1, 5, 10, 17 or 30 days) to determine the critical time period that

influences the DON [49]. An 8-year study in Germany used cross correlation maps to explore month-to-month correlations between the DON and climate variables, as well as time-lagged and interval-averaged correlations by considering a second time lag [13]. A 2-year study in five European countries examined time-lagged and interval-aggregated monthly and yearly means to test the associations between the abundance of questing *I. ricinus* nymphs and climate [81]. Despite this research effort, there is still uncertainty about which climate variables operating over what time scales drive the population ecology of *I. ricinus*.

Our study found that the relationship between the mean saturation deficit in the summer of that same year (SD_{S0}) and the DON differed among the four elevation sites (Figure 8). The relationship was positive linear for the low and high elevation sites, and it was negative quadratic for the medium and top elevation sites (Figure 8). The SD_{S0} is expected to have different effects on the spring and fall nymphs. With respect to the spring nymphs, increasing the SD is initially expected to increase the nymphal questing activity (the positive effects of higher temperatures outweigh the negative effects of lower relative humidity). However, the risk of desiccation and death both increase with high SD [50, 82], and at a certain threshold SD value, questing activity and survival will start to decrease for the spring nymphs (the negative effects of lower relative humidity outweigh the positive effects of higher temperatures). Thus, for the spring nymphs we expect a negative quadratic relationship between SD_{S0} and the DON, as observed at the medium and top elevation sites (Figure 8). With respect to the fall nymphs, a hot and dry summer (high SD) accelerates tick developmental rates, which under the direct development hypothesis, would increase the size of the fall nymphal peak of that calendar year [38, 42, 43, 45, 46]. In summary, the observed relationships between the SD_{S0} and the DON are broadly consistent with our expectations.

All three of our studies on this 15-year data set have found that RH (either acting alone or in combination with temperature to form the SD) in the present year (either annual or seasonal) was the most important climate variable for explaining variation in the DON or DIN [12, 36]. In our first study, the field-measured mean annual RH in the present year was negatively correlated with the annual DON [12]. In our second study, the weather station mean annual RH in the present year was negatively correlated with the DIN. In the present study, the best models in Table 5 included the summer SD in the present year (SD_{S0}) and the summer RH in the present year (RH_{S0}). However, one contradictory result in the present study was that the RH_{S0} was positively correlated with the DON (Additional file 1: Section 8). Thus, RH was always important for the ecology of *I. ricinus* but its correlation with the DON (negative or positive) differed among the three studies.

GAMs can model the bimodal phenology of *I. ricinus* nymphs: The bimodal non-linear phenology of *I. ricinus* nymphs is a challenge for statistical modelling. In our previous work, we avoided this complexity by analysing the total DON and DIN for each year and the same approach was used in a 14-year study in Switzerland that is near our study site [49], in a 10-year study in the Netherlands [44], and in a 13-year study in North America [14]. An 8-year study in Germany used different intercepts for the spring, summer, fall, and winter to deal with the non-linear phenology of *I. ricinus* nymphs [13]. We demonstrated that generalized additive models (GAMs) are a useful approach to model the bimodal non-linear phenology of *I. ricinus* nymphs because they allow the user to flexibly model the response variable as a non-parametric and non-linear smoothed function of the explanatory variables of interest. The smoothed function of the calendar day was an excellent fit to the seasonal phenology of *I. ricinus* nymphs (Additional file 1: Section 5). The other explanatory variables (e.g., beech masting score and climate variables) were initially modelled with non-parametric smoothed functions because we did not want to assume a linear function, but were subsequently replaced with parametric functions (e.g., linear or quadratic). In summary, we demonstrated that the bimodal non-linear phenology of *I. ricinus* ticks can be captured by GAMs using a combination of parametric and non-parametric functions of the explanatory variables of interest.

Conclusion: At our study location, the *I. ricinus* populations have a bimodal phenology at the lower elevation sites, but a unimodal phenology at the top elevation site. At the low and medium elevation sites, the fall nymphal peak in year *y*-1 was strongly correlated with the spring nymphal peak in year *y* over the 15 years of the study. In contrast, there was no correlation between the fall peak and the spring peak in the same calendar year. Inter-annual variation in the fall nymphal peak and spring nymphal peak were strongly associated with the beech masting index 1 year prior and 2 years prior, respectively. Fall nymphs had lower fat content than spring nymphs indicating that they are younger in age. All these results support the direct development hypothesis, and they contradict the diapause development hypothesis. In areas with a bimodal phenology, the DON and risk of tick-borne disease will increase 1 year later in the fall and 2 years later in the spring. Studies on the population ecology of *I. ricinus* should consider that the fall and peak that bookend the same winter contain the same generation of ticks. Studies on the annual abundance of *I. ricinus* should calculate this variable over the tick year (start of the fall in year *y*-1 to end of the summer of year *y*) and not the calendar year.

Additional files

Additional file 1: Section 1. Interpolation of the climate data from the weather stations. **Section 2.** Goodness of fit for the best model. **Section 3.** Effect of elevation site on the density of *I. ricinus* nymphs. **Section 4.** Correlation plots between the fall peak and the spring peak with different time lags. **Section 5.** Smoother function of calendar day predicts the bimodal phenology of *I. ricinus* nymphs at the four elevation sites. **Section 6.** Sequential modelling approach. **Section 7.** Comparison of the beech masting variables with different time lags and the inter-annual variation in the spring and fall peaks of the DON. **Section 8.** Full AIC-based model selection analysis. (DOCX).

Abbreviations

AIC: Akaike information criterion; ASL: Above sea level; BM: Beech masting; DIN: Density of infected nymphs; DON: Density of nymphs; GAMs: Generalized additive models; PR: Precipitation; RH: Relative humidity; SD: Saturation deficit; SN: Snow fall; T: Temperature; WMO: World Meteorological Organization.

Acknowledgements

We would like to thank Lise Gern for her financial support and for generously giving us these data. This study was part of the PhD thesis of Cindy Bregnard.

Declarations

Ethics approval and consent to participate

Not applicable

Consent for publication

Not applicable

Availability of data and materials

The raw data for this study are stored in the Additional file 2. The climate data are available from the Climap-net database of the Federal Office for Meteorology and Climatology (http://www.meteosuisse.admin.ch/home/service-et-publications/conseil-et-service/portail-de-donnees-dedie-aux-specialistes.html). The MASTREE database is available in the Ecology –

Ecological Society of America repository (http://onlinelibrary.wiley.com/doi/10.1002/ecy.1785/suppinfo).

Competing interests

The authors declare that they have no competing interests.

Funding

This study was supported by grants obtained by Lise Gern from the Swiss National Science Foundation: FN 32-57098.99, FN 3200B0-100657, FN 320000-113936 and FN 310030-127064 and by grants obtained by Lise Gern from the Federal Office of Public Health National Reference Center: 2009/10 (Projekt (911) 316) and 2011/13 (11.006911/ 304.0001-707). The doctoral salary of Cindy Bregnard was supported by the University of Neuchâtel. This research was also supported by two grants awarded to Maarten J. Voordouw, a Discovery Grant from the Natural Sciences and Engineering Research Council of Canada (RGPIN-2019-04483) and an Establishment Grant from the Saskatchewan Health Research Foundation (4583).

Authors' contributions

OR collected the ticks and the meteorological data in the field and managed the data. CH generated the data on the fat content in *I. ricinus* nymphs. CB and MJV analysed the data and wrote the manuscript. OK provided critical insight into how diapause structures the bimodal phenology of *I. ricinus* in continental Europe. KB provided critical insight into modelling the DON as a function of climate variables averaged over different temporal windows and with different time lags. All authors read and approved the final version of the manuscript.

REFERENCES

1. Lindgren E, Tälleklint L, Polfeldt T. Impact of climatic change on the northern latitude limit and population density of the disease-transmitting European tick *Ixodes ricinus*. Environ Health Perspect. 2000;108:119-23.
2. Jaenson TGT, Jaenson DG, Eisen L, Petersson E, Lindgren E. Changes in the geographical distribution and abundance of the tick *Ixodes ricinus* during the past 30 years in Sweden. Parasit Vectors. 2012;5:8.
3. Ogden NH, Lindsay LR, Morshed M, Sockett PN, Artsob H. The emergence of Lyme disease in Canada. CMAJ. 2009;180:1221-4.
4. Gasmi S, Ogden NH, Lindsay LR, Burns S, Fleming S, Badcock J, et al. Surveillance for Lyme disease in Canada: 2009-2015. Can Commun Dis Rep. 2017;43:194-9.
5. Brownstein JS, Holford TR, Fish D. Effect of climate change on Lyme disease risk in North America. EcoHealth. 2005;2:38-46.
6. Medlock J, Leach S. Impact of climate change on vector-borne disease in the UK. Lancet. 2015;15:159-99.
7. Rosenberg R, Lindsey N, Fischer M, Gregory C, Hinckley A, Mead P, et al. Vital signs : trends in reported vectorborne disease cases — United States and territories, 2004–2016. MMWR Morbidity and Mortality Weekly Report. 2018;67:1-6.
8. Jongejan F, Uilenberg G. The global importance of ticks. Parasitology. 2005;129:3-14.
9. Gray J, Kahl O, Zintl A. What do we still need to know about *Ixodes ricinus*? Ticks Tick Borne Dis. 2021;12:101682.
10. Hofmeester T, Coipan E, Van Wieren S, Prins H, Takken W, Sprong H. Few vertebrate species dominate the *Borrelia burgdorferi* sl life cycle. Environ Res Lett. 2016;11:043001.
11. Morán Cadenas F, Rais O, Humair PF, Douet V, Moret J, Gern L. Identification of host bloodmeal source and *Borrelia burgdorferi* sensu lato in field-collected *Ixodes ricinus* ticks in Chaumont (Switzerland). J Med Entomol. 2007;44:1109-17.
12. Bregnard C, Rais O, Voordouw MJ. Climate and tree seed production predict the abundance of the European Lyme disease vector over a 15-year period. Parasit Vectors. 2020;13:408.
13. Brugger K, Walter M, Chitimia-Dobler L, Dobler G, Rubel F. Seasonal cycles of the TBE and Lyme borreliosis vector *Ixodes ricinus* modelled with time-lagged and interval-averaged predictors. Exp Appl Acarol. 2017;73:439-50.

14. Ostfeld RS, Canham CD, Oggenfuss K, Winchcombe RJ, Keesing F. Climate, deer, rodents, and acorns as determinants of variation in Lyme-disease risk. PLoS Biol. 2006;4:e145.
15. Krawczyk AI, van Duijvendijk GLA, Swart A, Heylen D, Jaarsma RI, Jacobs FHH, et al. Effect of rodent density on tick and tick-borne pathogen populations: consequences for infectious disease risk. Parasit Vectors. 2020;13:34.
16. Perez G, Bastian S, Agoulon A, Bouju A, Durand A, Faille F, et al. Effect of landscape features on the relationship between *Ixodes ricinus* ticks and their small mammal hosts. Parasit Vectors. 2016;9:20.
17. Gray JS. Review The ecology of ticks transmitting Lyme borreliosis. Exp Appl Acarol. 1998;22:249-58.
18. Gray JS. The development and seasonal activity of the tick *Ixodes ricinus*: a vector of Lyme borreliosis. Rev MedVet Entomol. 1991;79:323-33.
19. Gray JS, Kahl O, S. Lane R, Levin M, Tsao J. Diapause in ticks of the medically important *Ixodes ricinus* species complex. Ticks Tick Borne Dis. 2016;7:992-1003.
20. Stanek G, Wormser GP, Gray J, Strle F. Lyme borreliosis. Lancet. 2012;379:461-73.
21. Randolph SE. Tick ecology: processes and patterns behind the epidemiological risk posed by ixodid ticks as vectors. Parasitology. 2004;129:37-65.
22. Ogden NH, Lindsay LR, Beauchamp G, Charron D, Maarouf A, O'Callaghan CJ, et al. Investigation of relationships between temperature and developmental rates of tick *Ixodes scapularis* (Acari: Ixodidae) in the laboratory and field. J Med Entomol. 2004;41:622-33.
23. Gray JS, Dautel H, Estrada-Peña A, Kahl O, Lindgren E. Effects of climate change on ticks and tick-borne diseases in europe. Interdiscip Perspect Infect Dis. 2009;2009:593232.
24. Ogden NH, Tsao JI. Biodiversity and Lyme disease: dilution or amplification? Epidemics. 2009;1:196-206.
25. Randolph SE. Ticks are not insects: consequences of contrasting vector biology for transmission potential. Parasitol Today. 1998;14:186-92.
26. Clotfelter E, Pedersen A, Cranford J, Ram N, Snajdr E, Nolan V, et al. Acorn mast drives long-term dynamics of rodent and songbird populations. Oecologia. 2008;154:493-503.
27. Schnurr JL, Ostfeld RS, Canham CD. Direct and indirect effects of masting on rodent populations and tree seed survival. Oikos. 2002;96:402-10.

28. Drobyshev I, Niklasson M, Mazerolle MJ, Bergeron Y. Reconstruction of a 253-year long mast record of European beech reveals its association with large scale temperature variability and no long-term trend in mast frequencies. Agric For Meteorol. 2014;192:9-17.
29. Drobyshev I, Övergaard R, Saygin I, Niklasson M, Hickler T, Karlsson M, et al. Masting behaviour and dendrochronology of European beech (*Fagus sylvatica* L.) in southern Sweden. For Ecol Manag. 2010;259:2160-71.
30. Piovesan G, Adams JM. Masting behaviour in beech: linking reproduction and climatic variation. Can J Bot. 2001;79:1039-47.
31. Övergaard R, Gemmel P, Karlsson M. Effects of weather conditions on mast year frequency in beech (*Fagus sylvatica* L.) in Sweden. Forestry. 2007;80:555-65.
32. Ostfeld RS, Levi T, Keesing F, Oggenfuss K, Canham CD. Tick-borne disease risk in a forest food web. Ecology. 2018;99:1562-73.
33. Ostfeld RS, Schauber EM, Canham CD, Keesing F, Jones CG, Wolff JO. Effects of acorn production and mouse abundance on abundance and *Borrelia burgdorferi* infection prevalence of nymphal *Ixodes scapularis* ticks. Vector Borne Zoonotic Dis. 2001;1:55-63.
34. Schauber EM, Ostfeld RS, Evans J, Andrew S. What is the best predictor of annual Lyme disease incidence: weather, mice, or acorns? Ecol Appl. 2005;15:575-86.
35. Brugger K, Walter M, Chitimia-Dobler L, Dobler G, Rubel F. Forecasting next season's *Ixodes ricinus* nymphal density: the example of southern Germany 2018. Exp Appl Acarol. 2018;75:281-8.
36. Bregnard C, Rais O, Voordouw MJ. Masting by beech trees predicts the risk of Lyme disease. Parasit Vectors. 2021;14:168.
37. Belozerov V. Diapause and biological rhythms in ticks. In: Obenchain FD, Galun R, editors. Physiology of Ticks: Pergamon; 1982. p. 469-500.
38. Korenberg EI. Seasonal population dynamics of *Ixodes* ticks and tick-borne encephalitis virus. Exp Appl Acarol. 2000;24:665-81.
39. Dautel H, Dippel C, Kämmer D, Werkhausen A, Kahl O. Winter activity of *Ixodes ricinus* in a Berlin forest. Int J Med Microbiol. 2008;298:50-4.
40. Steele G, Randolph S. An experimental evaluation of conventional control measures against the sheep tick, *Ixodes ricinus* (L.) (Acari: Ixodidae). I. A unimodal seasonal activity pattern. Bull Entomol Res. 1985;75.

41. Tälleklint L, Jaenson TG. Seasonal variations in density of questing *Ixodes ricinus* (Acari: Ixodidae) nymphs and prevalence of infection with *B. burgdorferi* s.l. in south central Sweden. J Med Entomol. 1996;33:592-7.
42. Perret JL, Guigoz E, Rais O, Gern L. Influence of saturation deficit and temperature on *Ixodes ricinus* tick questing activity in a Lyme borreliosis-endemic area (Switzerland). Parasitol Res. 2000;86:554-7.
43. Jouda F, Perret JL, Gern L. *Ixodes ricinus* density, and distribution and prevalence of *Borrelia burgdorferi* sensu lato infection along an altitudinal gradient. J Med Entomol. 2004;41:162-9.
44. Hartemink N, van Vliet A, Sprong H, Jacobs F, Garcia-Marti I, Zurita-Milla R, et al. Temporal-spatial variation in questing tick activity in the Netherlands: The effect of climatic and habitat factors. Vector Borne Zoonotic Dis. 2019;19:494-505.
45. Randolph SE, Green RM, Hoodless AN, Peacey MF. An empirical quantitative framework for the seasonal population dynamics of the tick *Ixodes ricinus*. Int J Parasitol. 2002;32:979-89.
46. Gray J. The development and questing activity of *Ixodes ricinus* (L.) (Acari: Ixodidae) under field conditions in Ireland. Bull Entomol Res. 1982;72:263-70.
47. Knap N, Durmiši E, Saksida A, Korva M, Petrovec M, Avšič-Županc T. Influence of climatic factors on dynamics of questing *Ixodes ricinus* ticks in Slovenia. Vet Parasitol. 2009;164:275-81.
48. Burtis JC, Sullivan P, Levi T, Oggenfuss K, Fahey TJ, Ostfeld RS. The impact of temperature and precipitation on blacklegged tick activity and Lyme disease incidence in endemic and emerging regions. Parasit Vectors. 2016;9:606.
49. Hauser G, Rais O, Morán Cadenas F, Gonseth Y, Bouzelboudjen M, Gern L. Influence of climatic factors on *Ixodes ricinus* nymph abundance and phenology over a long-term monthly observation in Switzerland (2000–2014). Parasit Vectors. 2018;11:289.
50. Perret J-L, Rais O, Gern L. Influence of climate on the proportion of *Ixodes ricinus* nymphs and adults questing in a tick population. J Med Entomol. 2004;41:361-5.
51. MacLeod J. *Ixodes ricinus* in relation to its physical environment: II. The factors governing survival and activity. Parasitology. 1935;27:123-44.
52. Lees AD. The water balance in *Ixodes ricinus* L. and certain other species of ticks. Parasitology. 1946;37:1-20.
53. Lees AD. The sensory physiology of the sheep tick, *Ixodes Ricinus* L. J Exp Biol. 1948;25:145-207.

54. van Oort BEH, Hovelsrud GK, Risvoll C, Mohr CW, Jore S. A mini-review of *Ixodes* ticks climate sensitive infection dispersion risk in the nordic region. Int J Env Res Public Health. 2020;17:5387.
55. Morán Cadenas F, Rais O, Jouda F, Douet V, Humair PF, Moret J, et al. Phenology of *Ixodes ricinus* and infection with *Borrelia burgdorferi* sensu lato along a north- and south-facing altitudinal gradient on Chaumont Mountain, Switzerland. J Med Entomol. 2007;44:683-93.
56. Jore S, Vanwambeke SO, Viljugrein H, Isaksen K, Kristoffersen AB, Woldehiwet Z, et al. Climate and environmental change drives *Ixodes ricinus* geographical expansion at the northern range margin. Parasit Vectors. 2014;7:11.
57. NFI TSNFI: Portrait des arbres forestiers les plus fréquents. https://www.lfi.ch/resultate/baumarten-fr.php (2017). Accessed April 12 2021.
58. Randolph SE, Storey K. Impact of microclimate on immature tick-rodent host interactions (Acari: Ixodidae): implications for parasite transmission. J Med Entomol. 1999;36:741-8.
59. Bogdziewicz M, Kelly D, Thomas PA, Lageard JG, Hacket-Pain A. Climate warming disrupts mast seeding and its fitness benefits in European beech. Nature Plants. 2020;6:88-94.
60. Ascoli D, Maringer J, Hacket-Pain A, Conedera M, Drobyshev I, Motta R, et al. Two centuries of masting data for European beech and Norway spruce across the European continent. Ecology. 2017;98:1473.
61. Knülle W, Rudolph D. Humidity relationships and water balance of ticks. vol. 1; 1982.
62. Herrmann C, Gern L. Search for blood or water is influenced by *Borrelia burgdorferi* in *Ixodes ricinus*. Parasit Vectors. 2015;8:6.
63. Herrmann C, Voordouw MJ, Gern L. *Ixodes ricinus* ticks infected with the causative agent of Lyme disease, *Borrelia burgdorferi* sensu lato, have higher energy reserves. Int J Parasitol. 2013;43:477-83.
64. Hurry G, Maluenda E, Sarr A, Belli A, Hamilton P, Duron O, et al. Infection with *Borrelia afzelii* reduces moulting time of *Ixodes ricinus* ticks. 2021.
65. R Development Core Team: R: A language and environement for statistical computing. Vienna, Austria: R Foundation for Statistical Computing; 2013.
66. Wood SN. Generalized additive models: an introduction with R. CRC press; 2017.
67. Bartoń K: MuMIn: Multi-model inference. R package version 1.43.17. https://CRAN.R-project.org/package=MuMIn (2020). Accessed April 12 2021.

68. Wickham H: ggplot2: Elegant graphics for data analysis. https://ggplot2.tidyverse.org (2016). Accessed April 12 2021.
69. Rubel F, Brugger K. Tick-borne encephalitis incidence forecasts for Austria, Germany, and Switzerland. Ticks Tick Borne Dis. 2020;11:101437.
70. Rubel F, Brugger K. Operational TBE incidence forecasts for Austria, Germany, and Switzerland 2019–2021. Ticks Tick Borne Dis. 2021;12:101579.
71. Rubel F, Walter M, Vogelgesang JR, Brugger K. Tick-borne encephalitis (TBE) cases are not random: explaining trend, low- and high-frequency oscillations based on the Austrian TBE time series. BMC Infect Dis. 2020;20:448.
72. Kurtenbach K, Hanincová K, Tsao JI, Margos G, Fish D, Ogden NH. Fundamental processes in the evolutionary ecology of Lyme borreliosis. Nature Reviews Microbiology. 2006;4:660-9.
73. Kiewra D, Kryza M, Szymanowski M. Influence of selected meteorological variables on the questing activity of *Ixodes ricinus* ticks in Lower Silesia, SW Poland. J Vector Ecol. 2014;39:138-45.
74. Li S, Heyman P, Cochez C, Simons L, Vanwambeke SO. A multi-level analysis of the relationship between environmental factors and questing *Ixodes ricinus* dynamics in Belgium. Parasit Vectors. 2012;5:149.
75. Schwarz A, Maier WA, Kistemann T, Kampen H. Analysis of the distribution of the tick *Ixodes ricinus* L. (Acari: Ixodidae) in a nature reserve of western Germany using Geographic Information Systems. Int J Hyg Environ Health. 2009;212:87-96.
76. Hubálek Z, Halouzka J, Juricova Z. Host-seeking activity of ixodid ticks in relation to weather variables. J Vector Ecol. 2003;28:159-65.
77. Mejlon HA, Jaenson TGT. Questing behaviour of *Ixodes ricinus* ticks (Acari: Ixodidae). Exp Appl Acarol. 1997;21:747-54.
78. Schulze TL, Jordan RA, Schulze CJ, Hung RW. Precipitation and temperature as predictors of the local abundance of *Ixodes scapularis* (Acari: Ixodidae) nymphs. J Med Entomol. 2009;46:1025-9.
79. Herrmann C, Gern L. Do the level of energy reserves, hydration status and *Borrelia* infection influence walking by *Ixodes ricinus* (Acari: Ixodidae) ticks? Parasitology. 2012;139:330-7.
80. Perret JL, Guerin PM, Diehl PA, Vlimant M, Gern L. Darkness induces mobility, and saturation deficit limits questing duration, in the tick *Ixodes ricinus*. J Exp Biol. 2003;206:1809-15.

81. Rosà R, Andreo V, Tagliapietra V, Baráková I, Arnoldi D, Hauffe HC, et al. Effect of climate and land use on the spatio-temporal variability of tick-borne bacteria in Europe. Int J Env Res Public Health. 2018;15:732.
82. Tagliapietra V, Rosà R, Arnoldi D, Cagnacci F, Capelli G, Montarsi F, et al. Saturation deficit and deer density affect questing activity and local abundance of *Ixodes ricinus* (Acari, Ixodidae) in Italy. Vet Parasitol. 2011;183:114-24.
83. Gray JS. Studies on the dynamics of active populations of the sheep tick, *Ixodes ricinus* L. in Co. Wicklow, Ireland. Acarologia. 1984;25:167-78.
84. Burri C, Morán Cadenas F, Douet V, Moret J, Gern L. *Ixodes ricinus* density and infection prevalence of *Borrelia burgdorferi* sensu lato along a north-facing altitudinal gradient in the Rhône Valley (Switzerland). Vector Borne Zoonotic Dis. 2007;7:50-8.
85. Estrada-Peña A, Martinez JM, Acedo CS, Quilez J, Cacho ED. Phenology of the tick, *Ixodes ricinus*, in its southern distribution range (central Spain). Med Vet Entomol. 2004;18:387-97.
86. Daniel M, Malý M, Danielová V, Kříž B, Nuttall P. Abiotic predictors and annual seasonal dynamics of *Ixodes ricinus*, the major disease vector of central Europe. Parasit Vectors. 2015;8:478.
87. Sormunen JJ, Klemola T, Vesterinen EJ, Vuorinen I, Hytönen J, Hänninen J, et al. Assessing the abundance, seasonal questing activity, and *Borrelia* and tick-borne encephalitis virus (TBEV) prevalence of *Ixodes ricinus* ticks in a Lyme borreliosis endemic area in southwest Finland. Ticks Tick Borne Dis. 2016;7:208-15.
88. Cayol C, Koskela E, Mappes T, Siukkola A, Kallio ER. Temporal dynamics of the tick *Ixodes ricinus* in northern Europe: epidemiological implications. Parasit Vectors. 2017;10:1-11.
89. Borde JP, Kaier K, Hehn P, Matzarakis A, Frey S, Bestehorn M, et al. The complex interplay of climate, TBEV vector dynamics and TBEV infection rates in ticks—Monitoring a natural TBEV focus in Germany, 2009–2018. PLOS ONE. 2021;16:e0244668.
90. Vogelgesang JR, Walter M, Kahl O, Rubel F, Brugger K. Long-term monitoring of the seasonal density of questing ixodid ticks in Vienna (Austria): setup and first results. Exp Appl Acarol. 2020;81:409-20.

Table 1. Type of phenology for *Ixodes ricinus* ticks in different countries in Europe.

Phenology	Country	Region	Studies
Unimodal	UK	Powys	[40]
Unimodal	Sweden	Bogesund	[41]
Unimodal	Switzerland	Chaumont Mountain	[42, 43]
Unimodal	Netherlands		[44]
Bimodal	Ireland	County Wicklow	[83]
Bimodal	Sweden	Bogesund	[41]
Bimodal	Crimea		[38]
Bimodal	Switzerland	Chaumont Mountain, Salins	[42, 43, 49, 50, 55, 84]
Bimodal	UK	Exmoor National Park, Mynydd Mallaen, Dorset	[45]
Bimodal	Spain	Rioja region	[85]
Bimodal	Czech Republic	Prague	[86]
Bimodal	Finland	Seili, Jyväskylä	[87, 88]
Bimodal	Germany	Haselmuehl	[89]
Bimodal	Austria	Vienna	[90]

Notes: *Ixodes ricinus* ticks (nymphs and adults) either have a unimodal or bimodal phenology. The phenology is shown for different countries and regions in Europe. The decision of whether a study found a unimodal or bimodal phenology was based on whether the authors of the study identified the mode of phenology as either unimodal or bimodal in the article.

Table 2. Acronym and definition of each variable used in the present study.

Acronym	Description
DON	Monthly density of nymphs per $100m^2$
S	Site name (factor with 4 levels: low, medium, high, top)
Y	Year of the study (covariate: 1, 2, …, 15)
D	Day of the year for the tick sampling (covariate: 1, 2, …, 365)
$BM_{1/1}$	Beech mast score in year *y*-1 (covariate: 1, 2, …, 5)
$BM_{2/2}$	Beech mast score in year *y*-2 (covariate: 1, 2, …, 5)
$BM_{2/1}$	Beech mast score with a 2-year time lag for the spring peak and a 1-year time lag for the fall peak (covariate: 1, 2, …, 5)
t	Temperature on day of sampling from the field-collected data (°C)
rh	Relative humidity on day of sampling from the field-collected data (%)
sd	Saturation deficit on day of sampling from the field-collected data (mmHg)
T_{Y0}	Mean annual temperature in year *y* from the weather station data (°C)
T_{Y1}	Mean annual temperature in year *y*-1 from the weather station data (°C)
T_{Y2}	Mean annual temperature in year *y*-2 from the weather station data (°C)
RH_{Y0}	Mean annual relative humidity in year *y* from the weather station data (%)
RH_{Y1}	Mean annual relative humidity in year *y*-1 from the weather station data (%)
RH_{Y2}	Mean annual relative humidity in year *y*-2 from the weather station data (%)
SD_{Y0}	Mean annual saturation deficit in year *y* from the weather station data (mmHg)
SD_{Y1}	Mean annual saturation deficit in year *y*-1 from the weather station data (mmHg)
SD_{Y2}	Mean annual saturation deficit in year *y*-2 from the weather station data (mmHg)
PR_{Y0}	Mean annual precipitation in year *y* from the weather station data (mm)
PR_{Y1}	Mean annual precipitation in year *y*-1 from the weather station data (mm)
PR_{Y2}	Mean annual precipitation in year *y*-2 from the weather station data (mm)
SN_{Y0}	Annual snowfall in year *y* from the weather station data (cm)
SN_{Y1}	Annual snowfall in year *y*-1 from the weather station data (cm)
SN_{Y2}	Annual snowfall in year *y*-2 from the weather station data (cm)
T_{F0}	Mean seasonal temperature of the fall in year *y* from the weather station data (°C; mean daily temperature was averaged over months of September, October, and November)
T_{S0}	Mean seasonal temperature of the summer in year *y* from the weather station data (°C; mean daily temperature was averaged over months of June, July, and August)
T_{L0}	Mean seasonal temperature of the spring in year *y* from the weather station data (°C; mean daily temperature was averaged over months of March, April, and May)
T_{W0}	Mean seasonal temperature of the winter in year *y* from the weather station data (°C; mean daily temperature was averaged over months of December, January, and February)
T_{F1}	Mean seasonal temperature of the fall in year *y*-1 from the weather station data (°C; mean daily temperature was averaged over months of September, October, and November)
T_{S1}	Mean seasonal temperature of the summer in year *y*-1 from the weather station data (°C; mean daily temperature was averaged over months of June, July, and August)
T_{L1}	Mean seasonal temperature of the spring in year *y*-1 from the weather station data (°C; mean daily temperature was averaged over months of March, April, and May)

T_{W1} Mean seasonal temperature of the winter in year *y*-1 from the weather station data (°C; mean daily temperature was averaged over months of December, January, and February)

T_{F2} Mean seasonal temperature of the fall in year *y*-2 from the weather station data (°C; mean daily temperature was averaged over months of September, October, and November)

T_{S2} Mean seasonal temperature of the summer in year *y*-2 from the weather station data (°C; mean daily temperature was averaged over months of June, July, and August)

T_{L2} Mean seasonal temperature of the spring in year *y*-2 from the weather station data (°C; mean daily temperature was averaged over months of March, April, and May)

T_{W2} Mean seasonal temperature of the winter in year *y*-2 from the weather station data (°C; mean daily temperature was averaged over months of December, January, and February)

RH_{F0} Mean seasonal relative humidity of the fall in year *y* from the weather station data (%; mean daily relative humidity was averaged over months of September, October, and November)

RH_{S0} Mean seasonal relative humidity of the summer in year *y* from the weather station data (%; mean daily relative humidity was averaged over months of June, July, and August)

RH_{L0} Mean seasonal relative humidity of the spring in year *y* from the weather station data (%; mean daily relative humidity was averaged over months of March, April, and May)

RH_{W0} Mean seasonal relative humidity of the winter in year *y* from the weather station data (%; mean daily relative humidity was averaged over months of December, January, and February)

RH_{F1} Mean seasonal relative humidity of the fall in year *y*-1 from the weather station data (%; mean daily relative humidity was averaged over months of September, October, and November)

RH_{S1} Mean seasonal relative humidity of the summer in year *y*-1 from the weather station data (%; mean daily relative humidity was averaged over months of June, July, and August)

RH_{L1} Mean seasonal relative humidity of the spring in year *y*-1 from the weather station data (%; mean daily relative humidity was averaged over months of March, April, and May)

RH_{W1} Mean seasonal relative humidity of the winter in year *y*-1 from the weather station data (%; mean daily relative humidity was averaged over months of December, January, and February)

RH_{F2} Mean seasonal relative humidity of the fall in year *y*-2 from the weather station data (%; mean daily relative humidity was averaged over months of September, October, and November)

RH_{S2} Mean seasonal relative humidity of the summer in year *y*-2 from the weather station data (%; mean daily relative humidity was averaged over months of June, July, and August)

RH_{L2} Mean seasonal relative humidity of the spring in year *y*-2 from the weather station data (%; mean daily relative humidity was averaged over months of March, April, and May)

RH_{W2} Mean seasonal relative humidity of the winter in year *y*-2 from the weather station data (%; mean daily relative humidity was averaged over months of December, January, and February)

SD_{F0} Mean seasonal saturation deficit of the fall in year *y* from the weather station data (mmHg; mean daily saturation deficit was averaged over months of September, October, and November)

SD_{S0} Mean seasonal saturation deficit of the summer in year *y* from the weather station data (mmHg; mean daily saturation deficit was averaged over months of June, July, and August)

SD_{L0} Mean seasonal saturation deficit of the spring in year *y* from the weather station data (mmHg; mean daily saturation deficit was averaged over months of March, April, and May)

SD_{W0} Mean seasonal saturation deficit of the winter in year *y* from the weather station data (mmHg; mean daily saturation deficit was averaged over months of December, January, and February)

SD_{F1} Mean seasonal saturation deficit of the fall in year *y*-1 from the weather station data (mmHg; mean daily saturation deficit was averaged over months of September, October, and November)

SD_{S1} Mean seasonal saturation deficit of the summer in year *y*-1 from the weather station data (mmHg; mean daily saturation deficit was averaged over months of June, July, and August)

SD_{L1} Mean seasonal saturation deficit of the spring in year *y*-1 from the weather station data (mmHg; mean daily saturation deficit was averaged over months of March, April, and May)

SD_{W1} Mean seasonal saturation deficit of the winter in year *y*-1 from the weather station data (mmHg; mean daily saturation deficit was averaged over months of December, January, and February)

SD_{F2} Mean seasonal saturation deficit of the fall in year *y*-2 from the weather station data (mmHg; mean daily saturation deficit was averaged over months of September, October, and November)

SD_{S2} Mean seasonal saturation deficit of the summer in year *y*-2 from the weather station data (mmHg; mean daily saturation deficit was averaged over months of June, July, and August)

SD_{L2} Mean seasonal saturation deficit of the spring in year *y*-2 from the weather station data (mmHg; mean daily saturation deficit was averaged over months of March, April, and May)

SD_{W2} Mean seasonal saturation deficit of the winter in year *y*-2 from the weather station data (mmHg; mean daily saturation deficit was averaged over months of December, January, and February)

PR_{F0} Mean seasonal precipitation of the fall in year *y* from the weather station data (mm; mean daily precipitation was averaged over months of September, October, and November)

PR_{S0} Mean seasonal precipitation of the summer in year *y* from the weather station data (mm; mean daily precipitation was averaged over months of June, July, and August)

PR_{L0} Mean seasonal precipitation of the spring in year *y* from the weather station data (mm; mean daily precipitation was averaged over months of March, April, and May)

PR_{W0}	Mean seasonal precipitation of the winter in year *y* from the weather station data (mm; mean daily precipitation was averaged over months of December, January, and February)
PR_{F1}	Mean seasonal precipitation of the fall in year *y*-1 from the weather station data (mm; mean daily precipitation was averaged over months of September, October, and November)
PR_{S1}	Mean seasonal precipitation of the summer in year *y*-1 from the weather station data (mm; mean daily precipitation was averaged over months of June, July, and August)
PR_{L1}	Mean seasonal precipitation of the spring in year *y*-1 from the weather station data (mm; mean daily precipitation was averaged over months of March, April, and May)
PR_{W1}	Mean seasonal precipitation of the winter in year *y*-1 from the weather station data (mm; mean daily precipitation was averaged over months of December, January, and February)
PR_{F2}	Mean seasonal precipitation of the fall in year *y*-2 from the weather station data (mm; mean daily precipitation was averaged over months of September, October, and November)
PR_{S2}	Mean seasonal precipitation of the summer in year *y*-2 from the weather station data (mm; mean daily precipitation was averaged over months of June, July, and August)
PR_{L2}	Mean seasonal precipitation of the spring in year *y*-2 from the weather station data (mm; mean daily precipitation was averaged over months of March, April, and May)
PR_{W2}	Mean seasonal precipitation of the winter in year *y*-2 from the weather station data (mm; mean daily precipitation was averaged over months of December, January, and February)

Table 3. Monthly density of nymphs (DON) per 100 m^2 for the four elevation sites on Chaumont Mountain over the 15 years of the study (2004 – 2018).

Site	Years	N	DON Mean	DON StdDev	DON Range	CND	DON2
Low	15	144	74.4	82.6	0.00 – 430.0	22,629	62.0
Medium	15	144	61.4	75.0	0.00 – 385.8	18,849	51.6
High	15	137	42.7	52.0	0.00 – 257.5	12,582	34.5
Top	15	133	10.6	14.5	0.00 – 80.8	3,000	8.2

Notes: Shown for each of the four elevation sites are the number of years, sample size (N; units are number of transects), mean (units are nymphs per 100 m^2), standard deviation, and the range of the monthly DON. For each elevation site, the expected sample size is 180 transects; missing transects are due to snow days when dragging for ticks was not possible. The DON is biased high due to the missing values for the snow days. In our previous study [12], we calculated the cumulative nymphal density (CND) for each calendar year by integrating the area under the curve of the seasonal phenology of the DON (per 100 m^2) from January 1 to December 31. When this CND is divided by 365 days, it gives a second estimate of density of nymphs (DON2) that is less biased by the missing snow days. For this reason, the estimates of DON2 are lower than the DON.

Table 4. Size of the spring and fall peaks of *I. ricinus* nymphs for the four elevation sites on Chaumont Mountain.

Cumulative spring peak (CSP)						
Site	N	CSP Mean	CSP StdDev	CSP Range	CND2	CSP (%)
Low	15	18,145	10,508	7,516 – 50,801	21,033	85.1
Medium	15	15,573	8,538	7,247 – 35,767	17,293	88.5
High	15	10,191	6,300	3,284 – 24,780	11,357	87.5
Top	15	2,693	1,416	842 – 4,974	2,826	94.5

Cumulative fall peak (CFP)						
Site	N	CFP Mean	CFP StdDev	CFP Range	CND2	CFP (%)
Low	15	2,887	2,456	507 – 9,462	21,033	14.9
Medium	15	1,720	1,303	308 – 4,361	17,293	11.5
High	15	1,166	925	249 – 2,763	11,357	12.5
Top	15	134	129	14 – 399	2,826	5.5

Notes: The size of the spring peak and the fall peak of *I. ricinus* nymphs are shown for each of the four elevation sites on Chaumont Mountain. To compare the size of the cumulative spring peak (CSP) and the cumulative fall peak (CFP), we integrated the area under the curve of the seasonal phenology of the DON (per 100 m^2) from January 1 to August 31 (CSP), and from September 1 to December 31 (CFP), respectively. The interpretation of the CSP and CFP are the numbers of *I. ricinus* nymphs that would have been captured if we had sampled for ticks every day over the corresponding calendar dates. For the CSP and the CFP, the sample size (N = 15 years), mean, standard deviation (StdDev), and range are shown. A second estimate of the cumulative nymphal density (CND2) was calculated by summing the CSP and the CFP. To express the two peaks as a percent, the CSP and the CFP were each divided by the CND2.

Table 5. Model selection results are shown for the generalized additive model (GAM) with negative binomial errors of the density of *I. ricinus* nymphs (DON) at the four elevation sites on Chaumont Mountain over 14 years (2004 to 2017).

Rank	Model structure	Df	logLik	AIC	ΔAIC	Weight1	Weight2	r^2
1	$DON \sim S+Y+S:Y+BM_{2/1}+t+t^2+s(day, by = S)+SD_{S0}+SD_{S0}^2+S:SD_{S0}+S:SD_{S0}^2$	49	-2117.8	4344.1	0.0	98.0	98.0	71.4
2	$DON \sim S+Y+S:Y+BM_{2/1}+t+t^2+s(day, by = S)+SN_{Y1}+SN_{Y1}^2+S:SN_{Y1}+S:SN_{Y1}^2$	49	-2122.3	4352.3	8.2	2.0	100.0	67.7
3	$DON \sim S+Y+S:Y+BM_{2/1}+t+t^2+s(day, by = S)+RH_{S0}+RH_{S0}^2+S:RH_{S0}+S:RH_{S0}^2$	49	-2123.4	4355.2	11.0	0.0	100.0	69.6
4	$DON \sim S+Y+S:Y+BM_{2/1}+t+t^2+s(day, by = S)+SD_{S0}+S:SD_{S0}$	45	-2128.8	4356.7	12.6	0.0	100.0	69.6
5	$DON \sim S+Y+S:Y+BM_{2/1}+t+t^2+s(day, by = S)+RH_{S0}+S:RH_{S0}$	45	-2130.4	4359.7	15.6	0.0	100.0	67.7
6	$DON \sim S+Y+S:Y+BM_{2/1}+t+t^2+s(day, by = S)+SD_{S0}+SD_{S0}^2$	43	-2138.7	4371.4	27.3	0.0	100.0	69.2
7	$DON \sim S+Y+S:Y+BM_{2/1}+t+t^2+s(day, by = S)+RH_{S0}$	42	-2140.8	4373.2	29.1	0.0	100.0	70.0
8	$DON \sim S+Y+S:Y+BM_{2/1}+t+t^2+s(day, by = S)+SD_{S0}$	42	-2141.0	4373.6	29.5	0.0	100.0	70.6
9	$DON \sim S+Y+S:Y+BM_{2/1}+t+t^2+s(day, by = S)+RH_{S0}+RH_{S0}^2$	43	-2140.6	4374.9	30.7	0.0	100.0	69.3
10	$DON \sim S+Y+S:Y+BM_{2/1}+t+t^2+s(day, by = S)+SN_{Y1}+S:SN_{Y1}$	44	-2142.5	4383.0	38.8	0.0	100.0	67.4
11	$DON \sim S+Y+S:Y+BM_{2/1}+t+t^2+s(day, by = S)+SN_{Y1}$	42	-2147.7	4386.4	42.3	0.0	100.0	66.8
12	$DON \sim S+Y+S:Y+BM_{2/1}+t+t^2+s(day, by = S)$	41	-2149.0	4386.8	42.6	0.0	100.0	67.1
13	$DON \sim S+Y+S:Y+BM_{2/1}+t+t^2+s(day, by = S)+SN_{Y1}+SN_{Y1}^2$	42	-2147.7	4388.8	44.7	0.0	100.0	66.7

Notes: The explanatory variables were site (S), year (Y), site:year interaction (S:Y), day (s(day, by = S)), beech mast score with different time lags for the spring peak and fall peak ($BM_{2/1}$), temperature on day of sampling ($t+t^2$), and 3 important weather station climate variables (SD_{S0}, SN_{Y1}, and RH_{S0}). All climate variables were modelled as linear or quadratic effects. To model the bimodal non-linear phenology of the DON, a site-specific smoother function was applied to the calendar day, s(day, by = S). The models are ranked according to their Akaike information criterion (AIC). Shown for each model are the model rank (Rank), model structure (see Table 2 for the list of acronyms of the explanatory variables), model degrees of freedom (Df), log-likelihood (logLik), Akaike information criterion (AIC), difference in the AIC value from the top model (ΔAIC), model weight (Weight1), cumulative model weight (Weight2), and adjusted r-squared value (r^2).

Table 6. Support for the 11 most important explanatory variables of the GAMs of the DON.

Rank	Explanatory variable of interest	Support (%)
1	Site	100.0
2	Year	100.0
3	Site:Year	100.0
4	$BM_{2/1}$	100.0
5	t	100.0
6	t^2	100.0
7	s(Day, by = Site)	100.0
8	SD_{S0}	97.9
9	SD_{S0}^2	97.8
10	$S:SD_{S0}$	97.9
11	$S:SD_{S0}^2$	97.8

Notes: The support for the 11 most important explanatory variables is shown from the AIC-based model selection table of the GAMs of the DON. This support is calculated as the sum of the Akaike weights for all the models in the set that include that particular explanatory variable. Additional file 1: Section 7 shows the results for all the explanatory variables.

Table 7. The parameter estimates from the best model in Table 5 are shown.

Type	Name	Estimate	s.e	t	p
Intercept	Low site	2.774	0.145	19.129	< 0.001
Contrast 1	Medium site	-0.503	0.181	-2.787	0.005
Contrast 2	High site	-0.152	0.253	-0.602	0.547
Contrast 3	Top site	-1.915	0.369	-5.183	< 0.001
Slope 1	Year (for Low site)	0.056	0.014	4.108	< 0.001
Slope 2	$BM_{2/1}$	0.232	0.017	14.014	< 0.001
Slope 3	t	9.616	1.229	7.823	< 0.001
Slope 4	t^2	-8.822	0.927	-9.520	< 0.001
Slope 5	SD_{S0} (for Low site)	-1.937	2.829	-0.685	0.494
Slope 6	SD_{S0}^2 (for Low site)	2.959	1.884	1.570	0.116
Contrast 4	Medium site: Year	-0.035	0.020	-1.790	0.073
Contrast 5	High site: Year	-0.091	0.019	-4.754	< 0.001
Contrast 6	Top site: Year	-0.142	0.022	-6.458	< 0.001
Contrast 7	Medium site: SD_{S0}	11.105	3.672	3.024	0.002
Contrast 8	High site: SD_{S0}	11.690	8.101	1.443	0.149
Contrast 9	Top site: SD_{S0}	-23.486	10.261	-2.289	0.022
Contrast 10	Medium site: SD_{S0}^2	-15.013	3.862	-3.887	< 0.001
Contrast 11	High site: SD_{S0}^2	-10.566	9.293	-1.137	0.256
Contrast 12	Top site: SD_{S0}^2	-19.070	6.638	-2.873	0.004
Smooth terms		Edf	Ref. df	F	p
s(D) – Low site		7.659	8.561	218.4	< 0.001
s(D) – Medium site		7.175	8.226	250.4	< 0.001
s(D) – High site		7.312	8.305	208.0	< 0.001
s(D) – Top site		5.997	7.123	187.9	< 0.001

Notes: In this best model, the DON response variable was modelled as a function of elevation site (Low, Medium, High, and Top), year, beech mast score with different time lags for the spring peak and fall peak ($BM_{2/1}$), linear and quadratic terms for temperature on the day of tick sampling (t and t^2), linear and quadratic terms for the weather station mean seasonal saturation deficit of the summer in the present year (SD_{S0} and SD_{S0}^2). Interactions are indicated by colons (:); for example, the parameter estimates for the site:year interaction are indicated by the terms Medium site: Year, High site: Year, and Top site: Year. For each parameter, the parameter type, parameter name, parameter estimate on the log scale, standard error on the log scale (s.e.), t-statistic (t), and p-values (p) are shown. To model the bimodal non-linear phenology of the DON, a site-specific smoother function was applied to the calendar day. For each of the 4 site-specific smoother functions of the calendar day, the effective degrees of freedom (edf), reference degrees of freedom (Ref. df), F-statistic (F), and p-value (p) are shown.

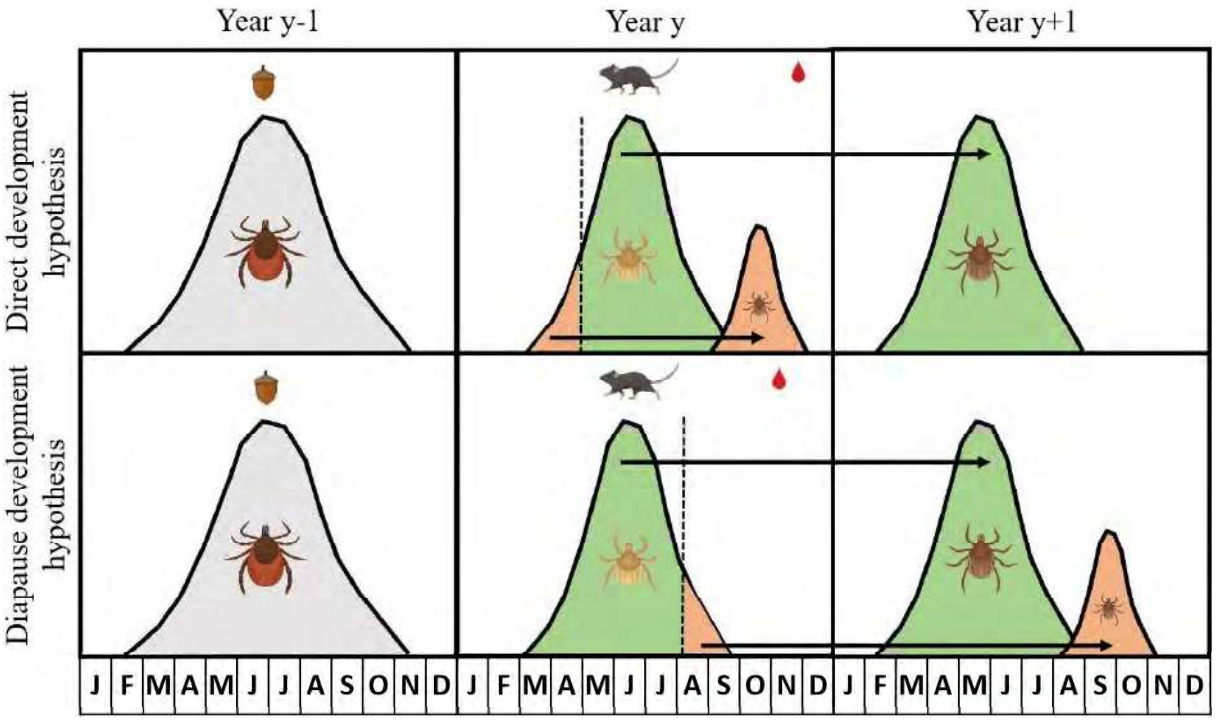

Figure 1. Two alternative (but not mutually exclusive) hypotheses for the fall peak are shown: the direct development hypothesis (top panel) and the developmental diapause hypothesis (bottom panel). The approximate 3-year life cycle of *I. ricinus* is shown by adult ticks (Year *y* – 1 in the left panel) that lay eggs, the larvae (Year *y* in the middle panel), and the nymphs (Year *y* + 1 in the right panel). The origin of the spring peak of nymphs (green peak in Year *y* + 1) is the same for both hypotheses and is as follows. Larvae that obtain their blood meal in the summer (green fraction in Year *y*), moult into unfed nymphs in the same year, enter behavioural diapause, overwinter, and quest as unfed nymphs the following spring (green peak in Year *y* + 1). The two hypotheses differ with respect to the origin of the fall nymphal peak (small orange peak). In the direct development hypothesis, larvae that obtain their blood meal early in the summer (orange fraction in Year *y*) moult into unfed nymphs in summer and quest as unfed nymphs that same fall (small orange peak in Year *y*). In the developmental diapause hypothesis, larvae that obtain their blood meal late in the summer (orange fraction in Year *y*), overwinter as engorged larvae, moult into unfed nymphs the following summer and quest as unfed nymphs the following fall (small orange peak in Year *y* + 1). The time lag between a masting event (Year *y* – 1) and the spring peak of nymphs (green peak in Year *y* + 1) is 2 years. In contrast, the time lag between a masting event and the fall peak of nymphs (small orange peak) is 1 year under the direct development hypothesis and 2 years under the developmental diapause hypothesis.

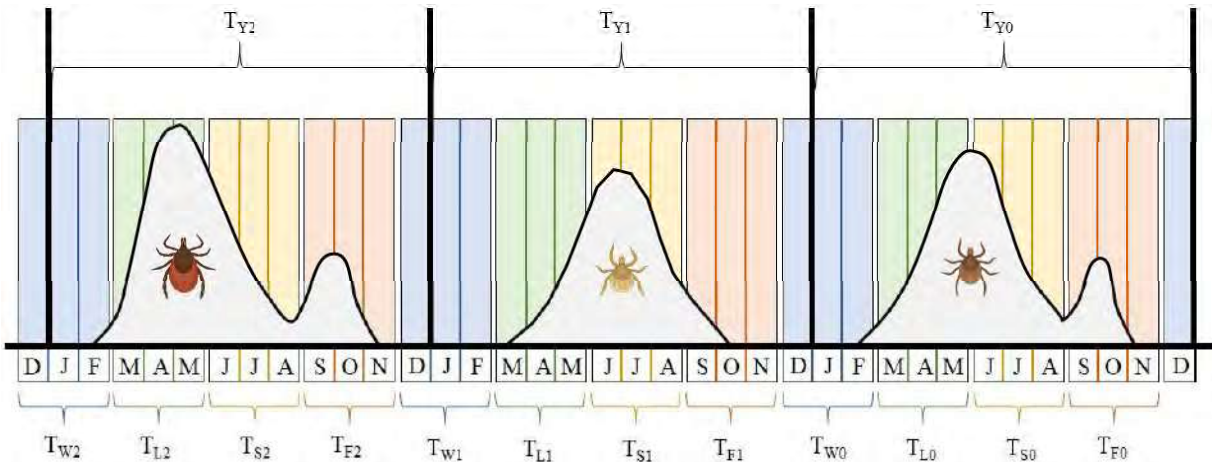

Figure 2. Visual representation of how the mean annual climate variables and the mean seasonal climate variables were calculated over 3 different years. The approximate 3-year life cycle of *I. ricinus* is shown by adult ticks that lay eggs (left panel), the eggs that hatch into larvae (middle panel), and the larvae that become nymphs (right panel). The bimodal or unimodal distribution in each panel represents the phenology of each tick stage. The three calendar years are shown by the vertical black lines, the months are shown by the bars that are labelled below the X-axis. The four seasons of winter, spring, summer, and fall are color-coded as blue, green, yellow, and orange, respectively. The response variable of interest is the density of nymphs (DON) in the right panel. For illustrative purposes, the explanatory variable is temperature (abbreviated as T). The 3 annual means of the temperature are T_{Y2}, T_{Y1}, and T_{Y0} (labelled at the top); the subscript 'Y' indicates that the temperature is averaged over the calendar year; the subscripts 0, 1, and 2 indicate the time lag (i.e., 0, 1, or 2 years before the year of the DON). There are 12 seasonal means of the temperature (labelled at the bottom); the subscripts 'W', 'L', 'S', and 'F' indicate that the temperature is averaged over the winter, lent (spring), summer, and fall; the subscripts 0, 1, and 2 indicate the time lag in years. For example, T_{W2} is the mean temperature of the winter two years before the year of the DON.

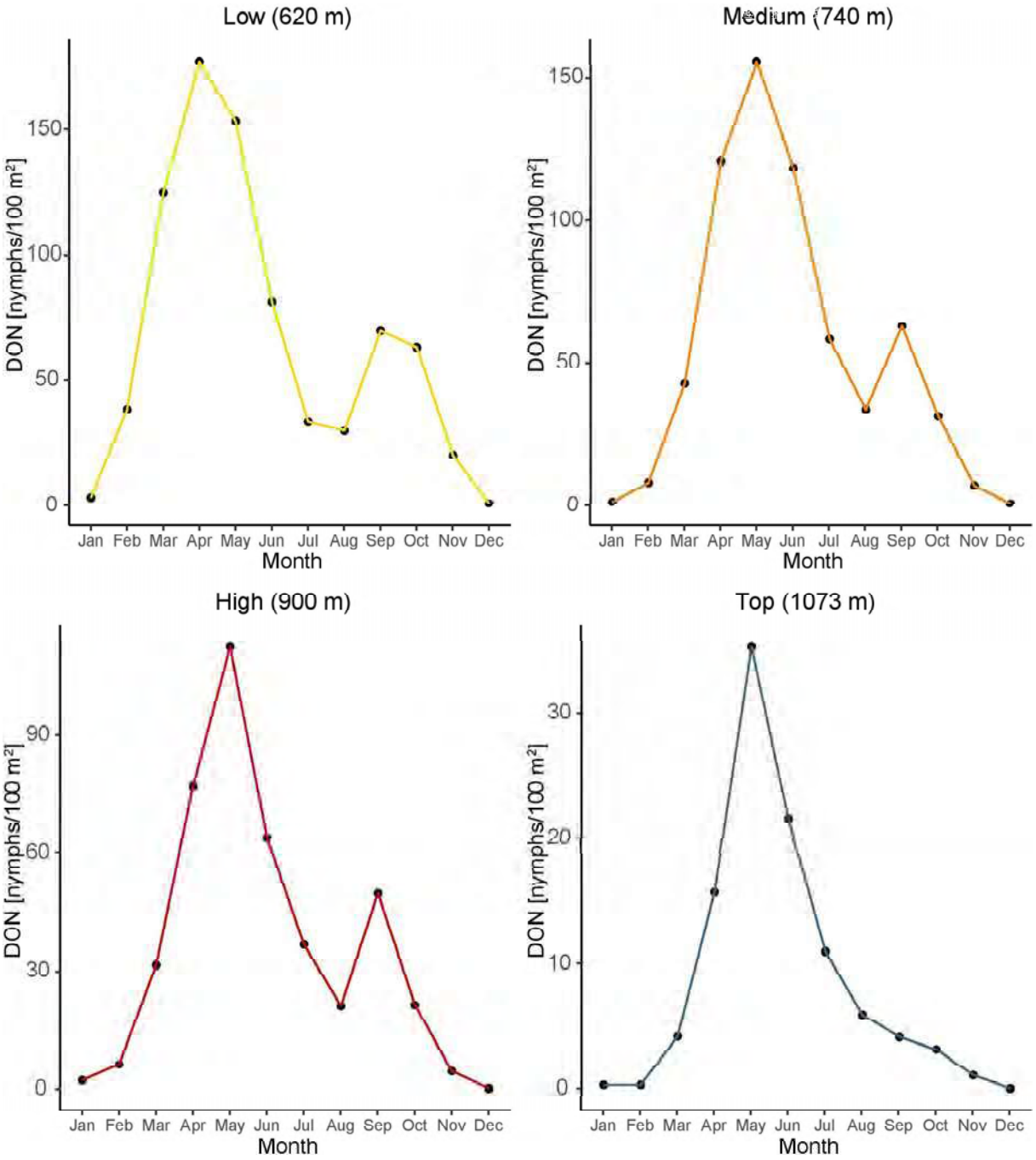

Figure 3. Seasonal changes in the DON over the calendar year at the four elevation sites. The DON is an estimate of the number of questing *I. ricinus* nymphs per 100 m^2 sampled by the dragging method each month. For each month, the data are averaged over the 15 years of the study (2004 – 2018). A bimodal phenology with a large peak of the DON in the spring and a smaller peak of the DON in the fall was observed at the low, medium, and high elevation sites, but not at the top elevation site where the phenology was characterized by a single peak in the spring.

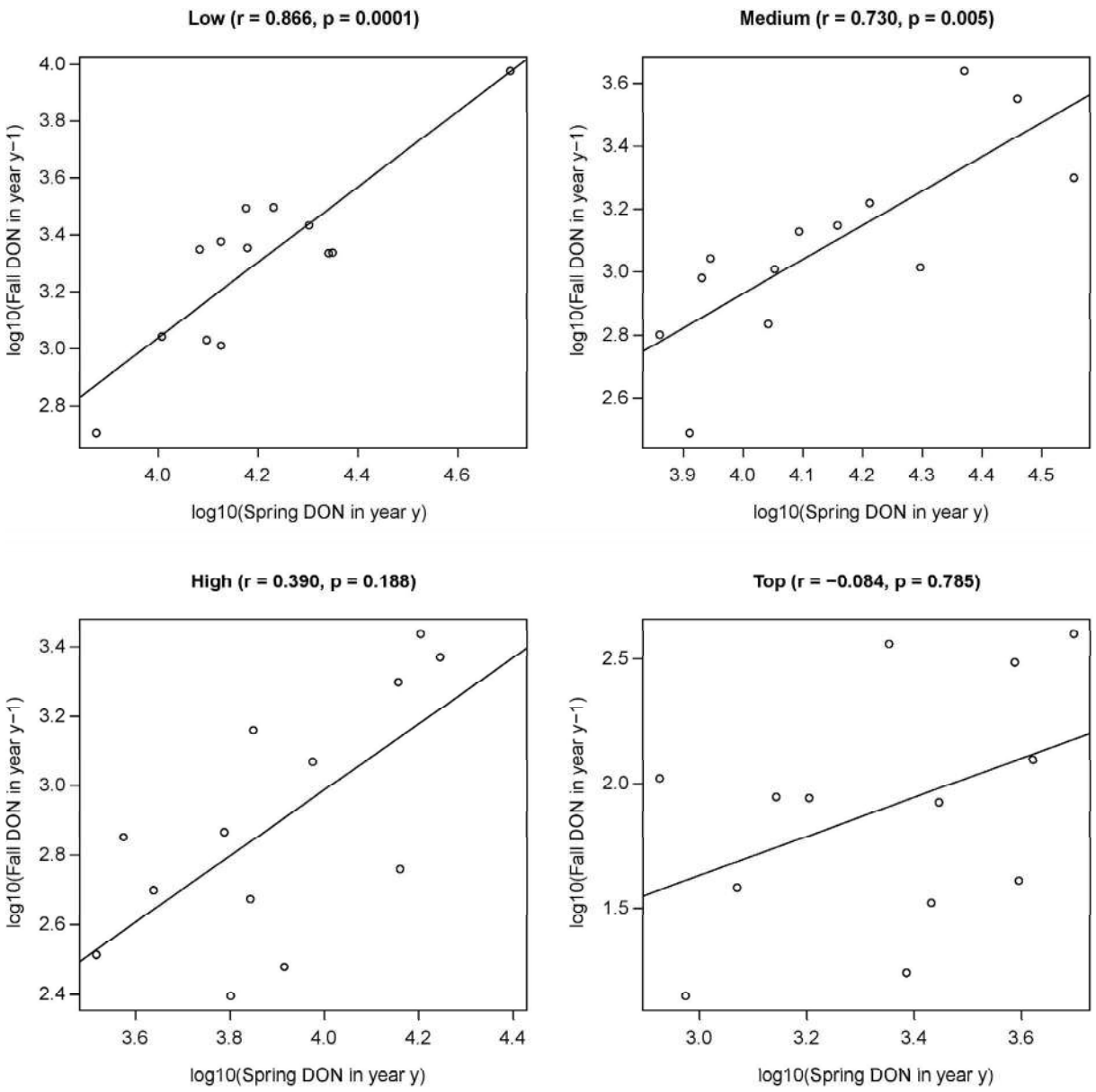

Figure 4. Correlation plot showing the relationship between the fall peak in year *y*-1 and the spring peak in year *y* for each of the four elevation sites. The fall peak in year *y*-1 is strongly correlated with the spring peak in year *y* for the low and medium elevation sites. The Pearson correlation coefficient (r) and the p-value (p) are shown in brackets at the top of each panel. These results support the direct development hypothesis and indicate that the tick year starts in the fall and ends the following summer.

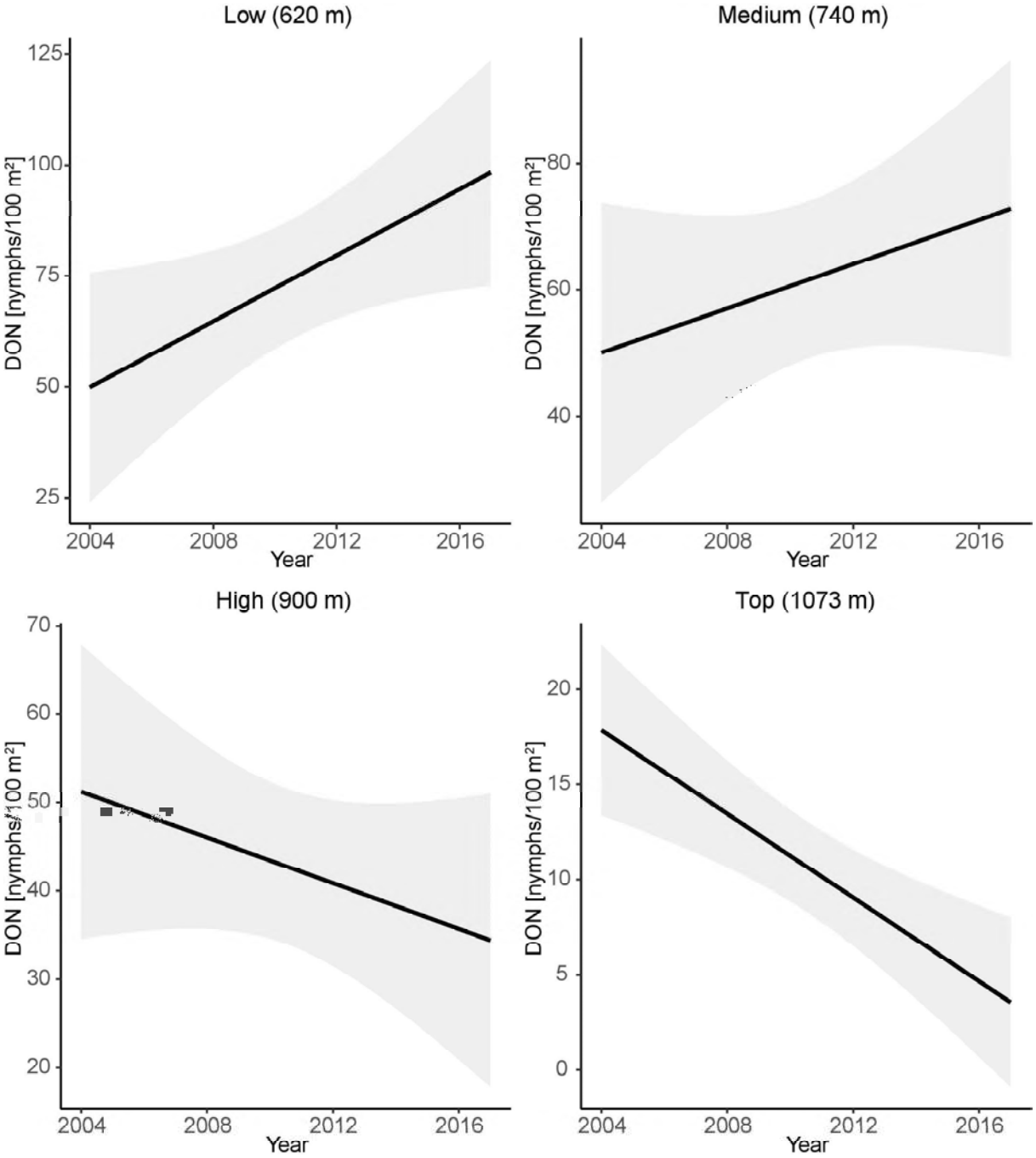

Figure 5. Effect of year on the density of nymphs (DON). The DON is an estimate of the number of questing *I. ricinus* nymphs per 100 m^2 sampled by the dragging method each month. The parameter estimates used to calculate the effect sizes were taken from Table 7. Over the 14-year study period, the DON increased by 119.0% at the low elevation, increased by 34.2% at the medium elevation, decreased by 38.7% at the high elevation, and decreased by 70.0% at the top elevation (partial r^2 = 6.6%).

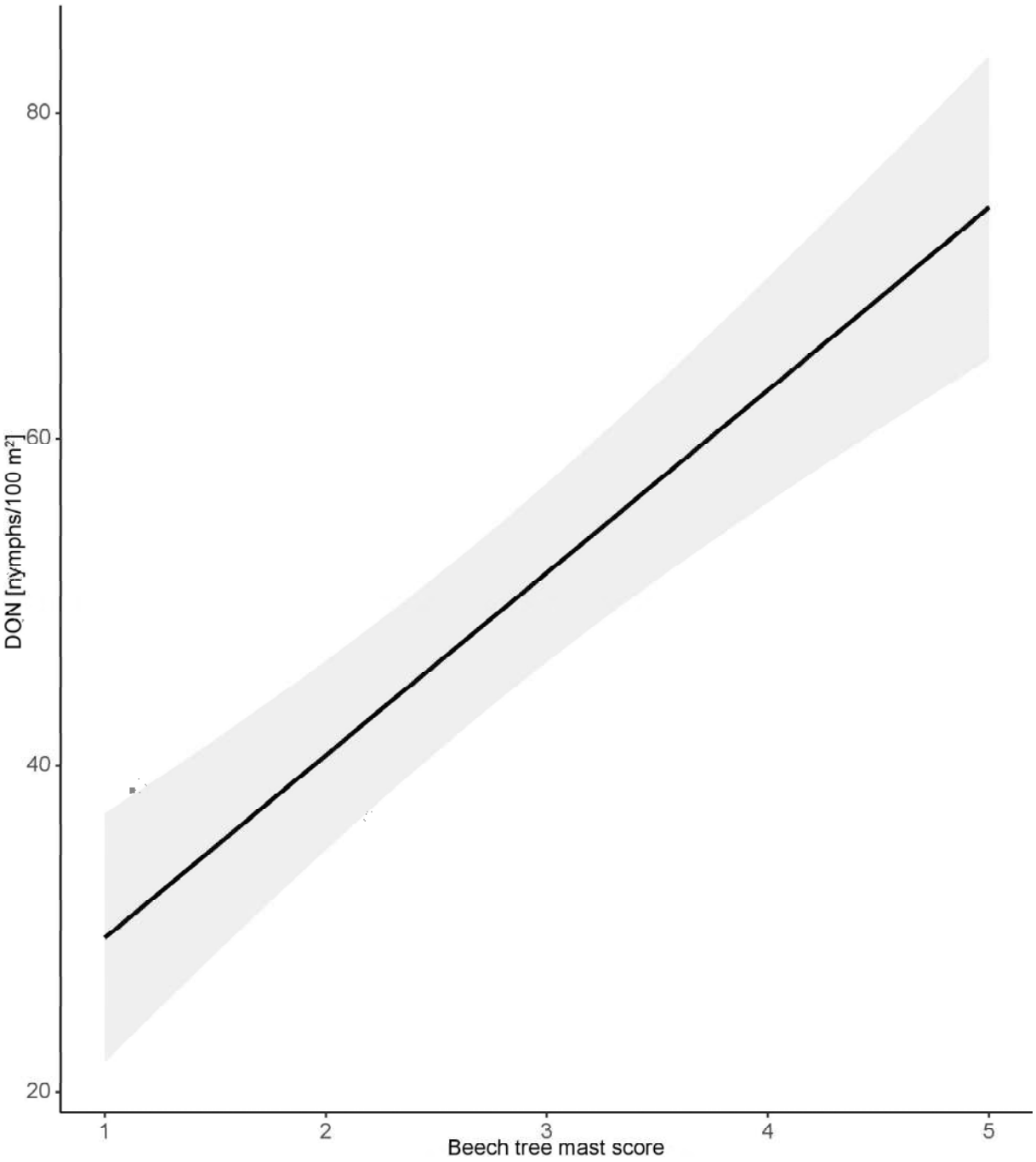

Figure 6. Effect of beech mast score with different time lags (2 years versus 1 year) for the spring and fall peak ($BM_{2/1}$) on the density of nymphs (DON). The beech tree mast score ($BM_{2/1}$) assumes a 2-year time lag for the spring nymphal peak and a 1-year time lag for the fall nymphal peak. The linear relationship shows that the DON increases with the beech mast score. The DON is an estimate of the number of questing *I. ricinus* nymphs per 100 m^2 sampled by the dragging method each month. Beech tree mast scores have values of 1, 2, 3, 4, and 5, which refer to very poor mast, poor mast, moderate mast, good mast, and full mast, respectively. The parameter estimates used to calculate the effect sizes were taken from Table 7. Increasing the

beech mast score from 1 (poor mast) to 5 (full mast) increased the DON by 152.9% at each of the four elevation sites (partial r^2 = 16.0%).

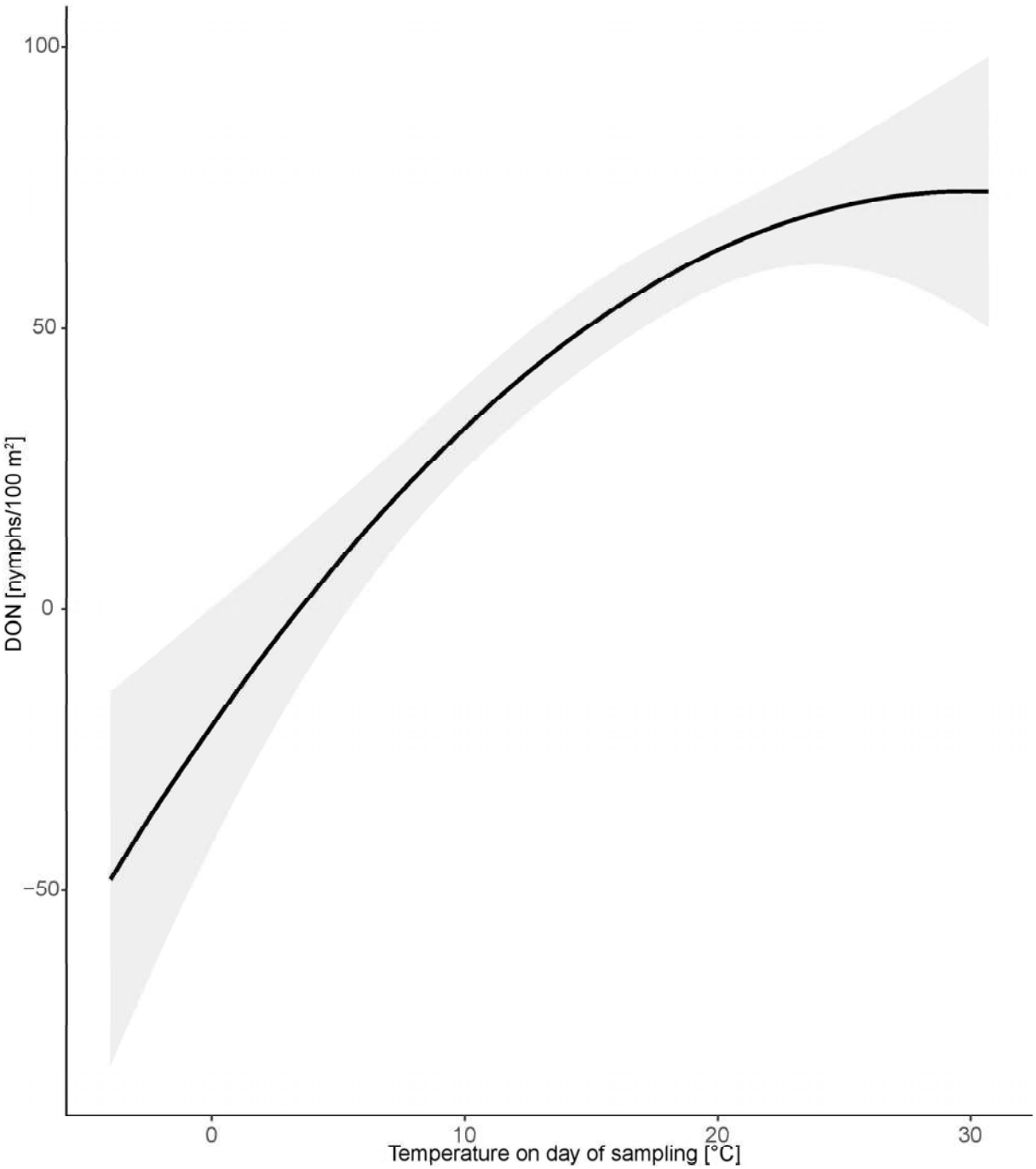

Figure 7. Effect of the field-measured temperature on the day of tick sampling on the density of nymphs (DON). The quadratic relationship shows that the DON increases with the temperature on the day of tick sampling and reaches a plateau at 30°C. The DON is an estimate of the number of questing *I. ricinus* nymphs per 100 m^2 sampled by the dragging method each month. Temperature has units of °C and was measured at 60 cm above the ground at the field site on the day of tick sampling. The parameter estimates used to calculate the effect sizes were taken from Table 7. The quadratic function of the field-measured temperature explained 0.0% of the variation in the DON (partial r^2 = 1.4%).

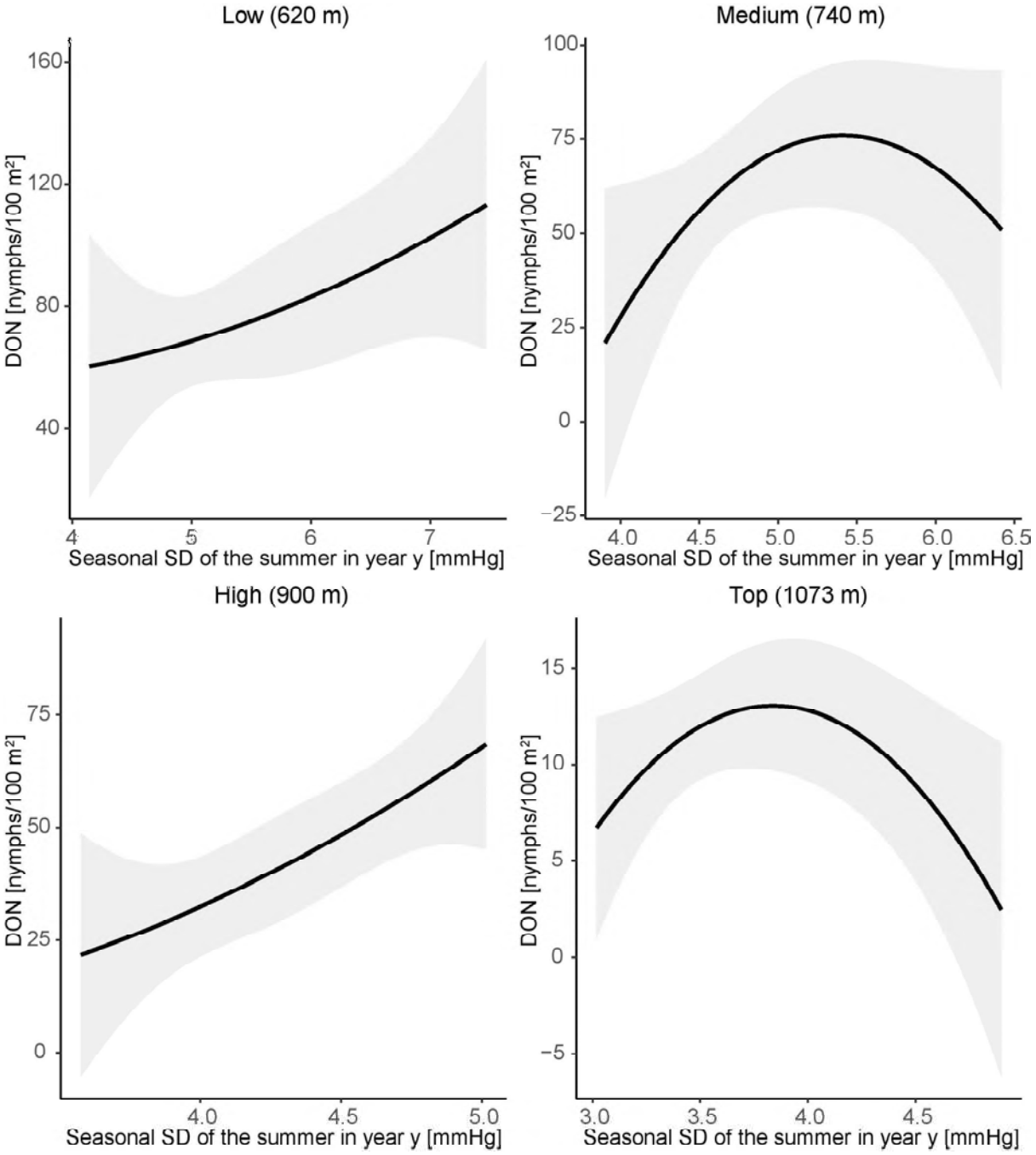

Figure 8. Effect of the mean saturation deficit in the summer of year *y* (SD_{S0}) on the density of nymphs (DON) at each of the four elevation sites. The SD_{S0} refers to the mean saturation deficit calculated over the summer months (1 June to 31 August) in the same year as the DON (i.e., no time lag). The relationship between the DON and the SD_{S0} is linear and positive for the low and high elevation sites and it is a negative quadratic for the medium and top elevation sites. The DON is an estimate of the number of questing *I. ricinus* nymphs per 100 m^2 sampled by the dragging method each month. The SD_{S0} has units of mmHg and was calculated from temperature and relative humidity data measured at 200 cm above the ground by two weather stations near the field site. The parameter estimates used to calculate the effect sizes were taken

from Table 7. The site-specific quadratic function of SD_{S0} explained 14.3% of the variation in the DON (partial r^2 = 4.3%).